ΑD			

Award Number: W81XWH-04-1-0887

TITLE: Pim-1: A Molecular Target to Modulate Cellular Resistance to Therapy in

Prostate Cancer

PRINCIPAL INVESTIGATOR: Michael Lilly, M.D.

CONTRACTING ORGANIZATION: Loma Linda University

Loma Linda, CA 92354

REPORT DATE: October 2007

TYPE OF REPORT: Annual

PREPARED FOR: U.S. Army Medical Research and Materiel Command

Fort Detrick, Maryland 21702-5012

DISTRIBUTION STATEMENT: Approved for Public Release;

Distribution Unlimited

The views, opinions and/or findings contained in this report are those of the author(s) and should not be construed as an official Department of the Army position, policy or decision unless so designated by other documentation.

REPORT DOCUMENTATION PAGE

Form Approved OMB No. 0704-0188

Public reporting burden for this collection of information is estimated to average 1 hour per response, including the time for reviewing instructions, searching existing data sources, gathering and maintaining the data needed, and completing and reviewing this collection of information. Send comments regarding this burden estimate or any other aspect of this collection of information, including suggestions for reducing this burden to Department of Defense, Washington Headquarters Services, Directorate for Information Operations and Reports (0704-0188), 1215 Jefferson Davis Highway, Suite 1204, Arlington, VA 22202-4302. Respondents should be aware that notwithstanding any other provision of law, no person shall be subject to any penalty for failing to comply with a collection of information if it does not display a currently valid OMB control number. PLEASE DO NOT RETURN YOUR FORM TO THE ABOVE ADDRESS.

1. REPORT DATE	2. REPORT TYPE	3. DATES COVERED
01-10-2007	Annual	1 Oct 2006 – 30 Sep 2007
4. TITLE AND SUBTITLE		5a. CONTRACT NUMBER
Pim-1: A Molecular Target to Modu	late Cellular Resistance to Therapy in Prostate	5b. GRANT NUMBER
Cancer	,	W81XWH-04-1-0887
		5c. PROGRAM ELEMENT NUMBER
6. AUTHOR(S)		5d. PROJECT NUMBER
• •		
Michael Lilly, M.D.		5e. TASK NUMBER
,,		
		5f. WORK UNIT NUMBER
Email: mlilly@uci.edu		
7. PERFORMING ORGANIZATION NAME(S) AND ADDRESS(ES)	8. PERFORMING ORGANIZATION REPORT
		NUMBER
Loma Linda University		
Loma Linda, CA 92354		
9. SPONSORING / MONITORING AGENCY	NAME(S) AND ADDRESS(ES)	10. SPONSOR/MONITOR'S ACRONYM(S)
U.S. Army Medical Research and M	lateriel Command	
Fort Detrick, Maryland 21702-5012		
-		11. SPONSOR/MONITOR'S REPORT
		NUMBER(S)
12 DISTRIBUTION / AVAIL ARILITY STATE	EMENT	

Approved for Public Release; Distribution Unlimited

13. SUPPLEMENTARY NOTES

Original contains colored plates: ALL DTIC reproductions will be in black and white.

14. ABSTRACT

The contract supports studies to define the role of the PIM1 kinase in acquired resistance to chemotherapy by prostate cancer cells. Data to date for specific aim #1 define a signaling pathway induced by docetaxel, involving sequential steps of STAT3 phosphorylation, expression of PIM1, and activation of NFkB signaling. Blockade of this pathway prevents drug-induced upregulation of NFkB activity, and sensitizes cells to docetaxel. Other studies (specific aim #2) focus on identifying a mechanism through which PIM1 activates NFkB. We have unambiguously identified S937 as the major PIM1 phosphorylation site on the NFKB1/p105 precursor protein, through use of LCM/MS/MS analysis. We have now shown that phosphorylation at S937 potentiates NFkB transcriptional activity. Additional data (specific aim #3) have been published to describe a small molecule inhibitor of PIM1. This molecule can sensitize prostate cancer cells to the cytotoxic effects of docetaxel in an additive or synergistic manner. Pharmacophore analysis has identified future modifications of the inhibitor.

15. SUBJECT TERMS

PIM1 kinase chemotherapy resistance prostate cancer

16. SECURITY CLAS	SIFICATION OF:		17. LIMITATION OF ABSTRACT	18. NUMBER OF PAGES	19a. NAME OF RESPONSIBLE PERSON USAMRMC
a. REPORT U	b. ABSTRACT U	c. THIS PAGE U	UU	67	19b. TELEPHONE NUMBER (include area code)

Table of Contents

ntroduction4	
Body4-6	
Key Research Accomplishments6	
Reportable Outcomes6	
Conclusions7	
References7	
Appendices7-69)

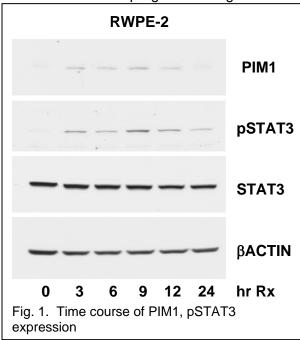
INTRODUCTION

Studies under this funded activity are focused on characterizing the role of the PIM1 gene in acquired resistance to chemotherapy drugs, by prostate cancer cells. The proposal included three specific aims: 1) to define a novel signal transduction pathway activated by docetaxel, 2) to characterize the mechanism through which PIM1 activates and regulates NFkB signaling, and 3) to explore genetic and pharmacologic means of inhibiting PIM1 activity or expression to enhance the sensitivity of prostate cancer cells to docetaxel and other chemotherapy drugs.

During the 02 year (October 1, 2006 through 9/30/2007) progress has been limited due the move of Dr. Lilly's laboratory from Loma Linda University to the University of California, Irvine. The Loma Linda laboratory was substantially shut down at the end of October, 2006. From that period until July, 2007 the grant was "in hiatus" as the two institutions negotiated an agreement through which the grant would remain at LLU, but all work would be performed by Dr. Lilly via a subcontract to UCI. A UCI account was finally established by the end of July, 2007 and the process of hiring new staff began. Nevertheless some progress has been made. Two papers have been published in well-known journals, describing the activity of our prototype PIM1 kinase inhibitor. In addition a third manuscript has been submitted to the *Journal of Biological Chemistry*.

BODY

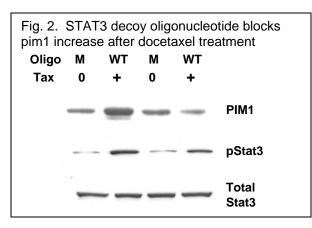
We will outline our progress through reference to the specific aims described above. The first



specific aim (specific aim #1)was to outline a signal transduction pathway activated by docetaxel and involving upregulation of PIM1 expression. This pathway has substantially defined. Using RWPE2 prostate cells, we noted that docetaxel treatment rapidly leads to an increase in expression of the PIM1 serine/threonine kinase. Expression becomes apparent at 3hrs after drug addition, peaks at 9-12hrs, and returns to baseline by 24hrs (Fig. 1). This increase in expression is accompanied by an increase in pim-1 mRNA, as shown by real time-PCR analysis (Fig. 2). Thus the effects of docetaxel are primarily transcriptional or posttranscriptional.

We next wanted to define mechanisms through which *pim-1* could be transcriptionally upregulated. Transcription of *pim-1* is known to be activated by STAT transcription factors and by NFkB transcription factors. We examined

the time course of STAT3 activation after docetaxel treatment (Fig. 1), and noted that it paralleled the course of pim-1 expression. We therefore suspected that docetaxel increased pim-1 expression in a STAT3-dependent manner. This was directly demonstrated by use of decoy oligonucleotides (Fig. 2). Double-stranded DNA oligonucleotides matching a known STAT3 binding site blocked the drug-induced upregulation of pim-1 expression, while a decoy based on a mutated (non-binding) STAT3 site did not. These data therefore establish a linear relationship among the following events: docetaxel treatment \rightarrow STAT3 activation \rightarrow pim-1 expression.

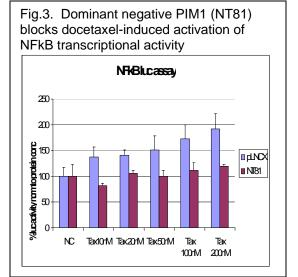


We hypothesized that NFkB transcriptional activation would be a downstream event in this signal transduction pathway, because many chemotherapy drugs and other stressors are known to activate NFkB. We engineered RWPE2 cells to constitutively express a NFkB-dependent promoter/luciferase plasmid, and found that docetaxel treatment increased NFkB transcriptional activity. We then transiently infected these cells with a *pim-1*-encoding retrovirus. *Pim-1* expression also consistently increased NFkB transcriptional activity. To determine if the drug-induced increase in NFkB

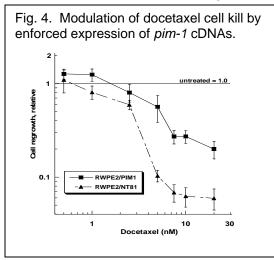
activity occurred in a *pim-1*-dependent manner, we then infected the reporter cell line with a retrovirus encoding a dominant-negative form of *pim-1*, pimNT81. The dominant negative *pim-1* cDNA completely blocked the drug-induced upregulation of NFkB activity, demonstrating that

pim-1 expression is a necessary upstream step in the drug-induced activation of NFkB (Fig. 3). In aggregate these studies establish a signal transduction pathway triggered by docetaxel treatment of RWPE2 prostate cancer cells.

To determine if this pathway modified drug toxicity, we examined the effects of enforced expression of wild-type or NT81 *pim-1* cDNAs of docetaxel cell kill (Fig. 4). Docetaxel produced dose-dependent cell kill in RWPE1, 2 cells. Enforced expression of wild-type *pim-1* cDNA markedly reduced cell death. In contrast, expression of the dominant negative NT81 cDNA enhanced cell death after docetaxel treatment. These data demonstrate that *pim-1* expression can modulate drug-induced cell death, and demonstrate that the survival pathway

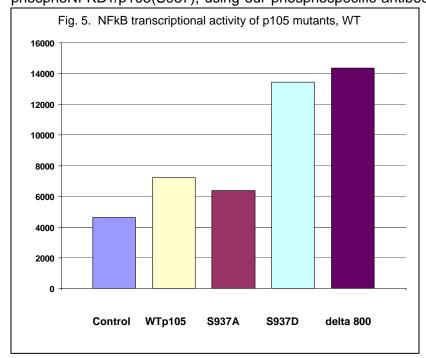


described above is a legitimate target for pharmacologic intervention. These data have been submitted to the Journal of Biological Chemistry (see manuscript in appendix).



The goal of **specific aim #2** was to define pathways through which the PIM1 kinase could activate NFkB transcriptional activity. We had hypothesized that PIM1 would phosphorylate the NFKB1/p105 precursor protein on serine-937, leading to proteolytic cleavage of the protein with release of active p50 protein as well as other sequestered NFkB components and the TPL2 kinase. In the previous reporting period we demonstrated that PIM1 can phosphorylate the p105 NFKB1 precursor on serine 937, a novel phosphorylation site. In addition we prepared a polyclonal antibody specific for this phosphorylation site. During the early part of this reporting period a

number of studies were undertaken to characterize the expression of phosphoNFKB1/p105(S937), using our phosphospecific antibody. An initial study used mutant



(S937D) p105 cDNAs to mimick the effect of These phosphorylation. "phosphomimic" proteins enhanced NFkB transcriptional whereas activity corresponding S937A mutant inhibits activity, compared to the wild type NFKB1 protein (Fig.5). In this experiment, HeLa cells were transfected with a luciferase reporter gene under the control of a synthetic consensus NFkB binding site, plus WT or mutant p105 cDNAs. Bars indicate the firefly luciferase activity of the transfectants, normalized to that of a Renilla luciferase transfection control plasmid. These data indicate that if

PIM1 phosphorylates S937 in vivo, it likely would enhance overall NFkB transcriptional activity.

The third specific aim (specific aim #3) proposed to use small molecule inhibitors of the PIM1 kinase as molecular probes to determine their effect on docetaxel sensitivity. describing one such molecule, the flavonol guercetagetin, was published as the cover article in the January, 2007 issue of Molecular Cancer Therapeutics (1; see appendix A). We have demonstrated that quercetagetin in a moderately potent (IC₅₀ = 340nM, specific, and cellpermeable inhibitor of PIM1 activity in prostate cancer cells. Key data include the demonstration that quercetagetin in competitive with ATP. A crystal structure of PIM1 in complex with quercetagetin, or with three other flavonoids, has been determined. We have also shown that quercetagetin is able to inhibit the activity of the PIM1 kinase in prostate cancer cells at an IC₅₀ of about 5.5µM. Interestingly the activity of the AKT kinase is not inhibited at all under these conditions. A companion article, presenting a pharmacophore analysis of flavonoid inhibitors of PIM1, has also been published recently (2; see appendix B). We have recently obtained, and begun characterizing, novel small molecule inhibitors of PIM1 from Exelixis Corporation and from Dr. Andrew Kraft (Hollings Cancer Center). These molecules show additive, or at some concentrations synergistic, cell growth inhibition in that PIM1 kinase acts to inhibit cell death caused by the cytotoxic drug docetaxel, and that blocking the activity of PIM can potentiate cell kill and overcome cytotoxic drug resistance.

KEY RESEARCH ACCOMPLISHMENTS THROUGH OCTOBER 31, 2007

- Definition of a novel survival pathway activated by docetaxel treatment, and involving sequential activation or expression of STAT3, PIM1, and NFkB components.
- A manuscript describing the above pathway has been submitted to *Journal of Biological Chemistry*, and is currently under revision.
- Identification of serine-937 as the major phosphorylation site for PIM1 on the p105/NFKB1 precursor protein

- Identication of quercetagetin as a moderately potent and specific, cell-permeable PIM1 kinase inhibitor
- Demonstration that XL-1075 and XL-1154 can show additive or synergistic cell kill in prostate cancer cells treated with docetaxel
- Abstract presented at the annual AACR meeting, Washington DC, April, 2006
- Paper describing the activity of quercetagetin as a PIM1 kinase inhibitor, published in January, 2007 issue of *Molecular Cancer Therapeutics* (cover article)
- Paper describing pharmacophore analysis of flavonoid inhibitors of PIM1, published in March, 2007 issue of Bioorganic and Medicinal Chemistry

REPORTABLE OUTCOMES

Manuscripts Published

Holder SL, Zemskova M, Bremner R, Neidigh J, **Lilly MB**: Identification of specific, cell-permeable small molecule inhibitor of the PIM1 kinase. *Mol Cancer Therapeutics* 6:163-72 (2007).

Holder SL, **Lilly MB**, Brown ML: Comparative Molecular Field Analysis of Flavonoid Inhibitors of the PIM-1 Kinase. *Bioorg Med Chem* (in press, 2007)

Manuscript Under Review

CONCLUSIONS

Our data demonstrate that PIM1 is a critical component of a survival/stress pathway activated by docetaxel treatment of prostate cancer cells. This pathway leads to activation of NFkB-dependent transcription, possibly by phosphorylation of p105/NFKB1 by PIM1 at serine-937. Targeting PIM1 kinase activity with quercetagetin, or other PIM1 kinase inhibitors, leads to additive or synergistic cell kill following docetaxel treatment.

REFERENCES

- 1. Holder SL, Zemskova M, Bremner R, Neidigh J, **Lilly MB**: Identification of specific, cell-permeable small molecule inhibitor of the PIM1 kinase. *Mol Cancer Therapeutics* Mol Cancer Ther. 6:163-72 (2007).
- 2. Holder SL, **Lilly MB**, Brown ML: Comparative Molecular Field Analysis of Flavonoid Inhibitors of the PIM-1 Kinase. *Bioorg Med Chem* (in press, 2007)

APPENDIX

Research data are presented throughout the body of this report. The appendix contains four items:

- A. Manuscript: Holder, et al., "Characterization . . . kinase." MCT
- B. Manuscript: Holder, et al., "Comparative . . . kinase." BMC
- C. Manuscript: Zemskova, et al., "The PIM . . . cells." JBC
- D. Curriculum vitae for Michael Lilly, MD

163

Characterization of a potent and selective small-molecule inhibitor of the PIM1 kinase

Sheldon Holder, ^{1,2,3} Marina Zemskova, ³ Chao Zhang, ⁴ Maryam Tabrizizad, ⁴ Ryan Bremer, ⁴ Jonathan W. Neidigh, ² and Michael B. Lilly ^{1,2,3}

¹Center for Molecular Biology and Gene Therapy, Departments of ²Biochemistry and Microbiology and ³Medicine, Loma Linda University School of Medicine, Loma Linda, California; and ⁴Plexxikon, Inc., Berkeley, California

Abstract

The pim-1 kinase is a true oncogene that has been implicated in the development of leukemias, lymphomas, and prostate cancer, and is the target of drug development programs. We have used experimental approaches to identify a selective, cell-permeable, small-molecule inhibitor of the pim-1 kinase to foster basic and translational studies of the enzyme. We used an ELISA-based kinase assay to screen a diversity library of potential kinase inhibitors. The flavonol quercetagetin (3,3',4',5,6,7hydroxyflavone) was identified as a moderately potent, ATP-competitive inhibitor (IC50, 0.34 µmol/L). Resolution of the crystal structure of PIM1 in complex with quercetagetin or two other flavonoids revealed a spectrum of binding poses and hydrogen-bonding patterns in spite of strong similarity of the ligands. Quercetagetin was a highly selective inhibitor of PIM1 compared with PIM2 and seven other serine-threonine kinases. Quercetagetin was able to inhibit PIM1 activity in intact RWPE2 prostate cancer cells in a dose-dependent manner (ED₅₀, 5.5 µmol/L). RWPE2 cells treated with quercetagetin showed pronounced growth inhibition at inhibitor concentrations that blocked PIM1 kinase activity. Furthermore, the ability of quercetagetin to inhibit the growth of other prostate epithelial cell lines varied in proportion to their levels of PIM1 protein. Quercetagetin can function as a moderately potent and selective, cell-permeable inhibitor of the pim-1 kinase, and may be useful for proof-of-concept studies to support the development of clinically useful PIM1 inhibitors. [Mol Cancer Ther 2007;6(1):163-72]

Received 7/10/06; revised 10/10/06; accepted 11/17/06.

Grant support: Department of Defense, Congressionally Directed Medical Research Program, Award W81XWH-041-0887.

The costs of publication of this article were defrayed in part by the payment of page charges. This article must therefore be hereby marked adventisement in accordance with 18 U.S.C. Section 1734 solely to indicate this fact.

Requests for reprints: Michael B. Lilly, Center for Molecular Biology and Gene Therapy, Lome Unide University School of Medicine, 11234 Anderson Street, Lome Linde, CA 92354. Phone: 909-558-8777; Fax: 909-558-0177. E-mai: milly@lb.edu

Copyright © 2007 American Association for Cancer Research. doi: 10.1158/1535-7163.MCT-06-0397

Mol Cancer Ther 2007;6(1), January 2007

Introduction

The pim family of serine-threonine kinases is composed of three highly homologous genes, pim-1, pim-2, and pim-3. These enzymes are increasingly being recognized as important mediators of survival signals in cancers, stress responses, and neural development (1–6). In addition, these kinases are constitutively expressed in some tumors and function as true oncogenes. Thus, they are of significant interest as targets for therapeutic intervention.

Small-molecule inhibitors are important molecular probes for studying protein kinases. In addition, they may serve as protype thempeutic agents for treating diseases resulting from unregulated kinase activity. Three prior reports have shown that known, promiscuous kinase inhibitors can inhibit PIM1 function in vitro. Jacobs et al. (7) showed that several staurosporine and bisindoyl-maleimide analogues, as well as the morpholino-substituted chromone LY294002, were able to inhibit PIM1 activity in vitro. Subsequently, Fabian et al. (8) presented an interaction map involving 113 kinases and 20 smallmolecule kinase inhibitors now under clinical study. Only three inhibitors had detectable binding to (and presumably inhibitory activity against) PIM1-two staurosporine analogues and flavopiridol, a flavonoid undergoing evaluation as an inhibitor of cyclin-dependent kinases. A recent report (9) confirmed the activity of bisindoylmaleimide derivatives as well as some flavonoids in vitro. All of the identified inhibitors either lacked specificity for PIM1 or were only modestly active at low micromolar concentrations, or both. Furthermore, none of these reports showed that the test agents could selectively inhibit PIM1 activity in

To further our basic and translational studies of the pim kinases, we have sought to identify small-molecule inhibitors of PIM1. We here report that the flavonol quercetagetin is a selective PIM1 inhibitor with nanomolar potency and can differentially inhibit the kinase in cellbased assays.

Materials and Methods

Cell Lines and Culture Methods

The prostate epithelial cell lines RWFE1, RWPE2, LNCaP, and PC3 were obtained from the American Type Culture Collection (Manassas, VA) and cultured in the recommended medium. We produced additional pools of RWPE2 prostate cells that overexpressed pim-1 through retroviral transduction. The coding region for the human pim-1 gene was cloned into the pLNCX retroviral vector (Clontech, Mountain View, CA). Infectious viruses were produced in the GP-293 packaging cell line by cotransfection with retroviral backbone plasmids (pLNCX or pLNCX/pim-1) and with pVSV-G, a plasmid that expresses the envelope

164 PIM1 Inhibitor

glycoprotein from vesicular stomatitis virus. Forty-eight hours after transfection, the medium was collected and the virus particles were concentrated as described in the manufacturer's protocol (Clontech). RWPE2 cells were plated at 1×10^5 per 60-mm plate 16 to 18 h before infection. Cells were infected with 5×10^4 viral particles in the presence of $8\,\mu g/mL$ polybrene. After 6 h of incubation, the virus-containing medium was replaced with fresh medium, and on the next day G418 (400 $\mu g/mL$) was added to select infected cells. After 10 days of selection, stable cell pools were established and PIM1 expression was verified by immunoblotting.

For growth-inhibition experiments, cells were plated onto 24-well plates and fixed with formaldehyde at intervals. Cell number was quantified by crystal violet staining (10).

Recombinant pim Kinases and Kinase Assays

We prepared recombinant PIM1 and PIM2 as glutathione S-transferase (GST) fusions in Escherichia coli, as described (11). For the inhibitor screening assays, a solid-phase kinase assay was developed based on our demonstration that PIM1 is a potent kinase for phosphorylating BAD on Ser112 (11, 12). Ninety-six-well flat-bottomed plates were coated overnight at 4°C with recombinant GST-BAD [1 µg/well in HEPES buffer: 136 mmol/L NaCl, 2.6 mmol/L KCl, and 20 mmol/L HEPES (pH 7.5)]. The plates were then blocked for 1 h at room temperature with 10 μg/mL bovine serum albumin in HEPES buffer. The blocking solution was then removed and 5 µL of each inhibitor, dissolved in 50% DMSO, were added to each well. Then, 100 µL of kinase buffer [20 mmol/L MOPS (pH 7.0), 125 mmol/L MgCl2, 1 mmol/L MnCl2, 1 mmol/L EGTA, 150 mmol/L NaCl, 10 µmol/L ATP, 1 mmol/L DTT, and 5 mmol/L β-glycerophosphate] containing 25 ng recombinant GST-PIM1 kinase were added to each well. The final concentration of each inhibitor was ~10 µmol/L. The plate was placed on a gel slab dryer prewarmed to 30°C, and the kinase reaction was allowed to proceed. The reaction was stopped after 60 min by removal of the reaction buffer, followed by the addition of 100 µL of HEPES buffer containing 20 mmol/L EDTA to each well. Phosphorylated GST-BAD was detected by an ELISA reaction, using as first antibody a monoclonal anti-phospho-BAD(S112) antibody (Cell Signaling, Danvers, MA), a secondary goat anti-mouse IgG-peroxidase conjugated antibody (Pierce, Rockford, IL), and Turbo-TMB peroxidase substrate (Pierce). The level of phosphorylated GST-BAD present was proportional to the absorbance at 450 nm.

For quantitative and kinetic studies of inhibitors against various BAD(S112) kinases, a solution phase assay was used. A biotinylated peptide based on the PIM1 phosphorylation site of human BAD was synthesized (GGAGA-VEIRSRHSSYPAGTE) and used as the assay substrate. Recombinant GST-PIM1 (25 ng/reaction) was preincubated with various concentrations of inhibitors in the previous kinase buffer (final volume 100 μL). The reaction proceeded by addition of substrate peptide, followed by incubation for 5 min in a 30 °C water bath. The reaction was terminated by transferring the mixture to a streptavidin-coated 96-well

plate (Pierce) containing $100~\mu\text{L/well}$ of 40~mmol/L EDTA. The biotinylated peptide substrate was allowed to bind to the plate at room temperature for 10~min. The level of phosphorylation was then determined by ELISA as described above. Curve fitting and enzyme analyses were done using GraphPad Prism version 4.00~for Windows (GraphPad Software, San Diego, CA). For the additional BAD(S112) kinases [PIM2, RSK2 (ribosomal S6 kinase 2), and PKA (cyclic AMP-dependent protein kinase)], reaction components were as described above. As with the PIM1 assays, an ATP concentration of $10~\text{\mu mol/L}$ was used. Furthermore, with each kinase, linear reaction velocities for the duration of the reaction were confirmed (data not shown).

To further assess the specificity of quercetagetin as a PIM1 inhibitor, its activity against a panel of serine-threonine kinases was also studied through a commercial kinase inhibitor profiling service (Kinase Profiler; Upstate Biotechnology, Charlottesville, VA). All Kinase Profiler assays were conducted using 10 µmol/L ATP concentrations.

Small-Molecule Library Screening

We obtained a library of 1,200 compounds that had structural affinity to known kinase inhibitors (TimTec, Inc., Newark, DE). The entire library was screened once with our solid-phase EUSA kinase assay, with each compound at ~10 μmol/L concentration. Positive hits were rescreened at the same concentration. Compounds that had reproducible activity at 10 μmol/L were then screened at a range of concentrations from 0.001 to 300 μmol/L. Additional flavonoids were purchased from Indofine Chemicals (Hillsborough, NJ) and were tested in a similar protocol.

Measurement of PIM1 Kinase Activity in Cells

RWPE2 cell pools, stably infected with empty retrovirus or pin-1-encoding retrovirus, were seeded in six-well plates at 5×10^5 cells per well. After 18 h, the normal supplemented keratinocyte medium was removed and replaced with supplement-free keratinocyte medium. Cells were then incubated for an additional 20 h. Quercetagetin, or an equivalent volume of DMSO, was added to the cells 3 h before the end of the starvation period. At the conclusion of the starvation period, the cells were washed twice with PBS and subsequently lysed in a denaturing buffer with protease, phosphatase inhibitors. The lysates were normalized by total protein content (BCA protein assay, Pierce), then analyzed by immunoblotting with the following antibodies: monoclonal anti-PIM1 (Santa Cruz Biotechnologies, Santa Cruz, CA); monoclonal anti-B-actin (Sigma, St. Louis, MO); monoclonal anti-BAD (Transduction Laboratories, Franklin Lakes, NJ); and monoclonal anti-phospho-BAD(S112), polyclonal anti-phospho-AKT(S473), and anti-AKT (all from Cell Signaling).

Cloning, Expression, Purification, and Crystallization

The production, purification, and characterization of recombinant 6His-tagged PIM1 proteins for crystallography have been described previously (13). To obtain cocrystals of complexes of the protein with ligands, the protein solution was initially mixed with the compound (dissolved

Mol Cancer Ther 2007;6(1). January 2007

in DMSO) at a final compound concentration of 1 mmol/L and then set up for crystallization. The protein was crystallized by a sitting-drop, vapor-diffusion experiment in which equal volumes of protein (10-15 mg/mL concentration) and reservoir solution [0.4-0.9 mol/L sodium acetate, 0.1 mol/L imidazole (pH 6.5)] were mixed and allowed to equilibrate against the reservoir at 4°C. The crystals routinely grew to a size of 200 × 200 × 800 μm in ~2 to 3 days.

Structure Determination

X-ray diffraction data were collected at Advanced Light Source (Berkeley, CA). All data were processed and reduced with MOSFLM and scaled with SCALA of the CCP4 suite of programs using the software ELVES. The space group of all crystals was determined to be P65, with the cell axes being approximately 99, 99, and 80, and one protein monomer being present in the asymmetrical unit. All structures were determined by molecular replacement using the apo PIM1 structure (1YWV; ref. 13) as a model, and refined by CNX and REFMAC5. Crystallographic statistics are reported in Supplementary Table S1.5 The coordinates and structure factors for the structures have been deposited with the RCSB Protein Data Bank (accession codes 2063, 2064, 2065).

Results

Screening of a Chemical Library with Structural Affinity to Known Kinase Inhibitors

As an initial approach to the identification of PIM1 inhibitors, we screened a library of small molecules whose structures were similar to those of known kinase inhibitors. Of the seven compounds that had reproducible inhibitory activity at 10 µmol/L, six were flavonoids [quercetin, luteolin, kaempferol, 7-hydroxyflavone, (S)-5,7-dihydroxy-8-(3-methylbut-2-ene)flavanone, and (R)-5,7-dihydroxyflavanone]. These compounds exhibited a range of inhibitory potencies (as IC₅₀) from 1.1 to 60 μmol/L. Thirty-seven other flavonoids failed to show detectable inhibitory activity at 10 µmol/L. These inactive compounds were characterized in most cases by bulky (charged or uncharged) groups at the 3, 3', 4', or 7 positions; lack of at least two hydrogen bond donors on the A or C rings; presence of glycoside linkages; or failure of all rings to adopt a planar conformation.

The most active compound in the chemical library was the flavonol quercetin (IC₅₀, 1.1 μmol/L), a known inhibitor of kinases and many other enzymes (14-19). Furthermore, six of the seven compounds with reproducible activity at 10 μmol/L were flavonoids. Hence, we screened additional flavonoids to identify molecules with inhibitory activity against the PIM1 kinase (Fig. 1). The most active molecule was the flavonol quercetagetin (IC₅₀, 0.34 μ mol/L). The four flavonoids with the highest inhibitory activity were characterized by the presence of five to six -OH groups

distributed between the A and B rings. In comparison, the hydroxyl groups on the B ring seemed to be more critical for the activity of the compounds than those on the A ring, as compounds with an unsubstituted B ring showed greatly reduced activity. Finally, a hydrophobic substituent at the 8 position was tolerated.

Quercetagetin Is a Selective, Potent Inhibitor of PIM1 In vitro

To assess the selectivity of quercetagetin for PIM1, we determined its IC₅₀ value toward the alternative BAD(S112) kinases RSK2, PKA, and PIM2 (Table 1). The IC50 of quercetagetin for PIM1 kinase was 0.34 µmol/L, whereas the corresponding values for the other kinases were 9- to 70-fold higher.

To further characterize the specificity of quercetagetin, its inhibitory activity was examined at 1 or 10 µmol/L against additional serine-threonine kinases (c-Jun-NH2-kinase 1, PKA, Aurora-A, c-RAF, and PKCθ; Fig. 2). At the lower concentration, the selectivity of quercetagetin was most apparent. In the presence of 1 µmol/L inhibitor, PIM1 activity was inhibited by 92%. In contrast, the activity of the other kinases was inhibited by only 0% to 41%. In aggregate, these studies established that quercetagetin was a severalfold more potent inhibitor for pin-1 kinase than for seven other serine-threonine kinases. In addition, quercetagetin was completely inactive against the c-abl tyrosine kinase when tested at the 200 μmol/L concentration (data not shown).

Crystallographic Analysis of Quercetagetin in Complex with PIM1

Recently, several crystal structures of the PIM1 kinase have been solved and presented, including apo forms and the enzyme in complex with a variety of ligands (7, 9, 13, 20, 21). Because the PIM1 protein has several unique structural features around its ATP-binding pocket, including the lack of the canonical hydrogen bond donor from the hinge region typically used by kinases to bind ATP-like ligands, we determined the crystal structure for the kinase in complex with three flavonoid inhibitors: quercetagetin, myricetin, and 5,7,3',4',5'-pentahydroxyflavone (Fig. 3).

The three flavonoid inhibitors show two distinct binding poses, denoted here as orientations I and II, respectively. Quercetagetin, the compound with two hydroxyl groups on the Bring, adopts orientation I, whereas the compounds with a trisubstituted B ring (myricetin and 5,7,3',4',5'pentahydroxyflavone) adopt orientation II.

The binding pose of quercetagetin in PIM1 (Fig. 3A) closely resembles that of quercetin in phosphatidylinositol 3-kinase y (1E8W; ref. 22) and that of fisetin in CDK6 (1XO2; ref. 23), designated here as orientation I. As seen in the two earlier structures (Fig. 3D and E), the 3-OH of the quercetagetin (Fig. 3A) makes a canonical hydrogen bond with backbone carbonyl oxygen of the hinge residue Glu¹²¹. In addition, the B ring of quercetagetin binds deep inside the PIM1 ATP-binding pocket, with the 4'-hydroxyl group hydrogen-bonded to the side chains of two highly conserved residues, Lys67 and Glu89. However, significant differences were also observed between the current

Supplementary data for this article are available at Molecular Cancer Therapeutics Online (http://mctaacrjournals.org/).

166 PIM1 Inhibitor

structure and the two reported structures. In both 1E8W and 1XO2, the 4-keto group of the chromenone core of the compound formed a hydrogen bond with the same hinge amide nitrogen [Val⁸⁸² in phosphatidylinositol 3-kinase γ (Fig. 3D) and Val¹⁰¹ in CDK6 (Fig. 3E)]. However, there is no direct interaction between the 4-keto group of quercetagetin and the amide nitrogen of the corresponding residue Pro^{123} in PIM1 because proline is incapable of acting as a hydrogen bond donor. Instead, the 4-keto group of quercetagetin makes close contact with the backbone $C\alpha$ of Arg^{122} (3.4 Å). It is not clear whether this interaction makes a positive contribution to the binding of quercetagetin to PIM1.

The B ring of quercetagetin binds deep inside the PIM1 ATP-binding pocket. The 4'-hydroxyl group forms hydrogen bonds with both Lys⁶⁷ and Glu⁸⁹, two of the most conserved residues in kinases. As has been noted, satisfying the hydrogen bonding requirements at this region is one of the determining features of binding of compounds to PIM1 (13).

When compared with quercetagetin, the chromenone core of myricetin (Fig. 3B) and 5,7,3',4',5'-pentahydroxy favone (Fig. 3C) has flipped 180° in PIM1 such that the B ring is now oriented toward the entrance of the ATP pocket. A possible explanation for adopting this orientation is that the interior of the ATP pocket cannot accommodate the B ring with three hydroxyl substitutions. Although they bind in the same orientation, there are important differences between the binding poses of the two compounds, which can be attributed to the presence or absence of the 3hydroxyl group. The 3-hydroxyl group in myricetin still makes a hydrogen bond with the carbonyl oxygen of Glu121, despite the difference in binding orientation. Because of the adjacent 4-keto group, the 3-hydroxyl is likely to be most acidic of all the hydroxyl groups in the compound, and, as a result, it dictates the overall positioning of the compound. Another interaction that may contribute to the observed binding pose is a hydrogen bond between the 3'-hydroxyl group of myricetin and the carbonyl oxygen of Pro123 (Fig. 3B). The importance of the 3-hydroxyl group is evident. The second compound, 5,7,3',4',5'-pentahydroxyflavone, lacking such a group, makes no direct interaction with the hinge region.

Quercetagetin Inhibits PIMI Kinase Activity in Intact Cells

To determine if quercetagetin could act as a cellpermeable PIM1 inhibitor, we examined the activity of the flavonol in RWPE2 prostate cancer cells. We studied the phosphorylation of endogenous BAD on Ser¹¹², under conditions of growth factor starvation, as an indicator of intracellular PIM1 activity (Fig. 4).

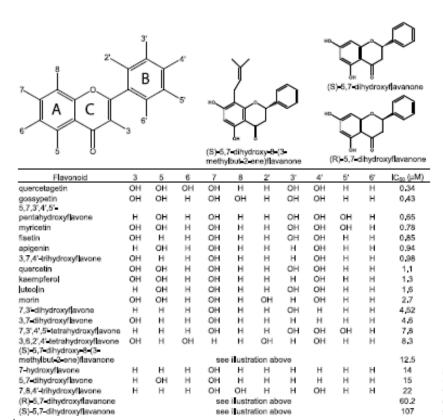


Figure 1. Identification of flavonoids with PIMI inhibitory activity. Structures of all studied flavonoids with detectable PIMI inhibitory activity, given with their IC₅₀ values.

Mol Cancer Ther 2007;6(1). January 2007

Table 1. Quercetagetin is a selective inhibitor of the PIM1 kinase over other BAD(\$112) kinases

Kinase	KC_{50} ($\mu mol/L$)	${\rm Log~IC_{50}~(\mu mol/L)}$	SE of log IC $_{50}$	R^2
PIM1	0.34	-0.46	0.12	0.98
PIM2	3.45	0.55	0.22	0.94
PKA	21.2	1.33	0.23	0.94
RSK2	2.82	0.45	0.09	0.99

NOTE All data were derived from nonlinear regression analyses using a three-parameter logistic that assumes a Hill coefficient of -1.

RWPE2 cells infected with a neo-expressing retrovirus showed little phospho-BAD(S112) when cultured overnight in basal serum-free medium. However, cells with enforced expression of PIM1 kinase had a 4-fold higher amount of phospho-BAD, reflecting the ability of the PIM1 protein to phosphorylate the endogenous BAD protein. When pim-1 expressing cells were treated with quercetagetin, phospho-BAD(S112) levels were markedly reduced in proportion to the concentration of the inhibitor. Half-maximal inhibition occurred at 5.5 µmol/L extracellular concentration. Quercetagetin did not inhibit the activity of the AKT kinase under these conditions, as indicated by persistent phos-phorylation of AKT on Ser⁴⁷³. These data indicate that quercetagetin was able to selectively block the ability of PIM1 to phosphorylate BAD in intact cells.

Quercet agetin Treatment Reproduces a Known pim-1 Knockdown Phenotype

If quercetagetin acts as a true PIM1 inhibitor, then it should reproduce a pim-1-dependent phenotype in the target cells. We have shown that PIM1 inhibition by genetic means (small interfering RNA) inhibits the proliferation of RWPE1 and RWPE2 cells (Supplementary Fig. S1).5 We therefore determined if quercetagetin could reproduce this phenotype. RWPE2 cells were treated with quercetagetin for up to 72 h (Fig. 5A). Marked dose-dependent growth inhibition was apparent by 24 h, leading to persistent growth arrest thereafter. Quercetagetin reproduced this pim-1 – dependent phenotype at a drug concentration that inhibited the enzyme in cells (ED50, 3.8 µmol/L; Fig. 5B). Similar results were seen in RWPE1 cells (data not shown). Apoptotic cells, showing cytoplasmic blebbing and detachment, were rare, but dividing cells virtually disappeared in cultures treated with quercetagetin at 6.25 µmol/L or higher concentrations (data not shown). DNA histograms obtained at 24 h after the addition of quercetagetin (6.25 µmol/L) or DMSO vehicle were very similar (Fig. 5C). Neither showed a <2n population suggestive of apoptosis. There was a slight increase in the proportion of cycling cells (S + G2-M) in the drug-treated samples.

A PIM1 inhibitor would be predicted to inhibit the growth of cells that express the molecular target, more than cells with little or no pim-1 expression. We examined the effects of quercetagetin on the growth of prostate cell lines that express a spectrum of PIM1 levels. RWPE2 cells expressed the highest amount of PIM1 protein; PC3 had an intermediate level; and LNCaP cells showed the lowest

amount of kinase protein (Fig. 6A). Treatment of the cells with various concentrations of quercetagetin for 72 h resulted in inhibition of cell growth (Fig. 6B). At all concentrations, RWPE2 cells were inhibited the most, being significantly more sensitive to quercetagetin growth inhibition than the other prostate cancer cell lines. PC3 cells showed intermediate growth suppression and were also significantly more sensitive than were LNCaP cells at quercetagetin concentrations of ≤12.5 µmol/L. Thus, the ability of the flavonol to inhibit proliferation was proportional to the amount of PIM1 protein in the target cells, particularly at lower drug concentrations. Although other interpretations are possible, these data support our observation that quercetagetin can act as a PIM1 inhibitor.

Discussion

The development of clinically useful small-molecule kinase inhibitors has been a seminal event in the world of oncology. Flavonoids were among the early scaffold structures identified as potential kinase inhibitors. However, although many flavones, isoflavones, and flavonols have been shown to regulate the activity of kinases in cell-based assays, fewer data exist to show that these molecules can directly bind and inhibit kinase targets both in vitro and in cells. It is clear that some flavonoids are ATP-competitive ligands for both tyrosine and serine-threonine kinases, as well as other ATP-binding enzymes. The flavonol quercetin is one such ligand, and its ability to directly bind to ATP-binding enzymes has been well shown. At low-micromolar concentrations, it directly binds and inhibits such diverse enzymes as the phosphatidylinositol 3-kinase (14), the epidermal growth factor receptor tyrosine kinase (15), retroviral reverse transcriptases (16), DNA gyrases (17), phosphodiesterases (18), and thioredoxin reductase (19). Other direct flavonoid inhibitors have been described for RSK2 kinase (24), mitogen-activated protein/extracellular signalregulated kinase 1 (25), and several cyclin-dependent kinases (23, 26-28). One such ligand, flavopiridol, has already entered clinical trials for the treatment of cancer. Others, such as PD98059, are familiar laboratory reagents for inhibition of kinase pathways. We now show, by means of crystallography, that quercetagetin is a direct ligand for the ATP-binding pocket of PIM1 kinase (Fig. 3).

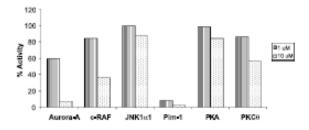


Figure 2. Quercetagetin is a selective inhibitor of PIM1 kinase. Inhibitor activity of quercetagetin at 1 and 10 µmol/L final concentration against a spectrum of serine-threonine kinases of a panel of kinases, assessed by KinaseProfiler assay. The activity in the presence of vehicle only was taken to be 100% activity. Columns, mean of duplicate determinations.

Mol Cancer Ther 2007;6(1), January 2007

168 PIM1 Inhibitor

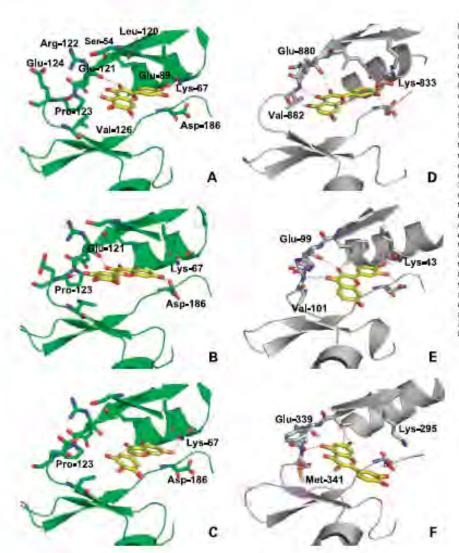


Figure 3. X-ray crystal structures of flavonoids bound to the ATPbinding sites of PIM1 and companson with structures of flavonoids in complex with other kinases. Of the three compounds coprystallized with PIM1, quercetagetin (A) orients the B ring inside the pocket (orientation i), whereas both myricetin (B) and 5,7,3',4',5' pentahydroxy flavone (C) fip the B ring out toward solvent (orientation ii). Both binding orientations have been observed in the crystal structures of flavonoids bound to other kinases. 1E8W (D, quercetn in complex with phosphatidylinostol 3 kinase y) and 1X02 (E, fisetin in complex with CDK6) represent orientation i, whereas 2HCK (F, quercetin n complex with HCK) exemplifies orientation II. All pictures show residues that form hydrogen bond with the inhibitors (Lys⁶⁷, Glu⁶⁸, Glu¹²¹, and Asp¹⁸⁶). In the PM1 structures, the three residues near the ATPbinding site that differentiate PIM1 from PIM2 (Ser⁵⁴, Glu ¹²⁴, and Val¹²⁶) are also shown. The inhibitors are colored by atom type: rad, oxygen atoma; yellow, carbon atoms. Dashed purple lines, hydrogen

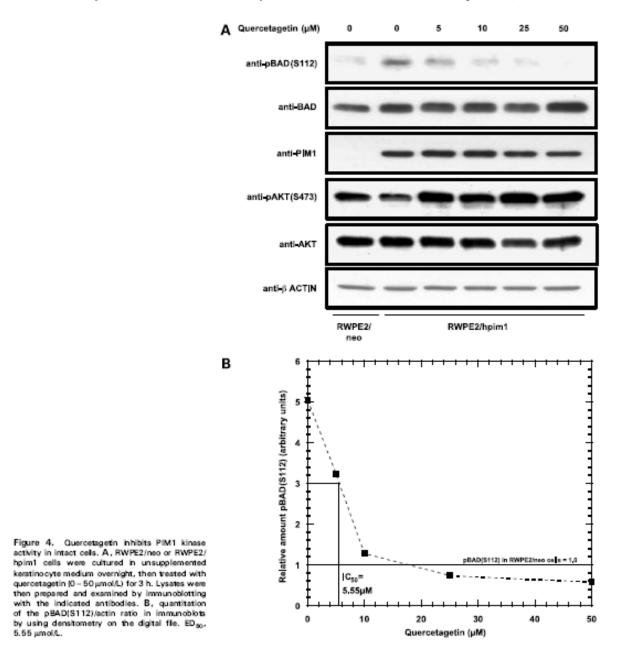
Specificity is always a concern with ATP pocket ligands. There are probably no absolutely selective inhibitors for a kinase but rather ligands that show a spectrum of affinities for their various targets. We have shown that quercetagetin is severalfold more active against PIM1 than against eight other serine-threonine kinases and a tyrosine kinase, either with in vitro assays or in cell cultures. Interestingly, quercetagetin showed 10-fold more selectivity for PIM1 than for the homologous PIM2 kinase (sequence identity 56%). The ATP-binding pockets of these two kinases are identical with the exception of three residues along the edge of the PIM1 ATP-binding pocket—Ser⁵⁴ (Ala⁵⁶ in PIM2), Glu¹²⁶ (Leu¹²⁰ in PIM2), and Val¹²⁶ (Ala¹²² in PIM2). Val¹²⁶ of PIM1 makes direct van der Waal's contact with the A ring of quercetagetin (Fig. 3A). Loss of such a contact due

to the Val-to-Ala substitution is likely a contributing factor to the reduced activity of the compound in PIM2. The other residues are located close to the hinge Arg¹²² (Arg¹¹⁸ in PIM2). The polar side chains of Ser⁵⁴ and Glu¹³⁴ can form hydrogen bonds with Arg¹²², thus affecting its conformation. Substitutions of these residues to hydrophobic amino acids in PIM2 will change the local environment (Fig. 3A).

The only large-scale examination of the specificity of flavonoid kinase inhibitors was reported recently by Fabian et al. (8). This investigation used a competitive binding assay to predict the inhibitor potency and specificity of the test agents. Flavopiridol was tested for binding affinity to 119 kinases. Twenty-three kinases bound flavopiridol under the test conditions, with binding constants ranging from 0.019 to 6.6 µmol/L. Interestingly, the tested cyclin-dependent

Mol Cancer Ther 2007;6(1). January 2007

kinases bound flavopiridol less well than did cakium/ calmodulin-dependent protein kinase kinase I. These data suggest that cyclin-dependent kinases may not be the only kinases inhibited in cells by flavopiridol. Both PIM1 and PIM2 were among the bound kinases, with binding constants of 0.52 and 0.65 µmol/L, respectively. Although there is no absolute correlation between binding constants and enzymatic activity, flavopiridol could conceivably inhibit the activity of both PIM1 and PIM2 in test systems. Because quercetagetin has not been tested against a large number of other kinases, we cannot predict what other enzymes would be perturbed by this flavonoid. It is likely, however, that its spectrum of selectivity will be substantially different from that of flavopiridol. Quercetagetin showed clear preference for inhibiting PIM1 over PIM2, whereas flavopiridol did not. Furthermore quercetagetin inhibited the activity of the Aurora-A kinase (IC₅₀, ~4 μmol/L), a kinase that did not bind flavopiridol (8). The substantial



Mol Cancer Ther 2007;6(1), January 2007

170 PIM1 Inhibitor

homology between Aurora-A kinase and PIM1 kinase likely contributed to the low-level inhibitory activity of quercetagetin for the former; Aurora-A and PIM1 are 29% identical over their entire kinase domains; and the ATP binding pockets have 68% conserved amino acids.

An earlier, smaller-scale study looked at the effect of the flavonol quercetin on the *in vitro* kinase activity of 25 kinases, none of which were *pim* family kinases (29). At the tested concentration (20 µmol/L), quercetin inhibited the enzymatic activity of eight of the kinases. The propensity of this flavonol to form aggregates in aqueous solution has been advanced as an explanation for its widespread enzyme-inhibitory activity *in vitro* (30). We have not detected quercetagetin aggregates at concentrations of <10 µmol/L in aqueous solution, using a light-scattering assay (data not shown). Thus, we feel that this artifact does not account for the ability of this flavonol to inhibit PIM1 at nanomolar concentrations.

Because of the potential ambiguities that may accompany the use of small-molecule kinase inhibitors, a series of standards have been proposed for their use (29). To validate the results, it is desirable to show that the effects of an inhibitor disappear when a drug-resistant mutant of the protein kinase is overexpressed. Although convincing, this standard often fails due to the lack of an identified mutant with the desired properties. No such mutant has been identified for any of the pim kinases. Another potential standard is to show that the cellular effect of the drug occurs at the same concentrations that prevents the phosphorylation of an authentic physiologic substrate of the protein kinase. We have seen in these studies that halfmaximal growth inhibition of prostate cancer cells occurred at a drug concentration (3.8 µmol/L) that approximated the IC₅₀ for PIM1 enzyme inhibition in cells (5.5 μmol/L). Furthermore, the selectivity for prostate cancer growth inhibition, in proportion to endogenous PIM1 levels, was greatest at 6.25 µmol/L. Higher concentrations suppressed growth more, but the relationship to endogenous PIM1 levels was obscured. These data suggest that, at relatively low concentrations (perhaps 5-10 µmol/L), the growthinhibitory effects of quercetagetin likely involve PIM1 antagonism. A third standard is to observe the same effect with at least two structurally unrelated inhibitors of the protein kinase. Previously described inhibitors of pim

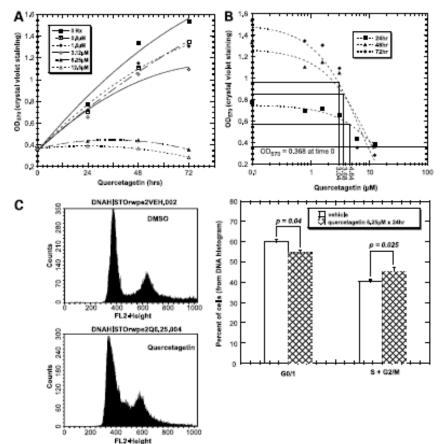


Figure 5. Quercetagetin inhibits growth of prostate cancer cells at concentrations that inhibit PIM1 kinase activity. A, growth curve of RWPE2 cells with different concentrations of quercetagetin. Cell number is measured by crystal violet staining. Points, mean of triplicate determinations from one of four similar experiments. B, calculation of EDso at 24, 48, and 72 h of drug exposure. Average ED₅₀ from all curves is 3.8 µmol/L. C, DNA histograms from RWPE2 cells treated with vehicle or quercetagetin 6.25 μmol/L × 24 h. Proportion of cells in G₀-1 or S + G₂-M fractions. Columns, mean of triplicate determinations from three independent experiments: bars, SD. P values show the probability of no difference by t test.

Mol Cancer Ther 2007;6(1). January 2007

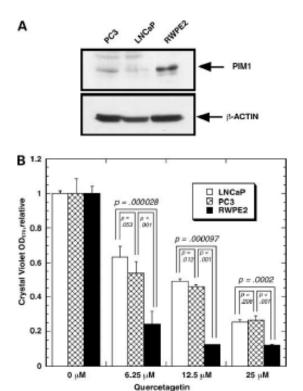


Figure 6. Quercetagetin inhibits the growth of prostate cancer cells in proportion to their content of PIM1. A, measurement of intracellular PIM1 in PC3, LNCaP, and RWPE2 prostate cancer cells by immunoblotting. B, growth inhibition by treatment of prostate cancer cells with guercetagetin for 72 h. Columns, mean of triplicate determinations from one of two similar experiments; bars, SD. P values were calculated by t tests and represent the probability that there is no difference between the two compared populations.

kinases are either less active or less specific flavonoids (7, 9), the same structural class as quercetagetin, or staurosporine analogues (8, 9, 21). We therefore used small interfering RNA as a genetic means to identify a pim-1dependent phenotype. Proliferation of prostate cells was suppressed with both the genetic and chemical inhibitors of PIM1 activity. These data show that quercetagetin is an authentic small-molecule inhibitor of PIM1 kinase.

The crystal structures of PIM1 complexed with quercetagetin, myricetin, and 5,7,3',4',5'-pentahydroxyflavonone show that flavonoids bind to PIM1 in two distinct orientations. Although interesting, this is not a surprising observation, as flavones have shown a variety of binding modes in kinases (9, 22, 23, 26-28). An examination of the intermolecular interactions of each flavonoid with PIM1 does not clearly reveal why one orientation was adopted over the other. However, it is possible that the presence of three hydroxyl groups on the B ring of myricetin and 5,7,3',4,5'-pentahydroxyflavone discourages these two flavonoids from adopting the binding orientation observed for quercetagetin. The hydrophobic side chain of Leu¹²⁰, which extends into the ATP pocket in the same region occupied by the B ring of quercetagetin (Fig. 3A), may be incompatible with the 5' hydroxyl group of myricetin and 5,7,3',4',5'-pentahydroxyflavone.

Both pim-1 and pim-2 can phosphorylate 4EBP-1, a regulator of protein translation (31, 32). Rapamycin was unable to block this effect. These data suggest that pim kinases may function in a parallel pathway to the phosphatidylinositol 3-kinase/AKT/mammalian target of rapamycin cascade to regulate and support protein synthesis under stress conditions. Because AKT-1 and PIM2 function cooperatively to induce lymphoma formation in transgenic mice (6), it may be necessary to target both pathways for effective antitumor effects. Several prototype AKT inhibitors have been described (33, 34). Our identification of quercetagetin as a PIM1 inhibitor provides a tool for tissue culture studies to investigate this hypothesis. Under the tested conditions, we found no evidence that quercetagetin inhibited the phosphorylation of AKT on Ser 473. Thus, it may be possible to combine inhibitors of these kinases to detect additive or synergistic effects resulting from the blockade of the two kinase pathways.

- 1. Wang Z, Ehattacharya N, Weaver M, et al. PIM1: a serine/threonine kinase with a role in cell survival, proliferation, differentiation, and tumorigenesis. J Vet Sci 2001;2:167 – 79.
- 2. Qian KC, Wang L, Hickey ER, et al. Structural basis of constitutive activity and a unique nucleotide binding mode of human PIM1 kinase. J Biol Chem 2005;280:6130 - 7.
- 3. Lilly M, Kraft A. Enforced expression of the Mr 33,000 PIM1 kinase enhances factor-independent survival and inhibits apoptosis in murine myeloid cells. Cancer Res 1997;57:5348-55.
- Pircher TJ, Zhao S, Geiger JN, Joneja B, Wojchowski DM. PIM1 kinase protects hematopoletic FDC cells from genotoxin-induced death. Oncogene 2000; 19:3684 - 92.
- Lilly M, Sandholm J, Cooper JJ, Koskinen PJ, Kraft A. The PIM1 serine kinese prolongs survival and inhibits apoptosis- related mitochondrial dysfunction in part through a bcl-2-dependent pathway. Oncogene 1999; 18:4022 - 31.
- 6. Hammerman PS, Fox CJ, Birnbaum MJ, Thompson CB. Pim and Akt oncogenes are independent regulators of hematopoletic cell growth and survival. Blood 2005;105:4477 - 83.
- 7. Jacobs MD, Black J, Futer O, et al. PIM1 ligand-bound structures reveal the mechanism of serine/threonine kinase inhibition by LY 294002. J Biol Chem 2005;280:13728-34.
- 8. Fabian MA, Biggs WH III, Treiber DK, et al. A small molecule-kinase interaction map for clinical kinase inhibitors. Nat Biotechnol 2005;23: 329-36
- 9. Bullock AN, Debreczeni JE, Fedorov CY, Nelson A, Marsden BD, Knapp S. Structural basis of inhibitor specificity of the human protooncogene provital insertion site in Moloney murine leukemia virus (PIM1) kinase. J Med Chem 2005;48:7604-14.
- 10. Kueng W, Silber E, Eppenberger U. Quantification of cells cultured on 96-well plates. Anal Biochem 1989;182:16-9.
- 11. Yan B, Zemskova M, Holder S, et al. The PIM-2 kinase phosphorylates BAD on serine 112 and reverses BAD-induced cell death. J Biol Chem 2003:278:45358 - 67.
- 12. Aho TL, Sandholm J, Peltola KJ, Mankonen HP, Lilly M, Koskinen PJ. PIM1 kinase promotes inactivation of the pro-apoptotic Bad protein by phosphorylating it on the Ser¹¹² gatekeeper site. FEBS Lett 2004;571:

Mol Cancer Ther 2007;6(1), January 2007

172 PIM1 Inhibitor

- Kumar A, Mandiyan V, Suzuki Y, et al. Crystal structures of protooncogene kinase PIM1: a target of aberrant somatic hypermutations in diffuse large cell lymphoma. J Mol Biol 2005;348:183 – 93.
- Mayr GW, Windhorst S, Hillemeier K. Antiproliferative plant and synthetic polyphenolics are specific inhibitors of vertebrate inositol-1,4,5trisphosphate 3-kinases and inositol polyphosphate multikinase. J Biol Chem 2006;280:13229 – 40.
- Lee LT, Huang YT, Hwang JJ, et al. Blockade of the epidermal growth factor receptor tyrosine kinase activity by quercetin and luteolin leads to growth inhibition and apoptosis of pancreatic tumor cells. Anticancer Res 2002;22:1615 – 27.
- Chu SC, Hsieh YS, Lin JY. Inhibitory effects of flavonoids on Moloney murine leukemia virus reverse transcriptase activity. J Nat Prod 1992;55: 179–83.
- Plaper A, Golob M, Hather I, Oblak M, Solmajer T, Jerala R. Characterization of quercetin binding site on DNA gyrase. Biochem Biophys Res Commun 2003;308:530 – 6.
- Ko WC, Shih CM, Lai YH, Chen JH, Huang HL. Inhibitory effects of flavonoids on phosphodiesterase isozymes from guinea pig and their structure-activity relationships. Biochem Pharmacol. 2004;68:2087 – 94.
- Lu J, Papp LV, Fang J, Rodriguez-Nieto S, Zhivotovsky B, Holmgren A. Inhibition of mammalian thioredoxin reductase by some flavonoids: implications for myricetin and quercetin anticancer activity. Cancer Res 2006;98:4410 – 8.
- Bullock AN, Debreczeni J, Amos AL, Knapp S, Turk BE. Structure and substrate specificity of the PIM1 kinase. J Biol Chem. 2005;280:41675 – 82.
- Debreczeni JE, Bullock AN, Atilla GE, et al. Ruthenium half-sandwich complexes bound to protein kinase pim-1. Angew Chem Int Ed Engl 2006; 45: 1580 – 5.
- Walker EH, Pacold ME, Perisic O, et al. Structural determinants of phosphoinositide 3-kinase inhibition by wortmannin, LY294002, quercetin, myricetin, and staurosporine. Mol Cell 2000;6:909-19.
- Lu H, Chang DJ, Baratte B, Meijer L, Schulze-Gahmen U. Crystal structure of a human cyclin-dependent kinase 6 complex with a flavonol inhibitor, fisetin. J Med Chem 2005;48:737 –43.

- Clark DE, Errington TM, Smith JA, Frierson HF, Jr., Weber MJ, Lannigan DA. The sering-threonine protein kinase, p90 ribosomal S6 kinase, is an important regulator of prostate cancer cell proliferation. Cancer Res 2005;85:3108 – 16.
- Alessi DR, Cuenda A, Cohen P, Dudley DT, Saltiel AR. PD 098059 is a specific inhibitor of the activation of mitogenectivated protein kinase kinase in vitro and in vivo. J Biol Chem. 1995;270:27489 – 94.
- De AW, Jr., Mueller Dieckmann HJ, Schulze-Gahmen U, Worland PJ, Sausville E, Kim SH. Structural basis for specificity and potency of a flavonoid inhibitor of human CDK2, a cell cycle kinase. Proc Natl Acad Sci U S A 1996;93:2735 – 40.
- Sicheri F, Moarefi I, Kuriyan J. Crystal structure of the Src family tyrosine kinase Hok. Nature 1997;385:602-9.
- De Azevedo WF, Jr., Mueller-Dieckmann HJ, Schulze-Gahmen U, Worland PJ, Sausville E, Kim SH. Structural basis for specificity and potency of a flavonoid inhibitor of human CDK2, a cell cycle kinase. Proc Natl Acad Sci U S A 1996;93:2735 – 40.
- Davies SP, Reddy H, Calvano M, Cohen P. Specificity and mechanism of action of some commonly used protein kinese inhibitors. Biochem J 2000:351:95 – 105.
- McGovern SL, Shokhet BK. Kinase inhibitors: not just for kinases anymore. J Med Chem 2003:48:1478-83.
- Fox CJ, Hammerman PS, Thompson CB. The Pim kinases control rapamycin-resistant T cell survival and activation. J Exp Med 2005;201: 259-86.
- Chen WW, Chan DC, Donald C, Lilly MB, Kraft AS. Pim family kinases enhance tumor growth of prostate cancer cells. Mol Cancer Res 2005;3: 443-51.
- Yang L, Dan HC, Sun M, et al. Akt/protein kinase B signaling inhibitor 2, a selective small molecule inhibitor of Akt signaling with antitumor activity in cancer cells overexpressing Akt. Cancer Res 2004; 64:4394 - 9.
- Barnett SF, Defeo Jones D, Fu S, et al. Identification and characterization of pieck strin-homology-domain-dependent and isoenzyme-specific Akt inhibitors. Biochem J 2005;385:399 – 408.

ARTICLE IN PRESS

Available online at www.sciencedirect.com

ScienceDirect

Biogranic & Medicinal Chemistry xxx (2007) xxx-xxx

Comparative molecular field analysis of flavonoid inhibitors of the PIM-1 kinase

Sheldon Holder, a,b,c Michael Lillya,b,c and Milton L. Brownd,*

*Center for Molecular Biology & Gene Therapy, Loma Linda University School of Medicine, Loma Linda, CA 92354, USA
*Department of Biochemistry and Microbiology, Loma Linda University School of Medicine, Loma Linda, CA 92354, USA
*Department of Medicine, Loma Linda University School of Medicine, Loma Linda, CA 92354, USA
*George town University Medical Center, Department of Oncology, Washington, DC 20057, USA

Received 24 December 2006; revised 23 May 2007; accepted 12 June 2007

Abstract—The PIM-1 protein, the product of the pim-l oncogene, is a serine/threonine kinase. Dysregulation of the PIM-1 kinase has been implicated in the development of human malignancies including lymphomas, leukemias, and prostate cancer. Comparative molecular field analysis (CoMFA) is a 3-D QSAR technique that has been widely used, with notable success, to correlate biological activity with the steric and electrostatic properties of ligands. We have used a set of 15 flavonoid inhibitors of the PIM-1 kinase, aligned de novo by common substructure, to generate a CoMFA model for the purpose of elucidating the steric and electrostatic properties involved in flavonoid binding to the PIM-1 kinase. Partial least squares correlation between observed and predicted inhibitor potency (expressed as $-\log IC_{50}$), using a non-cross-validated partial least squares analysis, generated a non-cross-validated $q^2 = 0.805$ for the training set (n = 15) of flavonoids. The CoMFA generated steric map indicated that the PIM-1-binding site was sterically hindered, leading to more efficient binding of planar molecules over (R) or (S) compounds. The electrostatic map identified that positive charges near the flavonoid atom C8 and negative charges near C4' increased flavonoid binding. The CoMFA model accurately predicted the potency of a test set of flavonoids (n = 6), generating a correlation between observed and predicted potency of $q^2 = 0.825$. CoMFA models generated from additional alignment rules, which were guided by co-crystal structure ligand orientations, did not improve the correlative value of the model. Superimposing the PIM-1 kinase crystal structure onto the CoMFA contours validated the steric and electrostatic maps, elucidating the amino acid residues that potentially contribute to the CoMFA fields. Thus we have generated the first predictive model that may be used for the rational design of small-molecule inhibitors of the PIM-1 kinase.

© 2007 Published by Elsevier Ltd.

1. Introduction

The PIM-1 protein is a serine/threonine kinase¹⁻³ that has been shown to be involved in the regulation of cell survival, differentiation, proliferation, and tumorigenesis (for review, see Refs. 4,5). The pim-1 gene was first identified as a preferential proviral insertion site of Moloney Murine Leukemia Virus in virally induced T-cell lymphomas in mice.⁶ In humans, pim-1 is expressed in normal lymphoid tissues (bone marrow, spleen, thymus, and lymph nodes), testis, and circulating myeloid cells.^{7,8} Although its specific role is not known, the PIM-1 kinase has been shown to be an integral part

of growth factor signaling.⁹⁻¹⁷ Additionally, the PIM-1 kinase is involved in regulating the activity of phosphatases^{18,19} and transcription factors, ^{20,21} and has been shown to phosphorylate heterochromatin protein 1 (HP1), ²² Pim-1 associated protein 1 (PAP-1), ²³ and the nuclear mitotic apparatus protein (NuMA), ²⁴ all nuclear proteins involved in chromatin remodeling. The PIM-1 kinase has also been shown to phosphorylate and inactivate the pro-apoptotic protein BAD. ^{25,26}

While the PIM-1 kinase is involved in numerous signaling events in normal cells, pɨn-I knockout mice only exhibit a minimal phenotype. The near normal phenotype of these mice is attributed to functional compensation by other members of the PIM family of kinases, namely PIM-2 and PIM-3.²⁷ Not surprisingly, hematopoietic cells taken from triple knockout mice devoid of PIM-1. PIM-2, and PIM-3 demonstrated to have an

0968-0896/5 - see front matter © 2007 Published by Elsevier Ltd. doi:10.1016/j.bmc.2007.06.025

Keywords: Pim-1; Comparative molecular field analysis (CoMFA); Flavonoids; Kinase inhibitors.

^{*}Corresponding author. Tel.: +1 202 687 8603; fax: +1 202 687 7659; e-mail: mb544@georgetown.edu

BMC 5803 ARTICLE IN PRESS No. of Pages 11
16 June 2007 Disk used

S. Holder et al. / Bioorg. Med. Chem. xxx (2007) xxx-xxx

impaired response to growth factors.²⁸ While the absence of pin-1 showed minimal adverse effects in mice, over-expression of pim-1 has been shown to have significant effects on cell survival. In vitro studies reveal that enforced expression of pin-1 caused increased cellular proliferation, decreased apoptosis and cell death, increased cell survival,²⁹ and protection from toxin-induced cell death³⁰ in the murine bone marrow FDCP1 cell line. Enforced expression of human pin-1 in FDCP1 cells also resulted in IL-3-independent cell survival,³¹ Furthermore, pin-1 has been shown to cooperate with both c-myc and N-myc in hematopoietic oncogenesis⁸ and significant over-expression of pin-1 has been demonstrated in clinical cases of lymphoma, ^{32,33} leukemia,⁷ and prostate cancer. ^{34,35}

Comparative molecular field analysis (CoMFA) is a three-dimensional quantitative molecular modeling technique used to study relationships between ligand structure (steric and electrostatic properties) and biological activity. The final validated model can be used for the design of novel ligands and to predict the functional activity of those ligands before synthesis.

In addition to its successful use to evaluate the properties of the binding sites of kinase-specific inhibitors, ³⁶⁻³⁸ the CoMFA methodology has shown utility in evaluating the ligand-binding sites of numerous receptors, ³⁹⁻⁵⁴ calcium channels, ⁵⁵ chromosome p450 enzymes, ⁵⁶⁻⁶⁰ human immunodeficiency virus-1 integrase, ⁶¹ and β-tubulin. ⁶² In each case the CoMFA models demonstrated a strong correlation between predicted and experimental ligand activity.

We have constructed CoMFA models, aligned with and without crystal structure guidance, for flavonoid ligands of the PIM-1 kinase using a training set of 15 flavonoid probes for which we have determined the inhibitory potency against the PIM-1 kinase. Here we describe the electrostatic and steric properties of the CoMFA model. We demonstrated its utility as a predictive model of flavonoid potency using a test set of six flavonoids that were not included in the training set. We also validated the model by overlay with a PIM-1 kinase crystal structure to elucidate the amino acid residues that may provide an explanation of the CoMFA contours.

Q2 2. Results

100

110

Simple correlations between PIM-1 kinase inhibition and flavonoid $\log P$ (Fig. 1) or molecule dipole (Fig. 2) resulted in poor correlations. This suggested that other parameters are important for kinase inhibition.

Hence we generated CoMFA models of flavonoid inhibitors of the PIM-1 kinase. The structures and corresponding $-\log IC_{50}$ values for the training set of flavonoids are presented in Table 1. A cross-validated partial least squares analysis determined the optimum number of components for use in non-cross-validated analysis to be 2 (Table 2).

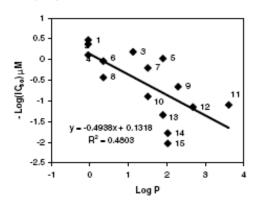


Figure 1. Predictive value of log P versus inhibitor potency for the training set.

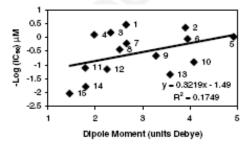


Figure 2. Predictive value of dipole moment versus inhibitor potency for the training set.

Using the alignment rule for model I (Fig. 3), a non-cross-validated partial least squares regression analysis of potency, expressed as $-\log IC_{50}$, and CoMFA descriptors generated a CoMFA model with $q^2=0.805$ for the training set (see Table 1 and Fig. 4a). The CoMFA model provided an improved correlation to flavonoid potency compared with $\log P$ ($R^2=0.4803$) or dipole moment ($R^2=0.1749$) for the same set of data.

120

130

140

We validated the CoMFA model by determining how accurately it could predict the IC₅₀ values of a test set of compounds (flavonoids not included in the training set; Table 3). We compared the CoMFA predicted $-\log IC_{50}$ with the experimental $-\log IC_{50}$ for each flavonoid in the test set. The model showed a strong correlation between predicted $-\log IC_{50}$ and experimental $-\log IC_{50}$ with a correlation coefficient of $R^2=0.829$ (Fig. 4b). These data demonstrated that the CoMFA model could successfully predict the potency of flavonoid inhibitors of the PIM-1 kinase not present in the training set.

The steric and electrostatic contributions to the model were determined to be 0.626 and 0.374, respectively, and are represented graphically in Figure 5. For electrostatic contributions the model predicts that increased binding will result by placing more negative charge near the flavonoid C4′ position and more positive charges near C8. For steric contributions the model predicts that

ARTICLE IN PRESS

S. Holder et al. | Bioorg, Med. Chem. xxx (2007) xxx-xxx

Table 1. Structures and non-cross-validated PLS analysis for the training set using multiple alignments

Compound	R_1	R_2	R_3	R.	R ₅	R ₆	R_7	R_{π}	R ₉	R ₁₀
1 (quercetagetin)	ОН	OH	OH	OH	Н	Н	OH	OH	Н	Н
2 (gossypetin)	OH	OH	н	он	OH	H	OH	он	H	н
3	H	OH	H	он	H	H	OH	OH	он	н
4 (myricetin)	OH	OH	H	он	H	H	OH	ОН	он	н
5 (apigenin)	H	OH	н	он	H	H	H	OH	H	н
6 (quercetin)	OH	OH	H	он	H	H	OH	OH	H	н
7 (luteolin)	H	OH	н	он	н	H	OH	OH	H	н
8 (morin)	OH	OH	н	он	H	OH	H	он	H	н
9	H	H	H	он	H	H	OH	H	H	H
10	H	H	H	он	H	H	OH	ОН	он	н
12	H	H	н	он	H	H	H	H	H	н
13	H	н	н	OH	OH	H	H	OH	н	н

Compound		Model I -log IC ₅₀ (μM)			del II C ₅₀ (μM)	Mod- -logIC	el III 50 (μΜ)	
	Obsd	Pred*	Res	Pred*	Res	Preda	Res	
1	0.47	0.20	0.27	0.28	0.19	0.32	0.15	
2	0.37	0.21	0.16	0.31	0.06	0.34	0.03	
3	0.19	0.23	-0.05	0.29	-0.11	0.02	0.17	
4	0.11	0.28	-0.18	-0.10	0.21	0.005	0.1	
5	0.03	0.09	-0.06	0.19	-0.17	0.21	-0.18	
6	-0.04	-0.25	0.21	-0.29	0.24	-0.39	0.35	
7	-0.20	-0.12	-0.08	-0.16	-0.04	-0.19	-0.01	
8	-0.43	-0.78	0.35	-0.82	0.39	-0.80	0.37	
9	-0.66	-0.98	0.33	-0.91	0.25	-0.88	0.22	
10	-0.89	-0.86	-0.03	-0.84	-0.05	-0.67	-0.23	
11	-1.10	-1.76	0.67	-1.77	0.68	-1.82	0.72	
12	-1.15	-0.98	-0.17	-0.91	-0.23	-0.89	-0.26	
13	-1.34	-0.89	-0.46	-0.89	-0.45	-0.86	-0.48	
14-(R)	-1.78	-1.05	-0.73	-1.03	-0.75	-1.01	-0.77	
15-(S)	-2.03	-1.78	-0.25	-1.81	-0.22	-1.84	-0.19	

Table 2. Cross-validated partial least squares analysis using multiple alignments

Components	Mo	del I	Mod	iel II	Model III		
	s	R ²	s	R ²	s	R^2	
1	0.682	0.303	0.686	0.296	0.711	0.244	
2	0.610	0.487	0.630	0.452	0.654	0.409	
3	0.679	0.416	0.669	0.433	0.696	0.386	
4	0.691	0.450	0.731	0.385	0.728	0.390	
5	0.778	0.374	0.760	0.401	0.787	0.358	
6	0.861	0.318	0.819	0.382	0.864	0.312	

s, standard error for the estimate of $-\log IC_{50}$; R^2 , correlation coefficient. Optimum number of components for model I is $2(R^2 = 0.487)$, model II is 2 $(R^2 = 0.452)$, model III is $2(R^2 = 0.409)$.

adding bulk near the C3' and C6' positions will improve binding.

We examined the interactions of the most potent PIM-1 antagonist, quercetagetin (IC₅₀ = $0.34 \mu M$), and those of the least potent flavonoid, compound 15 (IC₅₀ =

107 µM), with the steric and electrostatic contours of the model. The model elucidates at least one reason for the dramatic differences in potency between these two flavonoid compounds. As illustrated in Figure 6, quercetagetin lies almost completely flat within the contours. In this position the C3' and C4' hydroxyl groups on the

Please cite this article in press as: Holder, S. et al., Bisong. Med. Chem. (2007), doi:10.1016/j.bmc.2007.06.025

150

Obsd, observed value; pred, predicted value; res, residual.

*Generated from CoMFA non-cross-validated run (see Section 4). R² = 0.805 (model II), 0.800 (model III), 0.781 (model III).

4		S. Holder et al. J. Bisser, Med. Chem. vxv. (2007), vxvvxv.	
16 June 2007	Disk used		
BMG 5800		ARTICLE IN PRESS	No. of Pages 11

a

HO OH HO

Figure 3. CoMFA model alignment rules. (a) In model I compounds 2-21 were aligned by overlapping atoms indicated by red circles. (b) In model II myricetin was aligned to quercetagetin according to their respective poses within the co-crystallized PIM-1 structures. To achieve this alignment the protein crystal structure backbones of PIM-1/quercitagetin and PIM-1/myricetin were aligned. The relationship of the quercetagetin pose to the myricetin pose is illustrated by overlap of atoms indicated by blue squares and red circles. Compounds 2, 3, 5-21 were aligned to quercetagetin as in model I (indicated by green triangles). (c) In model III compounds 3 and 10 were aligned to the co-crystallized pose of myricetin. Compounds 2, 5-9, 11-21 were aligned to the co-crystallized pose of quercetagetin. (d) The crystal poses of quercetagetin (blue) and myricetin (green) in the PIM-1 ATP-binding pocket.

B ring are directed toward the area revealed by the model as favorable for negative charges (red contours). In contrast, compound 15 has a chiral center at the C2 position and does not lie flat within the contours (because of the sp³ hybridization). The B ring of this flavonoid is positioned deep within a region where the model predicted less bulk would improve binding (yellow contour). Hence the model elucidates the steric interactions that make compound 15 a poor PIM-1 kinase inhibitor, that is, the position of the B ring produces steric hindrances that discourage flavonoid binding.

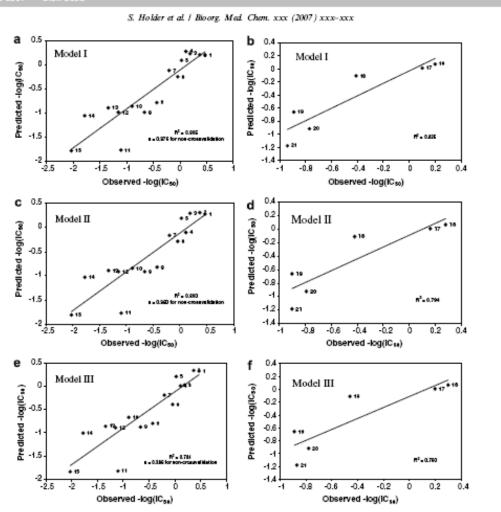
We sought to further validate the CoMFA model by comparing the steric and electrostatic contours of the model with a PIM-1 kinase crystal structure. We have previously reported the crystal structure of the PIM-1 kinase in complex with quercetagetin. ⁶³ We superimposed the quercetagetin in the PIM-1 co-crystal structure onto the quercetagetin in the CoMFA training set and examined the amino acid residues involved in flavonoid binding. In the areas where the model predicts improved binding by the addition of more positive charges, there are potential interactions with negatively charged acidic side chains (Glu¹²¹, Asp¹²⁶, Asp¹³¹, Glu¹⁷¹). Similarly, the electrostatic contour favoring negative charges envelops the positively charged side chain of Lys⁶⁷ (Fig. 6a).

The steric fields were also confirmed by the PIM-1 kinase crystal structure. The bulky side chains of Val⁵², Ala⁶⁵, and Leu¹²⁶ sterically hinder large groups in the re-

gion identified in the crystal structure that corresponds to regions in the CoMFA model where reduced bulk will improve binding. The model also identified a solvent exposed area near C7 as a region where reduced bulk would improve binding. Additionally, the side chain of Phe⁴⁹ and those of Ile¹⁶⁴ and Ile¹⁸⁵ form two hydrophobic pockets. The model accurately identified both of these pockets as regions where the addition of bulk would improve binding (Fig. 6b). Hence, a comparison of the electrostatic and steric CoMFA fields with the PIM-1 kinase crystal structure validates the striking accuracy of this CoMFA model of the PIM-1 kinase.

To address the finding that flavonoids bind to the PIM-1 kinase in at least two different orientations we created additional CoMFA models using alternate alignment rules (Fig. 3). Model II, in which myricetin was aligned in the training set of compounds according to its crystal pose rather than by superimposition onto quercetagetin over their common substructure, showed no improvement over model I to predict the potencies of the test set of compounds (Fig. 4). Similarly, model III, in which myricetin and compounds 3 and 10 were aligned in the training set according to the crystal pose of myricetin, showed no improvement over model I in predicting the potencies of the test set compounds (Fig. 4).

In light of the sterically restricted nature of the PIM-1 kinase ATP binding site we evaluated the relationship between volume and potency for flavonoid inhibitors



ARTICLE IN PRESS

Figure 4. Training and test set analyses using multiple alignment rules. The correlation between predicted and observed potencies for the training set using CoMFA models I, II, and III (a, c, e, respectively) is shown. The test set results for models I, II, and III are presented in panels b, d, and f, respectively.

of the PIM-1 kinase. Figure 7 demonstrates what appears to be an optimum volume near 218 Å³ (the volume of quercetagetin) for flavonoid antagonists of PIM-1. Flavonoids with volumes larger or smaller than 218 Å³ are progressively worse inhibitors of the PIM-1 kinase.

21.0

220

3. Discussion

Here we have described the generation of the first CoM-FA model for PIM-1 kinase ligands using flavonoid probes. Sixty-three percent of the contributions to the model were steric, while only 37% were electrostatic, suggesting that flavonoid binding to the PIM-1 kinase is influenced predominantly by steric factors rather than by electrostatic factors.

The steric contours reveal that the PIM-1 kinase ATPbinding site is sterically hindered above and below the plane of the bound flavonoid. It is likely that the planar conformation of the flavone class of compounds is what allows them to fit well into the sterically restricted space within the PIM-1 kinase ATP-binding site. In contrast, (R)- and (S)-flavanones (compounds 11, 14, and 15), which have a chiral carbon at the C2 position, are inferior PIM-1 kinase antagonists compared to the flavones (see Fig. 6 and Table 1). Our model was able to predict the relative order in regard to enantioselective inhibition (R > S) of compounds 14 and 15. It appears that a planar conformation is advantageous for inhibition and presumably would not be limited to the flavonoid class of compounds. It is more likely that this favorable characteristic will be found in small-molecule inhibitors of the PIM-1 kinase as a group.

230

240

As demonstrated in Figure 7, the volume of the ligand also appears to play a role in the potency of flavonoid compounds as PIM-1 kinase antagonists. This feature

IBMC 8803 ARTICLE IN PRESS No. of Pages 11
16 June 2007 Disk used

S. Holder et al. | Bisorg. Med. Chem. xxx (2007) xxx-xxx

Table 3. Observed and predicted potencies for the test set using multiple alignments

16-21

Compound	R ₁	R ₂	R ₃	R4	R ₅	R ₆	R,	Rg	R _o	R 10
16 (fisetin)	ОН	н	н	OH	Н	Н	ОН	OH	н	н
17	OH	H	H	OH	H	H	H	OH	H	H
18 (kaempferol)	ОН	OH	H	OH	H	H	H	OH	H	H
19	ОН	H	H	OH	H	H	H	H	H	H
20	OH	H	OH	H	H	OH	H	OH	H	H
21	H	OH	H	OH	H	H	H	H	H	H

Compound		Model I -log IC ₂₀ (μM)		1.00	del II co (μΜ)	Mod —logIC	el III so (µM)
	Obsd	Pred	Res	Pred	Res	Pred	Res
16 (fisetin)	0.07	0.20	-0.13	0.28	-0.21	0.30	-0.23
17	10.0	0.10	-0.09	0.16	-0.15	0.20	-0.19
18 (kaempferol)	-0.11	-0.41	0.30	-0.42	0.31	-0.46	0.35
19	-0.66	-0.89	0.23	-0.90	0.24	-0.89	0.23
20	-0.92	-0.77	-0.15	-0.79	-0.13	-0.78	-0.14
21	-1.18	-0.94	-0.24	-0.90	-0.28	-0.87	-0.31

Q1 Obsd, observed value; pred, predicted value; res, residual; "Generated from CoMFA non-cross-validated run (see Section 4).

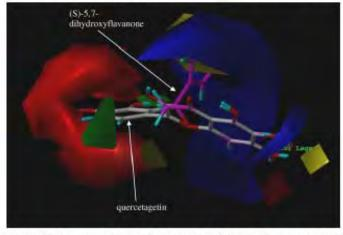


Figure 5. Comparison of the most and least potent flavonoid inhibitors of the PIM-1 kinuse within the contours of the CoMFA model. Quercetagetin, the most potent inhibitor, is pictured in gray. (S) 5,7-Dihydroxyflavanone (15), the poorest inhibitor, is pictured in purple. For the electrostatic contours increased binding is predicted by placing more positive (+) charges near blue areas and more negative (-) charges near red areas. The steric contours predict increased binding by placing more bulk near green areas and less bulk near yellow areas.

is related to the sterically restricted nature of the binding site. It appears that the potency of a flavonoid is reduced when the volume of the flavonoid is too small to adequately fill the ATP-binding pocket. Similarly, if the volume of the flavonoid is too large the restrictive nature of the binding pocket results in reduced efficiency of binding and inferior potency. A volume approaching 218 Å³, the volume of quercetagetin, appears near optimal for flavonoid inhibitors of the PIM-1 kinase

The CoMFA model generated a superior correlation to observed flavonoid potency than simple correlation to either $\log P$ or dipole moment. It is important to note that the flavonoid potencies used to generate the CoMFA model were determined using a solid phase in vitro kinase assay. Because $\log P$ is a predictive measure of absorption, it is plausible that determining the flavonoid potencies using a cellular assay would improve the correlation between $\log P$ and observed flavonoid potency. Nonetheless, the utility of the CoMFA model as a pre-

Please cite this article in press as: Holder, S. et al., Bioorg. Med. Chem. (2007), doi:10.1016/j.bmc.2007.06.025

2.50

260



S. Holder et al. I Bloorg. Med. Chem. xxx (2007) xxx-xxx



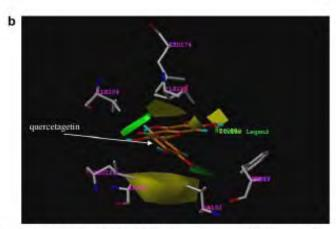


Figure 6. Characterization of the electrostatic and steric CoMFA fields with a superimposed PIM-1 kinase crystal structure. The crystal structure of the PIM-1 kinase in complex with quercetagetin is superimposed on the CoMFA fields using the positions of quercetagetin in the crystal and in the model. For clarity, only the amino acid residues contributing to the properties of a CoMFA contour are shown. The pictured flavonoid is the CoMFA model quercetagetin structure; to reduce visual clutter the PIM-1 crystal quercetagetin structure is not shown. (a) For the electrostatic contours increased binding is predicted by placing more positive (+) charges near thus areas and more negative (-) charges near red areas. (b) The steric contours predict increased binding by placing more bulk near green areas and less bulk near yellow areas.

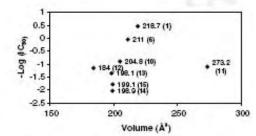


Figure 7. The volume of a flavonoid is related to its potency as an inhibitor of the PIM-1 kinase. The labels on the points represent the volume of each inhibitor. The bold numbers in parentheses identify the compound according to number as presented in Table 1.

dictive model of flavonoid potency was demonstrated by its ability to accurately predict the potency of the test set of flavonoids. These data suggest that the model may be an effective tool for the in silico design and prediction of additional flavonoid inhibitors of the PIM-1 kinase. Further experiments will be conducted to determine the accuracy of using the model to determine the potency of small molecules that are not in the flavonoid class of compounds.

Additionally, the PIM-1 kinase crystal structure strongly supports the CoMFA model by providing reasonable rationale in regard to the amino acid residues that may contribute to the steric and electrostatic contours of the model. This type of analysis is fairly unique, as CoMFA models are usually employed when the structure of the enzyme or receptor protein is unknown. Similar types of analyses, where the contours of a CoMFA model for a protein were combined with a crystal structure of the enzyme, have been described. 36,65-68 In each case, as in our case, the combination of the CoMFA contours with the enzyme structure elucidated spe-

Please cite this article in press as: Holder, S. et al., Bloorg. Med. Chem. (2007), doi:10.1016/j.bmc.2007.06.025

270

280

350

390

BMC 5803 ARTICLE IN PRESS No. of Pages 11
16 June 2007 Disk used

S. Holder et al. | Bioorg, Med. Chem. xxx (2007) xxx-xxx

cific potential ligand-enzyme interactions and allowed for a more informed and predictive structure-based design effort.

Our analysis elucidated the three-dimensional contributions of specific amino acid residues to the steric and electrostatic properties of the PIM-1 kinase ATP-binding site. Results from these studies may provide invaluable information for the design of potent, selective inhibitors of the PIM-1 kinase.

290

300

320

Quercetagetin, quercetin, myricetin, and compound 3 share a common flavone scaffold and differ only in the number and positions of substituted hydroxyl groups onto the flavone backbone. Hence, our previous work demonstrating that these flavones do not all bind to the PIM-1 kinase in the same orientation was quite unexpected. 63

One of the weaknesses of CoMFA is the choice of the alignment rule. We show for the first time that caution must be used in aligning compounds even when they appear to have a common pharmacophore. The varied orientation of flavonoid binding to the PIM-1 kinase presented a potential limitation of the CoMFA model. The alignment rule used to create model I did not take into account the varied binding orientations (crystal poses) that could be present in the training set of flavonoids. However, alignment rules incorporating the crystal orientations of compounds in the training set (model II) did not improve the ability of the model to predict the potencies of the test set of compounds. This unique example provides strong evidence of the robustness in a correlated partial least squares in regard to establishing alignment rules.

It should be noted that, as a class of compounds, flavonoids have been shown to be inhibitors of other kinases in addition to the PIM-1 kinase. Protein kinase C⁶⁹ and protein kinase A⁷⁰ activity have been shown to be inhibited by flavonoids, with IC₅₀ values in the millimolar range. In contrast, flavonoids inhibit the PIM-1 kinase in the micromolar and submicromolar ranges.

Flavonoids are promiscuous compounds, in that their effect is not limited to the kinase class of enzymes. Flavonoids have been shown to induce mammalian topoisomerase II-dependent cleavage, 71 and inhibit both mitochondrial NADH-oxidase 72 and HIV-1 integrase. 73 Flavonoids have also been shown to inhibit soybean lipoxygenase and stimulate cyclooxygenase. 74 Gastric H+, K+-ATPase, 75 reverse transcriptases, 76 and DNA and RNA polymerases 76 are also inhibited by flavonoids. Common to many of these studies, regardless of the target enzyme, is the observation that the polyhydroxylated core plays a major role in the potency of flavonoids. This polyhydroxylation is also an important contributor to flavonoid promiscuity.

Comparing the hydroxylation patterns of quercetagetin and myricetin, as in Figure 3d, suggests that the trihydroxylated ring of the flavonoids is preferentially oriented toward the same region when bound to the PIM-1 kinase. This general rule appears true whether the trihydroxylated ring is ring A (as in quercetagetin) or ring B (as in myricetin). An alignment rule based on this general rule would require compounds 3 and 10 to bind to the PIM-1 kinase in an orientation similar to myricetin, rather than quercetagetin. Such an alignment was employed for model III, with no improvement in the predictive value of the model.

The structure of myricetin is similar to that of quercetagetin, hence the two compounds share similar properties when aligned according to their common substructure (as in model I). Interestingly, when aligned according to their crystal orientations (as in models II and III) these two compounds still share similar spatial electrostatic and steric properties (see Fig. 3). This relationship likely contributes to the success of our model. Our findings demonstrate the utility of ligand-based methods, such as CoMFA, in elucidating structure activity relationships; particularly in cases were the binding orientations of ligands are unknown.

Thus the outcome of the three predictive models presented here demonstrates that with our training and test set of compounds CoMFA is sufficiently robust to provide predictive models despite the varied binding orientations of flavonoids to the PIM-1 kinase. The utility of our model has been demonstrated by its successful use to predict the potencies of the test set of flavonoids ($r^2 = 0.829$). Hence we present here the first predictive model that may be used for the rational design of small-molecule PIM-1 kinase inhibitors.

4. Methods

4.1. PIM-1 activity

The IC₅₀'s used in the CoMFA were recently reported for PIM-1 kinase activity (Holder, S., Zemskova, M., Zhang, C., Tabrizizad, M., Bremer, R., Neidigh, J. W., Lilly, M. B. Characterization of a potent and selective small-molecule inhibitor of the PIM1 kinase. Mol. Cancer Ther. 2007, 6, 163–172). These values were used without correction or normalization.

4.2. Molecular modeling

The octanol-water partition coefficient (log P) for each flavonoid was calculated using Chemdraw version 6.0 (Cambridgesoft, Cambridge, MA). Molecular dipoles were calculated using MOPAC with default settings. The molecular volume (Å³) of each compound was calculated in SYBYL. The structures and IC₅₀ values of the set of flavonoids that form the training set are listed in Table 1. Table 3 lists the structures and IC₅₀ values for the flavonoids that form the test set.

The structures of all of the compounds were constructed in the BUILD/EDIT mode of SYBYL and energy-minimized by the conjugate gradient method using the Tripos force field⁶⁴ from a starting geometry of PIM-1 bound quercetagetin (2O3P). The flavonoids in the

BMC 5803 ARTICLE IN PRESS No. of Pages 11
16 June 2007 Disk used

S. Holder et al. / Bioorg. Med. Chem. xxx (2007) xxx-xxx

training and the test sets have a common double sixmembered ring structure; hence atoms in this common sub-structure were used to create the alignment rule for model I. All of the structures in the training set were aligned over the atoms C4, C5, C6, C7, and C8 of quercetagetin from the co-crystal structure with the PIM-1 kinase. Similarly, the flavonoids in the test set were also aligned over the atoms C4, C5, C6, C7, and C8. CoMFA, using default parameters, was calculated in the QSAR option of SYBYL 6.5. The CoMFA grid spacing was 2.0 Å in the x, y, and z directions, and the grid region was automatically generated by the CoMFA routine to encompass all molecules with an extension of 4.0 Å in each direction. An sp³ carbon (sterics) and a charge of +1.0 (electrostatics) were used as probes to generate the interaction energies at each lattice point. The default value of 30 kcal/mol was used as the maximum electrostatic and steric energy cutoff.

410

430

450

Using the training set of flavonoids, cross-validated and non-cross-validated partial least squares analyses (PLS) were performed within the SYBYL/QSAR routine. Cross-validation of the dependent column (-logIC₅₀) and the CoMFA column was performed with 2.0 kcal/mol column filtering. Scaled by the CoM-FA standard deviation, the cross-validated analysis generated an optimum number of components equal to 2 and $q^2 = 0.495$ (Table 2). PLS analysis with noncross-validation, performed with two components, generated a standard error of estimate of 0.376, a probability $(R^2 = 0)$ equal to 0.000, an F value $(n_1 = 2,$ $n_2 = 12$) of 24.792, and a $q^2 = 0.805$ (Table 1). The relative steric (0.626) and electrostatic (0.374) contributions to the final model were contoured as the standard deviation multiplied by the coefficient at 80% for favored steric (contoured in green) and favored positive electrostatic (contoured in blue) effects and at 20% for disfavored steric (contoured in yellow) and favored negative electrostatic (contoured in red) effects, as shown in Figures 5-7.

On the basis of this analysis, the IC₅₀ values of the test set of flavonoids were predicted and correlated to the observed IC₅₀ values as determined in our laboratory (Table 3). The CoMFA contours were also compared with a PIM-1 crystal structure. A PIM-1 kinase crystal structure with bound quercetagetin (the most potent flavonoid inhibitor of the PIM-1 kinase among those we have assayed) was superimposed with atoms O1, C2, C3, C4, C5, C6, C7, and C8, onto the quercetagetin structure in the training set of compounds used to create the CoMFA model.

A crystal structure of myricetin in complex with the PIM-1 kinase revealed a surprisingly distinct and different binding orientation than quercetagetin. ⁶³ Hence a second CoMFA alignment rule was employed (model II), in which myricetin was aligned to quercetagetin according to their crystal poses rather than by their common substructure as in model I. To accomplish this alignment the two crystal structures of the PIM-1 kinase in complex with quercetagetin and myricetin (RCSB Protein Data Bank codes 2063, 2064, respectively) were

superimposed over their protein backbones. The two PIM-1 kinase structures are notably similar, with an RMSD over the complete protein backbone of only 0.58 Å. Quercetagetin and myricetin were extracted from their respective PIM-1 kinase protein structures to achieve a ligand alignment and orientation based on the crystal poses. The remaining compounds in the training set were aligned to quercetagetin by their common substructure, as in model I.

Based on their respective hydroxylation patterns, compounds 3 and 10 were identified as likely candidates for binding to the PIM-1 kinase in a similar pose to myricetin, rather than that of quercetagetin (see the discussion section for a detailed explanation). Consequently a third alignment rule was employed (model III), where myricetin and compounds 3 and 10 were aligned in the crystal pose of myricetin, while the remaining compounds in the training set were aligned in the quercetagetin crystal pose.

Acknowledgments

We thank Ryan Bremer and Plexxikon, Inc. for making the co-crystal structures of PIM-1 bound to quercetagetin and myricetin available to us in advance of publication for use in this study. We thank the Drug Discovery Program at Georgetown Medical Center for financial support.

References and notes

- Hoover, D.; Friedmann, M.; Reeves, R.; Magnuson, N. S. J. Biol Chem. 1991, 266, 14018–14023.
- Padma, R.; Nagarajan, L. Cancer Res. 1991, 51, 2486– 2489.
- Saris, C. J.; Domen, J.; Berns, A. EMBO J. 1991, 10, 655– 664.
- Wang, Z.; Bhattacharya, N.; Weaver, M.; Petersen, K.; Meyer, M.; Gapter, L.; Magnuson, N. S. J. Vet. Sci. 2001, 2, 167–179.
- Bachmann, M.; Moroy, T. Int. J. Biochem. Cell Biol. 2005, 37, 726–730.
- Ouypers, H. T.; Selten, G.; Quint, W.; Zijlstra, M.; Maandag, E. R.; Boelens, W.; van Wezenbeek, P.; Melief, C.; Berns, A. Cell 1984, 37, 41–150.
- Amson, R.; Sigaux, F.; Przedborski, S.; Flandrin, G.; Givol, D.; Telerman, A. Proc. Natl. Acad. Sci. U.S.A. 1989, 86, 8857–8861.
- van Lohuizen, M.; Verbeek, S.; Krimpenfort, P.; Domen, J.; Saris, C.; Radaszkiewicz, T.; Berns, A. Cell 1989, 56, 673–682.
- Domen, J.; van der Lugt, N. M.; Laird, P. W.; Saris, C. J.; Berns, A. Leukemia 1993, 7(Suppl. 2), S108–S112.
- Domen, J.; van der Lugt, N. M.; Laird, P. W.; Saris, C. J.; Clarke, A. R.; Hooper, M. L.; Berns, A. *Blood* 1993, 82, 1445–1452.
- Lilly, M.; Le, T.; Holland, P.; Hendrickson, S. L. Oncogene 1992, 7, 727–732.
- Miura, O.; Miura, Y.; Nakamura, N.; Quelle, F. W.; Witthuhn, B. A.; Ihle, J. N.; Aoki, N. Blood 1994, 84, 4135-4141.
- Shirogane, T.; Fukada, T.; Muller, J. M.; Shima, D. T.; Hibi, M.; Hirano, T. *Immunity* 1999, 11, 709–719.

ARTICLE IN PRESS 16 June 2007 Disk used	
10 S. Holder et al. Bioorg. Med. Chem. xxx (2007) xxx-xxx	
 Wingett, D.; Long, A.; Kelleher, D.; Magnuson, N. S. J. Immunol 1996, 156, 549-557. Yip-Schneider, M. T.; Horie, M.; Broxmeyer, H. E. Blood 1995, 85, 3494-3502. Zhu, N.; Ramirez, L. M.; Lee, R. L.; Magnuson, N. S.; Bishop, G. A.; Gold, M. R. J. Immunol 2002, 168, 744-754. Krumenacker, J. S.; Narang, V. S.; Buckley, D. J.; Buckley, A. R. J. Neuroimmunol. 2001, 113, 249-259. Wong, G.; Koehler, K. F.; Skolnick, P.; Gu Ananthan, S.; Schonholzer, P.; Hunkeler, W.; Zh Cook, J. M. J. Med. Chem. 1993, 36, 1820-1830. Myers, A. M.; Charifson, P. S.; Owens, C. E.; Ku McPhail, A. T.; Baldessarini, R. J.; Booth, R. G.; S. D. J. Med. Chem. 1994, 37, 4109-4117. Thomas, B. F.; Compton, D. R.; Martin, B. R.; S. F. Mol. Pharmacol. 1991, 49, 656-665. 	nang, W.; l. ila, N. S.; ; Wyrick,
 Mochizuki, T.; Kitanaka, C.; Noguchi, K.; Muramatsu, T.; Asai, A.; Kuchino, Y. <i>J. Biol. Chem.</i> 1999, 274, 18659–18666. Wang, Z.; Bhattacharya, N.; Meyer, M. K.; Seimiya, H.; Dahlgren, T.; Herslof, M.; Yang, Y.; Lamb 	i, H. B.;
Tsuruo, T.; Tonani, J. A.; Magnuson, N. S. Arch Biochem Biophys. 2001, 390, 9-18. Nelson, D. L.; Regan, J. W. J. Med. Chem. 1 4006-4014.	1993, 36,
 Rainio, E. M.; Sandholm, J.; Koskinen, P. J. J. Immunol. 2002, 168, 1524–1527. Leverson, J. D.; Koskinen, P. J.; Orrico, F. C.; Rainio, E. M.; Jalkanen, K. J.; Dash, A. B.; Eisenman, R. N.; Ness, M. SAR QSAR Environ. Res. 1999, 10, 215–237. 	eehan, D.
 S. A. Mol. Cell 1998, 2, 417-425. Koike, N.; Maita, H.; Taira, T.; Ariga, H.; Iguchi-Ariga, S. M. FEBS Lett. 2000, 467, 17-21. Mor, M.; Rivara, S.; Silva, C.; Bordi, F.; Plazz Spadoni, G.; Diamantini, G.; Balsamini, C.; Ta Fraschini, F.; Lucini, V.; Nonno, R.; Stankov J. Med. Chem. 1998, 41, 3831-3844. 	arzia, G.;
 M.; Tamai, K.; Takahashi, K.; Ariga, H.; Iguchi-Ariga, S. M. Eur. J. Biochem. 2000, 267, 5168-5178. Bhattacharya, N.; Wang, Z.; Davitt, C.; McKenzie, I. F.; Xing, P. X.; Magnuson, N. S. Chromosoma 2002, 111, 80-95. Moro, S.; van Rhee, A. M.; Sanders, L. H.; Jaco A. J. Med. Chem. 1998, 41, 46-52. Sicsie, S.; Serraz, I.; Andrieux, J.; Bremont, B.; Allainmat, M.; Poncet, A.; Shen, S.; Langlois, M. Chem. 1997, 40, 739-748. 	; Mathe-
 Yan, B.; Zemskova, M.; Holder, S.; Chin, V.; Kraft, A.; Koskinen, P. J.; Lilly, M. J. Biol. Chem. 2003, 278, 45358–45367. Aho, T. L.; Sandholm, J.; Peltola, K. J.; Mankonen, H. P.; Gantchev, T. G.; Ali, H.; van Lier, J. E. J. Med. 1994, 37, 4164-4176. 	
 Lilly, M.; Koskinen, P. J. FEBS Lett. 2004, 571, 43-49. Laird, P. W.; van der Lugt, N. M.; Clarke, A.; Domen, J.; Linders, K.; McWhir, J.; Berns, A.; Hooper, M. Nucleic Acids Res. 1993, 21, 4750-4755. Mikkers, H.; Nawijn, M.; Allen, J.; Brouwers, C.; Verhoeven, E.; Jonkers, J.; Berns, A. Mol. Cell Biol. 2004, 24, Albava, E.; Juvonen, R. O. Toxicol. In Vitro 2 	d, T. L.; 15-5554. nen, M.;
6104-6115. 29. Lilly, M.; Sandholm, J.; Cooper, J. J.; Koskinen, P. J.; Kraft, A. Oncogene 1999, 18, 4022-4031. 30. Pircher, T. J.; Zhao, S.; Geiger, J. N.; Joneja, B.; 59. Ekins, S.; Bravi, G.; Wikel, J. H.; Wrighton, Pharmacol. Exp. Ther. 1999, 291, 424-433.	S. A. J.
 Wojchowski, D. M. Oncogene 2000, 19, 3684-3692. 31. Lilly, M.; Kraft, A. Cancer Res. 1997, 57, 5348-5355. 32. Akasaka, H.; Akasaka, T.; Kurata, M.; Ueda, C.; Shimizu, A.; Uchiyama, T.; Ohno, H. Cancer Res. 2000, 60, 2335-2341. 33. Pasqualucci, L.; Neumeister, P.; Goossens, T.; Nanjan- 34. C. X. Acta Pharmacol Sin. 2004, 25, 950-958. 	kel, J. H. E. Drug
gud, G.; Chaganti, R. S.; Kuppers, R.; Dalla-Favera, R. Nature 2001, 412, 341-346. 34. Dhanasekaran, S. M.; Barrette, T. R.; Ghosh, D.; Shah, R.; Varambally, S.; Kurachi, K.; Pienta, K. J.; Rubin, M. A.; Chinnaiyan, A. M. Nature 2001, 412, 822-826. 62. Brown, M. L.; Rieger, J. M.; Macdonald, T. L. Med Chem. 2000, 8, 1433-1441. 63. Holder, S.; Zemskova, M.; Zhang, C.; Tabrizi Bremer, R.; Neidigh, J. W.; Lilly, M. B. Mol. Can 2007, 6, 163-172.	izad, M.;
 Valdman, A.; Fang, X.; Pang, S. T.; Ekman, P.; Egevad, L. Prostate 2004, 60, 367-371. Thaimattam, R.; Daga, P.; Rajjak, S. A.; Banerjee, R.; Buolamwini, J. K.; Assefa, H. J. Med. Chem. 2 	_
 Iqbal, J. Bioorg. Med. Chem. 2004, 12, 6415-6425. Sperandio da Silva, G. M.; Sant'Anna, C. M.; Barreiro, E. J. Bioorg. Med. Chem. 2004, 12, 3159-3166. Ducrot, P.; Legraverend, M.; Grierson, D. S. J. Med Desiraju, G. R.; Gopalakrishnan, B.; Jetti, R. K. 	
Chem. 2000, 43, 4098-4108. 39. Rieger, J. M.; Brown, M. L.; Sullivan, G. W.; Linden, J.; Macdonald, T. L. J. Med. Chem. 2001, 44, 531-539. 40. Peng, Y.; Keenan, S. M.; Zhang, Q.; Kholodovych, V.; 62. Tammela, P.; Ekokoski, E.; García-Horsman, A.;	a, M. E.; 4857. 559–572. ; Talman,
 Welsh, W. J. J. Med. Chem. 2005, 48, 1620–1629. Kim, K. H.; Greco, G.; Novellino, E.; Silipo, C.; Vittoria, A. J. Comput. Aided Mol. Des. 1993, 7, 263–280. Greco, G.; Novellino, E.; Fiorini, I.; Nacci, V.; Campiani, Seyler 1992, 373, 205–211. 	
 Greco, G.; Novellino, E.; Fiorini, I.; Nacci, V.; Campiani, G.; Ciani, S. M.; Garofalo, A.; Bernasconi, P.; Mennini, T. J. Med. Chem. 1994, 37, 4100-4108. Seyler 1992, 373, 205-211. Austin, C. A.; Patel, S.; Ono, K.; Nakane, H.; F. M. Biochem. J. 1992, 282(Pt 3), 883-889. 	Fisher, L.

ARTICLE IN PRESS

S. Holder et al. / Bioorg. Med. Chem. xxx (2007) xxx-xxx

- Hodnick, W. F.; Bohmont, C. W.; Capps, C.; Pardini, R. S. Biochem. Pharmacol. 1987, 36, 2873– 2874.
- Fesen, M. R.; Pommier, Y.; Leteurtre, F.; Hiroguchi, S.; Yung, J.; Kohn, K. W. Biochem. Pharmacol. 1994, 48, 595-608.
- Robak, J.; Shridi, F.; Wolbis, M.; Krolikowska, M. Pol J. Pharmacol Pharm. 1988, 40, 451–458.
 Murakami, S.; Muramatsu, M.; Tomisawa, K. J. Enzyme Inhib. 1999, 14, 151–166.
 Ono, K.; Nakane, H.; Fukushima, M.; Chermann, J. C.; Barre-Sinoussi, F. Eur. J. Biochem. 1990, 190, 469–476.

THE PIMI KINASE IS A CRITICAL COMPONENT OF A SURVIVAL PATHWAY ACTIVATED BY DOCETAXEL, AND PROMOTES SURVIVAL OF DOCETAXEL-TREATED PROSTATE CANCER CELLS

Marina Zemskova¹, Eva Sahakian¹, Svetlana Bashkirova¹, Michael Lilly^{1,2}

From Center for Health Disparities and Molecular Medicine, Departments of Medicine & Microbiology, Loma Linda University School of Medicine, Loma Linda, CA¹; Chao Family Comprehensive Cancer Center, University of California, Irvine, Irvine, CA²

Running head: PIM1 mediates docetaxel resistance

Address correspondence to: Michael Lilly, MD, Chao Family Comprehensive Cancer Center, Bldg. 56, Rm 248, University of California, Irvine, 101 The City Drive, Orange, CA 92868, telephone 714-456-5153, FAX 714-456-2242, e-mail: mlilly@uci.edu

A defining characteristic of solid tumors is the capacity to divide aggressively and disseminate under conditions of nutrient deprivation, limited oxygen availability, and exposure to cytotoxic drugs or radiation. Survival pathways are activated within tumor cells to cope with these ambient stresses. We here describe a survival pathway activated by the anti-cancer drug docetaxel in prostate cancer cells. Docetaxel activates STAT3 phosphorylation and transcriptional activity, which in turns induces expression of the PIM1 gene, encoding a serine-threonine kinase activated by many cellular stresses. Expression of PIM1 improves survival of docetaxel-treated prostate cancer cells, and PIM1 knockdown, or expression of a dominant-negative PIM1 protein, sensitize cells to the cytotoxic effects of docetaxel. PIM1 in turn mediates docetaxel-induced activation of NFkB transcriptional activity, and PIM1 depends in part on NFxB p65 protein for its prosurvival effects. The PIM1 kinase plays a critical role in this STAT3-> PIM1→ NFκB stress response pathway, and serves as a target for intervention to enhance the therapeutic effects of cytotoxic drugs such as docetaxel.

A defining characteristic of solid tumors is the capacity to divide aggressively and metastasize under conditions of nutrient deprivation and limited oxygen availability. These microenvironmental stresses arise from inadequate perfusion as the primary tumor rapidly outgrows its initial blood supply, and from dramatic structural abnormalities of tumor vessels that lead to aberrant microcirculation. Survival pathways are activated within tumor cells to cope with these ambient stresses. Examples include stress pathways that respond to hypoxia (1), oxidative stress (2), and unfolded protein/endoplasmic reticulum stresses (3). In addition to these microenvironmental stresses, anti-cancer treatment can cause additional stresses to cancer cells. These added insults call forth additional responses that can augment the survival mechanisms of the malignant cells and impair overall cell kill. Key participants in stress response pathways induced by cytotoxic drugs include AKT- and other kinase-dependent pathways (4-8), NFkB pathways (9), and mediators of DNA repair (10).

Among the potential survival proteins in cancer cells are the PIM family of kinases, including the PIM1, PIM2, and PIM3 genes. These small, cytoplasmic serine-threonine kinases function as true oncogenes, promoting the development of cancer in animal models, either alone (11) or synergistically with other oncogenes such as MYC (12). In normal and malignant cells PIM kinases are highly regulated at the transcriptional level. Expression is induced by many cellular stresses, including cytokines (13), oncogenes (14), hypoxia (15), heat shock (16), and toxin exposure (17). In addition, PIM kinases are constitutively expressed in a variety of leukemias and lymphomas (18), in head and neck squamous cell carcinomas (19), as well as in prostate cancer (20-22). Therefore PIM kinases may mediate in part the process of carcinogenesis.

PIM kinases have been shown to promote cell survival in the face of cytokine withdrawal, as well as exposure to ionizing radiation and doxorubicin (13,23,24). This is accomplished in part through phosphorylation of the pro-

apoptotic protein BAD on serine-112, leading to its sequestraton by 14-3-3 (25,26). It is unknown whether PIM kinases participate in induced cytoprotective responses following treatment of cancer cells with chemotherapeutic agents. Since the PIM1 kinase has been implicated in the development or progression of prostate cancer, we have examined its role in cell responses to docetaxel, the primary cytotoxic agent used to treat prostate cancer (27,28). We here present data showing that PIM1 expression is induced by docetaxel Furthermore, PIM1 is a key treatment. component of a survival pathway that includes STAT3 and NFxB transcriptional complexes.

Experimental Procedures

Reagents. Docetaxel pharmaceutical grade solution (Sanofi) was diluted in unsupplemented keratinocyte medium (Invitrogen) immediately before each experiment. 3-(4, 5-Dimethyl-2-thiazolyl)-2,5-diphenyl-2H-tetrazolium bromide (MTT) was prepared as stock solutions in PBS. The following monocbnal antibodies were used: anti-β-ACTIN (clone AC-15; Sigma), anti-PIM1 (clone 12H8; Santa Cruz), anti-BCL_M. (clone H-5; Santa Cruz), anti-phospho-STAT3 (Tyr705) (clone 3E2; Cell Signaling), anti-total STAT3 (clone 84; BD Biosciences), and anti-human cyclin B1 (clone GNS-1; BD Biosciences).

Cell Culture and generation of stable clones. RWPE-1 and RWPE-2 prostate epithelial cell lines (both from ATCC) were maintained in keratinocyte medium (Invitrogen) supplemented with 5 ng/mL human recombinant EGF, 0.05 mg/mL bovine pituitary extract, 100 units/mL penicillin and 100 µg/mL streptomycin (MediaTech). RWPE-1 cells are immortalized but not tumorigenic; RWPE-2 cells are both immortalized and tumorigenic in immunodeficient animals.

For some experiments we produced additional pools of RWPE-1 and RWPE-2 prostate cells that overexpressed wild-type or dominant-negative PIM1 cDNAs (23) through retroviral transduction. The coding regions for the human PIM1 gene or a dominant-negative variant (NT81) were cloned into the pLNCX retroviral vector (Clontech). To produce infectious viruses the GP-293 packaging cell

line was co-transfected with retroviral backbone plasmids (pLNCX, pLNCX/PIM1 pLNCX/NT81) and with pVSV-G, a plasmid that expresses the envelope glycoprotein from vesicular stomatitis virus, using the calcium phosphate method. After 48 hours of incubation the medium was collected and the virus particles were concentrated by centrifugation. Prostate cells were plated at 1 x 105 per 60-mm plate 16-18 hours before infection. Cells were infected with 5 x 10⁴ viral particles per plate in the presence of 8 µg/ml polybrene. After 6 hours of incubation the virus-containing media was replaced with fresh media, and on the next day G418 400 µg/mL was added to select stably infected cell populations. After 10 days of selection stable cell pools were established and expression of the PIM1 transgenes was verified by Western blot analysis.

For reporter gene assays, RWPE-2 cells stably expressing a NFkB-luciferase reporter plasmid were prepared. The parental cell line was co-transfected with the reporter gene plasmid (Strategene) and a puromycin resistance Puromycin-resistant clones were screened for expression of firefly luciferase in response to stimulation with tumor necrosis factor alpha (Peprotech). Two high-responding clones were combined to create a pool. In some experiments this pool of reporter cells was with further infected PIM1-encoding retroviruses as described above, and further pools were selected by treatment of the cultures with G418.

Determination of cell viability and apoptosis. To determine cell survival following docetaxel treatment, both short-term (MTT) and long-term (regrowth) assays were used. For the former, cells were seeded into 96-well plates (1-2 x 104 cells/well) and allowed to adhere overnight. Docetaxel was added and the cells were incubated for various period of time. Metabolically active cells were measured by the MTT assay. For regrowth assays, cells were plated at 5 x 10⁴/well of 12-well plates, and allowed to adhere overnight. Docetaxel was then added for 24hrs. Cells were subsequently trypsinized, and dilutions were plated in fresh medium in 24-well plates, and allowed to grow for 6-7 days. Cell numbers were then enumerated by crystal violet staining (29).

To measure caspase activation following docetaxel treatment, the carboxyfluorescein FLICA apoptosis detection kit was used (Immunochemistry Technologies). The stained cells were analyzed with a FACScalibur flow cytometer.

DNA histogram analysis. After docetaxel treatment for 24 hours the floating and adherent cells were harvested and combined, washed with PBS, then fixed with cold 70% ethanol and stored at 4°C. The cells were then washed with PBS and were resuspended in 1 ml of PBS containing 25 μg/ml propidium iodide, 0.1% Triton X100, and 40 μg/ml RNAase A. After incubation at least 30 min at 4°C the cells then were analyzed by FACScalibur flow cytometer using channel FL3.

Luciferase reporter assays. Cells (4 x 10⁴/well) were plated in 24-well plates and allowed to adhere overnight. Cells then were untreated or not with docetaxel and incubated for 6 hours. The level of luciferase expression was determined in triplicate using a luciferase assay system (Promega) according to the manufacturer's protocol. The luminescent signal recorded using a plate luminometer (Berthold Technologies). Luciferase activity was normalized to total protein concentrations, as measured by the Bradford method.

Western blotting. Cells (5-7 x 105) were washed with cold PBS and lysed in 100 μl of lysis buffer (20mM Tris-HCl pH 7.5, 1% SDS, 50mM NaCl, 1mM EDTA supplied with 1mM phenylmethylsulfonyl fluoride and protease inhibitor cocktail Set V (Calbiochem). The lysates were sonicated and the protein concentration was measured using the BCA™ Protein assay kit (Pierce). Up to 70 µg of total protein/lane were subjected to 12% SDS-PAGE and transferred to polyvinylidene membranes. The membranes were blocked with 5% skimmed milk in TBST (20 mM Tris-HCl, pH 7.5, 150 mM NaCl, 0.1% Tween 20), and then incubated overnight in 5% of skimmed milk or 5% bovine serum albumin in TBST with primary antibodies (dilution 1:1000) at 4° C with constant shaking. After washing with TBST, the membranes were exposed to peroxidase-coupled secondary antibodies for 1 hour at room temperature. Membranes then washed again with TBST. Detection of the protein was performed by using the chemiluminescent SuperSignal West Femto or Pico Maximum Sensitivity substrate (Pierce).

Real-Time PCR Total RNA was extracted with TRIzol Reagent (Invitrogen) and singlestranded cDNA was constructed by Superscript III polymerase (Invitrogen) and oligo-dT primers. Real-Time PCR was performed using iCycler (Bio-Rad) and SYBR Green PCR master-mix reagents (QIAGEN). The following PIM1 Forward 5'primers were used: AACTGGTCTTCCTTTTTTGGTT-3'; PIM1 Reverse 5'-TACCATGCCAACTGTACA CAC-CFL 5'-(cofilin) Forward GAGCAAGAAGGAGGATCTGGT-3': Reverse 5'-CAATTCATGCTTGATCCCTGT- The PIM1 primer concentration was 2μM and the CFL (cofilin) primer concentration was 0.3µM per reaction.

STAT3 decoy and mutant control decoy oligonucleotide treatment. The STAT3 decoy and mutant decoy oligonucleotides utilized previously described sequences (30). RWPE-2 cells were seeded into 6-well plates (5-7 x 10⁵/well) and allowed to grow. Twenty-four hours later the cells were treated with STAT3 decoy oligonucleotide (50nM) or mutant control oligonucleotide (50 nM) using TransIT*-OligoTransfection Reagent (Mirus). Incubation times of cells with decoy oligonucleotides varied between experiments (see figure legends).

siRNA studies. In some cases (NFkB siRNA studies) cells were transfected with NFKB1 (= p50) siRNA, RELA (= p65) siRNA, or control siRNA (Santa Cruz). One day prior to transfection, 5 x 105 cells/well were seeded in 6well plates. Twenty-four hours later the cells were transfected with siRNAs using the TransIT-TKO* Transfection Reagent (Mirus), and incubated overnight. The cells were then trypsinized, counted, and plated into 24-well plates (5-7 x 104/well) for luciferase assay, performed 24 hours later (48 hours after transfection). Alternately, for immunoblot analysis, the cells were plated in 6-well plates, transfected with siRNAs, and lysed after 48 hours after transfection. For docetaxel treatment the cells were seeded into a 96-well plate (1-2 x 10⁴ cell/well, 100 μl total volume) and allowed to adhere for 12hrs. They were then transfected with siRNAs using TransIT-TKO® Transfection Reagent (Mirus). Twenty-four hours later docetaxel (100 nM) was added to the cells, and incubation continued for 48 hours. The MTT assay was then performed.

Alternately (PIM1 siRNA studies) specific and control siRNA sequences were cloned into pSILENCER (Ambion) plasmid and used for transfection. The PIM1-targeting sequence was 5'- AACATCCTTATCGACCTCAATCGCG-3' and the control sequence was GCCTACCGTCAGGCTATCGCGTATC Plasmids were transiently transfected into RWPE-2 cells with a Nucleofector device (Amaxa) and incubated for 24 hours. Then, cells were trypsinized and re-plated with density 5 x 10⁵ cells/well in 6-well plates for immunoblot assay and 2 x 10° cells/well into 96-well plate for cell viability analysis. Next day, 48 hours after transfection, 100nM of Docetaxel was applied, then the cells were incubated for an additional 6 hours, lysed and used for an imuunoblotting assay with anti-PIM1 antibody was performed to detect PIM1 knockdown. Alternatively, for cell survival assay, 100nM of docetaxel was added for 24, 48 or 72 hours. The cell viability was measured with MTT assay.

RESULTS

Docetaxel increases expression of PIM1 mRNA and protein in prostate epithelial cell lines. To investigate the effect of docetaxel on the expression of the PIM1 kinase, we treated RWPE-1 and RWPE-2 prostate epithelial cells with pharmacological concentrations docetaxel that approximate those observed in plasma within 24 hours after administration Expression of PIM1 protein was analyzed by immunoblotting. Docetaxel induced expression of the kinase by 3 hours, with maximum expression between 612 hours, and then a decline to near-baseline levels thereafter (Fig. 1 A-D). Quantitative analysis of the densitometry data showed that PIM1 expression increased 2.5-7-fold during this The increase was statistically interval. significant at 3, 6, and 9 hours in eleven of twelve cell/dose combinations (Fig. 1 A-D), and of borderline significance in the last combination. Elevated PIM1 levels were less consistently seen at the later time points (12, 24

hours). Similar results were seen with either RWPE-1 or RWPE-2 cells, and with either 10nM or 100nM docetaxel concentrations.

To explore whether docetaxel-mediated induction of PIM1 expression transcriptionally regulated, real-time reversetranscription-PCR analysis was used (Fig. 2). Docetaxel induced up-regulation of the PIM1 transcript level in both RWPE-1 and RWPE-2 cells treated with either 10nM or 100nM of drug. The results of real-time reverse-transcription-PCR analysis, showing a two- to four-fold increase of PIM1 mRNA expression, were in direct agreement with the docetaxel-induced upregulation of PIM1 protein detected by Western blot. The level of PIM1 mRNA increased gradually in the presence of 10nM of docetaxel. With the higher drug concentration (100nM) there was more rapid up-regulation of PIM1 transcript.

Previous studies suggest that the PIM1 protein increases during the G2/M phase of the cell cycle (31). Since docetaxel treatment has been reported to cause G2/M arrest, it was possible that the increase in PIM1 protein that accompanies drug treatment might merely reflect a change in cell cycle distribution. We used DNA histogram analysis to identify changes in cell cycle distributions in RWPE-2 cells after docetaxel treatment (Fig. 3A). There was no overall increase in the G2/M cell population after 24 hours of low-dose (10nM) docetaxel treatment, compared with vehicletreated cells (p = 0.31 for no difference, based on 6 independent experiments). A large increase in G2/M cells was observed after treatment of RWPE-2 cells with a higher concentration (100nM) of docetaxel for 24 hours. Treatment with 10nM of docetaxel failed to induce the mitotic arrest, but increased the proportion of cells in sub-G1 fraction, with DNA content lower than 2N. DNA loss occurred when cells passed through transient mitotic block forming multimininucleated interphase cells (32). The data of DNA histogram analysis were confirmed by DAPI staining and phase-contrast microscopy after incubation of RWPE-2 cells with 10nM or 100nM of docetaxel for 24 hours (data not shown). Variable G2/M arrest was confirmed by immunoblotting to detect expression of cyclin B1 (a G2/M phase marker). There was no

change in cyclin B1 expression within 24 hours after 10nM docetaxel treatment, but a time-dependent increase of cyclin B1 protein was apparent after 100 nM docetaxel exposure (Fig. 3B, right panel). During both treatments, however, PIM1 expression increased between three and twelve hours of exposure, independent of the extent of G2/M arrest and cyclin B1 expression.

Endogenous and enhanced expression of PIM1 protects prostate epithelial cells from docetaxel-induced cell death and apoptosis. To determine whether PIM1 can protect prostate cells from docetaxel-triggered cell death, we infected RWPE-2 cells with retroviruses encoding a PIM1 cDNA (pLNCX/PIM1), or an empty retrovirus (pLNCX). Pools of stablytransduced cells were selected treated with docetaxel (10nM or 100nM) for up to 72 hours. and then analyzed by MTT assay to measure metabolically active cells. Enforced expression of wild-type PIM1 kinase was able to consistently improve cell survival, as reflected by the MTT assay, at time points up to 72 hours after the start of docetaxel exposure (Fig. 4). A statistically significant survival advantage was seen at both low (10nM) and high (100nM) drug concentrations, and in both RWPE-1 (data not shown) and RWPE-2 cells.

To determine if ambient levels of PIM1 can protect RWPE-2 cells from docetaxel toxicity, we introduced control and PIM1-specific siRNA oligonucleotides into target cells. Control siRNA oligonucleotides were unable to block the docetaxel-induced increase in PIM1 In contrast, PIM1 siRNAs expression. substantially prevented the increase in kinase expression following drug exposure (Fig. 5A). Down-regulation of endogenous PIM1 kinase expression led to enhanced cell kill up to 72hrs The drug after drug application (Fig. 5B). sensitization was statistically significant at every time point. To confirm the protective effect of endogenous PIM1 kinase, we also introduced a dominant-negative enzyme (PIM1/NT81) into RWPE-1 and RWPE-2 cells by retroviral This truncated protein was transduction. expressed well (Fig. 6A and B). As was seen with the knockdown experiments, the NT81 mutant kinase also sensitized cells to the cytotoxic effect of docetaxel.

experiments clearly demonstrate that ambient levels of PIM1 are protective against docetaxelinduced cell death.

Docetaxel has previously been shown to induce cell death in part by apoptosis (33-35). Therefore, we measured caspase activation by a fluorescent caspase activity assay in drug-treated cells as an index of docetaxel cytotoxicity. The wild-type PIM1 kinase decreased drug-induced caspase activation, consistent with its previously demonstrated survival activity (Fig. 5, 6C). The dominant-negative PIM1 kinase markedly enhanced drug-induced caspase activation, and the effect was statistically significant in both prostate cell lines.

The drug effect reflected by the MTT and caspase assays was not great, and its reversal by PIM1 expression, while statistically significant, was still quantitatively modest. These data reflect the fact that docetaxel does not produce massive, immediate apoptotic cell death. To better measure the protective effects of PIM1 kinase on the proliferative potential of docetaxel-treated cancer cells, we used a regrowth assay (Fig. 7). Since RWPE-2 cells form loose colonies and aggregates, we were not able to count discrete colonies; thus, the studies are technically not clonogenic or colony-growth RWPE-2/PIM1 and RWPE-2/NT81 cells were treated with various concentrations of docetaxel for 24 hours, then were trypsinized and plated in fresh medium (without drug) and allowed to grow for 6-7 days. Cell growth was then quantified by staining with crystal violet Docetaxel produced dose-dependent inhibition of growth in both cell lines. However, growth inhibition was up to 8-fold greater in the RWPE-2/NT81 cells, particularly at the drug concentrations of 5nM or higher. Thus the presence of biologically active PIM1 kinase markedly inhibited docetaxel-induced cell death.

The STAT3 transcription factor mediates induction of PIM1 by docetaxel. To identify mechanisms by which docetaxel could induce PIM1 expression, we examined the activation status of STAT3 and STAT5 transcriptional factors, known mediators of PIM1 transcription, after docetaxel treatment. STAT5 was not consistently phosphorylated in RWPE-1 or RWPE-2 cells (data not shown). The level of phosphoSTAT3 (Tyr705) was strongly and

rapidly increased after 10nM and 100nM treatment of RWPE-1 and RWPE-2 cells (Fig. 8A-D), while the total amount of STAT3 protein was not changed. Docetaxel induced phosphorylation of STAT3 simultaneously with up-regulation of PIM1 expression. These results suggested docetaxel-induced expression of PIM1 may be dependent of activation of the STAT3 transcriptional factor.

To determine if docetaxel induces PIM1 expression in a STAT3-dependent manner, we used double-stranded STAT3 oligonucleotides (30) to selectively abrogate STAT3 transcriptional activity. RWPE-2 cells were incubated with wild-type or mutantsequence STAT3 decoys for 48 hours. PIM1 expression was then analyzed by immunoblotting (Fig. 9A). STAT3 decoys, but not mutant decoys, decreased PIM1expression, as well as expression of the known STAT3 target gene BCLx_L. These results demonstrate that STAT3 transcriptional activity controlled basal PIM1 gene expression in RWPE-2 prostate cells. STAT3 decoy treatment was not associated with decreased levels of either STAT3 protein or tyrosine phosphorylated STAT3.

To further define the role of STAT3 transcriptional activity in docetaxel-dependent PIM1 expression, we treated RWPE-2 cells with STAT3 or mutant decoy oligonucleotides for 18 hours. Docetaxel was then added for an additional 6 hours. As shown (Fig. 9B), the STAT3 decoy did not prevent docetaxel-induced phosphorylation of STAT3, but did inhibit the effect of the drug on PIM1. In contrast, the mutant oligonucleotides had no effect on PIM1 expression. These results identify STAT3 as an upstream mediator through which docetaxel induces expression of the PIM1 kinase.

Docetaxel activates NFkB transcriptional activity in a PIM1-dependent manner. Inhibition of the NFkB transcriptional complex sensitizes prostate cancer cells to paclitaxel (another taxane) and enhances drug-induced apoptosis (36). We hypothesized that the protective role of PIM1 in docetaxel-induced apoptosis could be mediated through activation of NFkB transcriptional activity as well. We initially investigated the effect of PIM1

expression on NFkB transcriptional activity. RWPE-2 cells stably expressing an NFkB-dependent luciferase expression plasmid were infected with retroviruses encoding PIM1 or empty retrovirus only. Enhanced expression of PIM1 consistently increased NFkB transcriptional activity about two-fold (Fig. 10).

We then treated the NFkB reporter cell line with docetaxel. Cells were incubated for 6 hours with docetaxel, and then were assayed for luciferase activity. As shown (Fig.11) docetaxel increased NFkB directed luciferase expression in a concentration-dependent manner. Co-expression of a dominant-negative PIM1 protein substantially blocked drug-induced activation of NFkB transcriptional activity at each docetaxel concentration (Fig.11).

The protective effect of PIM1 expression from docetaxel-induced death depends in part on NFκB activation. To determine if PIM1enhances survival of docetaxel-treated cells through NFxB activation, we used siRNA to inhibit expression of the RELA (p65) and NFKB1 (p105, p50) proteins, the two components of the major NFkB complex. Figure 12A shows that basal and PIM1dependent activation of NFcB is decreased by p65/RELA and p50/NFKB1 Immunoblotting confirmed the knockdown of the corresponding p65/RELA and p50/NFKB1 proteins (Fig. 12B).

A survival analysis, based on the MTT assay, was then performed on docetaxel-treated cells (Fig. 13A, B). With all siRNA treatments, RWPE-2/PIM1 cells showed improved survival compared to that of cells infected with pLNCX virus alone (Fig. 13A). The p65/RELA and p50/NFKB1 siRNAs reduced survival of both cell lines. The p50/NFKB1 siRNA did not significantly impair the survival of docetaxeltreated RWPE-2/pLNCX cells, while it did have a significant effect on RWPE-2/PIM1 cells. In contrast p65/RELA siRNAs significantly enhanced docetaxel cell kill in both cell lines. These data suggested that cells with high expression of PIM1 (RWPE-2/PIM1) might be more sensitive to the effects of NFkB siRNAs than were cells with low levels of PIM1 (RWPE-2/pLNCX). We then reanalyzed the data by normalizing the survival of p65/RELA

and p50/NFKB1 siRNA-treated cells to that of cells treated with docetaxel and control siRNA. The p65/RELA and p50/NFKB1 siRNAs enhanced docetaxel induced cell kill of RWPE-2/PIM1 cells to a greater extent than they enhanced kill of RWPE-2/pLNCX (= vector only) cells. This enhancement was of borderline significance for p50/NFKB1 siRNA (p = 0.057), but was highly significant for p65/RELA These results demonstrate that the p65/RELA and p50/NFKB1 proteins mediate resistance to docetaxel cell kill. Their effects are more pronounced in prostate cells with higher PIM1 levels that in similar cells with lower amounts of PIM1. These data demonstrate that the ability of PIM1 to decrease docetaxelinduced cell kill depends in part on the p65/RELA, and possibly the p50/NFKB1, protein.

DISCUSSION

The present study assessed the up-regulation of PIM1 expression following docetaxel treatment of prostate epithelial cells. Docetaxel induced expression of PIM1 in a time-dependent manner, and PIM1 expression was independent of cell cycle arrest. Apoptosis is involved in docetaxel's antitumor effects, both in cultured cells and clinical settings (34,35,37). Our results demonstrated that PIM1 inhibited docetaxel-induced apoptosis. Recent work has indicated that other modes of cell death may also contribute significantly to the overall therapeutic response to docetaxel (33). Whether PIM1 modulates these other forms of docetaxel-induced cell death requires further investigation.

Cellular stressors are known to activate survival pathways. Among these stressors are a wide variety of anti-neoplastic agents, such as cytotoxic drugs (including taxanes; 6,7,10,39), tyrosine and serine-threonine kinase inhibitors (4,5), and triterpenes such as betulinic acid (38). These agents are capable of transiently activating kinases and other survival mediators, such as AKT, ERK1, and NFkB transcriptional activity. It appears that drug-induced activation of survival signaling pathways can impair the cytotoxic effects of chemotherapy drugs both in vivo and in vitro (9,40), and inhibition of

activated kinases can potentiate cytotoxic drug cell kill (40-44).

Our data document the existence of a STAT3→ PIM1→ NFxB survival pathway that is activated by docetaxel, and which mediates docetaxel resistance. The linear relationships among the pathway components were established by temporal correlations as well as by blocking experiments using siRNAs and oligonucleotide decoys. Resistance to docetaxel has previously been ascribed to tubulin mutations (45), as well as to MDR-dependent effects (46,47) and to limited tissue penetration (48). Fewer data exist to implicate transient or acquired resistance mediated through survival pathways. A previous report has shown that stable overexpression of STAT1 is associated with docetaxel resistance in prostate cancer cell lines (49). In addition, genetic inhibition of EGFR expression has been shown to sensitize head-and-neck cancer cells to docetaxel (50). The involvement of PIM kinases in induced resistance to cytotoxic drugs has not been documented thus far. However, activation of AKT has often been described (6.51). The PIM kinases and AKT kinases have been described as mediating separate but parallel survival pathways (52). At times they also phosphorylate the same substrates. Thus the involvement of PIM kinases in induced resistance to cytotoxic drugs may be anticipated in cells where the kinase is expressed.

The mechanism through which docetaxel activates the STAT3→PIM1→ NFκB pathway is unknown at present. Docetaxel induces an increase in reactive oxygen species (ROS), as do many cytotoxic drugs (53). This form of oxidizing stress inhibits phosphatase activity, leading to an increase in tyrosine phosphorylation of multiple proteins (54-56). Transactivation of receptor-type tyrosine kinases (such as the EGFR) has been shown in cells stressed by ROS, and by cytotoxic agents including paclitaxel (57-59). Docetaxel can transactivate the EGFR, and EGFR inhibitors can act synergistically with taxanes to enhance cancer cell kill (43,51). However, we continue to see expression of pSTAT3 or PIM1 proteins following docetaxel treatment of RWPE-2 cells pretreated with an EGFR inhibitor (data not shown). ROS have previously been shown to

activate JAK kinase signaling in some cells lines, possibly providing a mechanism for STAT activation as well (60,61). ROS can also activate STAT proteins without JAK kinase activation (62). Regardless of the most proximal mediators, activated STAT3 is a known mediator of ROSinduced survival signals. Furthermore STAT transcription factors are known upstream mediators of PIM1 transcription, at least in hematopoietic cells (63-65). Our data demonstrate that STAT3 regulates PIM1 expression in prostate cells as well. The decoy studies establish a linear relationship between STAT3 and PIM1 as downstream mediators of docetaxel survival signals. Since prostate cancer cells frequently express activated STAT3 and PIM1, this relationship may occur constitutively as well (66-68).

Our identification of a drug-induced signaling pathway leading to NFxB activation is consistent with the known effects of docetaxel (69-71). While many prostate cancer cell lines constitutive activation of NFkB transcriptional complexes, docetaxel can further increase NFkB transcriptional activity (70). Our studies indicate that, in RWPE-2 cells, docetaxel activates NFxB in a PIM1-dependent manner. Previous reports have shown that the related PIM2 kinase can activate NFkB activity (72), although alternative opinions about the PIM1 kinase have been presented (73). PIM2 activates NFxB activity through phosphorylation and activation of the COT/TPL2 kinase, a kinase with known IkB kinase-like activity (72). Clarification as to whether the PIM1 kinase acts through this mechanism or through another pathway will require further studies.

A decrease in NFkB expression or activity would be predicted to increase docetaxel-induced cell death in both RWPE-2/pLNCX and RWPE-2/PIM1 cell lines (36), and this was in fact seen (Fig. 13). However, cells with higher expression of the PIM1 kinase were more sensitive to the blockage of NFkB function (Fig. 13 B). Compared with their effects in RWPE-2/pLNCX cells, p65/RELA siRNAs were significantly more effective at potentiating docetaxel-induced death in RWPE-2/PIM1 cells. P50/NFKB1 siRNAs were also more active against cells with high levels of PIM1, but the

effect was of borderline significance. These data suggest that the pro-survival effect of PIM1 kinase in docetaxel-treated cells likely involves members of the NFxB transcriptional complex. particularly p65/RELA. The observation that inhibition of NFkB only partially enhances docetaxel-induced cell death in PIM1 expressing cells is consistent with the ability of the kinase to protect cells through other mechanisms, as well as the incomplete knockdown of the target protein in RWPE-2 cells. Nevertheless, the result demonstrates that PIM1, like PIM2 (72), can mediate NFxB activation, and that PIM1 also requires NFkB transcriptional activity for the development of the full drug-resistance phenotype.

The survival response induced by low concentrations of docetaxel is reminiscent of the concept of hormesis. A controversial body of literature documents that stressors (including radiation, gases, toxins, exercise, and others) can produce biphasic dose-response curves in various assay systems (74,75). At low doses a protective (hormetic) response is generated, while at high doses toxicity is the result. Hormesis has been invoked to explain the beneficial effects of calorie restriction, exercise. and various phytochemicals in disease prevention. In many cancer cells lines, cytotoxic agents also generate a classic biphasic hormetic dose-response curve (76-78). demonstrates the same phenomenon in our experimental system. There is a 24% increase in regrowth/survival of RWPE-2/PIM1 cells treated with low concentrations (0.5-1.0nM) of docetaxel, compared to the survival of untreated RWPE-2/PIM1 cells (p<0.001). In contrast, survival of RWPE-2/NT81 cells treated similarly is worse than that of RWPE-2/PIM1 cells and there is no enhancement of survival at low drug concentrations. Our data strongly suggest that the PIM1 kinase participates in cytotoxic-drug induced hormesis. PIM1 is also increased in response to a wide variety of cellular stressors growth factors, oncogenes, heat, radiation, toxins, oxidative stress, and hypoxia. Thus one may postulate that PIM1 is a general mediator of hormesis, or protective stress responses induced by low level environmental stresses. Recently. small molecule inhibitors of the PIM kinases

have been described in vitro and in cell-based systems (79-81). Targeting the PIM1 kinase may be a beneficial addition to traditional docetaxelbased chemotherapy regimen. However it will be important to determine if the same maneuver will increase normal tissue toxicity as well.

REFERENCES

- Welsh, S. J., Koh, M. Y., and Powis, G. (2006) Semin Oncol 33(4), 486-497
- Dairkee, S. H., Nicolau, M., Sayeed, A., Champion, S., Ji, Y., Moore, D. H., Yong, B., Meng, Z., and Jeffrey, S. S. (2007) Oncogene
- Feldman, D. E., Chauhan, V., and Koong, A. C. (2005) Mol Cancer Res 3(11), 597-605
- Burchert, A., Wang, Y., Cai, D., von Bubnoff, N., Paschka, P., Muller-Brusselbach, S., Ottmann, O. G., Duyster, J., Hochhaus, A., and Neubauer, A. (2005) Leukemia 19(10), 1774-1782
- Shi, Y., Yan, H., Frost, P., Gera, J., and Lichtenstein, A. (2005) Mol Cancer Ther 4(10), 1533-1540
- di Palma, A., Matarese, G., Leone, V., Di Matola, T., Acquaviva, F., Acquaviva, A. M., and Ricchi, P. (2006) Mol Cancer Ther 5(5), 1318-1324
- Ling, X., Bernacki, R. J., Brattain, M. G., and Li, F. (2004) J Biol Chem 279 (15), 15196-15203
- Okano, J., and Rustgi, A. K. (2001) J Biol Chem 276(22), 19555-19564
- Cusack, J. C., Jr., Liu, R., and Baldwin, A. S., Jr. (2000) Cancer Res 60(9), 2323-2330
- Anderson, K. M., Alrefai, W. A., Anderson, C. A., Ho, Y., Jadko, S., Ou, D., Wu, Y. B., and Harris, J. E. (2002) Anticancer Res 22(1A), 75-81
- van Lohuizen, M., Verbeek, S., Krimpenfort, P., Domen, J., Saris, C., Radaszkiewicz, T., and Berns, A. (1989) Cell 56(4), 673-682
- Verbeek, S., van Lohuizen, M., van der Valk, M., Domen, J., Kraal, G., and Berns, A. (1991) Mol Cell Biol 11(2), 1176-1179
- Lilly, M., Le, T., Holland, P., and Hendrickson, S. L. (1992) Oncogene 7(4), 727-732
- Nieborowska-Skorska, M., Hoser, G., Kossev, P., Wasik, M. A., and Skorski, T. (2002) Blood 99(12), 4531-4539
- Teh, B. G. (2004) Hokkaido Igaku Zasshi 79(1), 19-26
- Shay, K. P., Wang, Z., Xing, P. X., McKenzie, I. F., and Magnuson, N. S. (2005) Mol Cancer Res 3(3), 170-181
- DaSilva, L., Cote, D., Roy, C., Martinez, M., Duniho, S., Pitt, M. L., Downey, T., and Dertzbaugh, M. (2003) Toxicon 41(7), 813-822
- Amson, R., Sigaux, F., Przedborski, S., Flandrin, G., Givol, D., and Telerman, A. (1989) Proc Natl Acad Sci U S A 86(22), 8857-8861
- Beier, U. H., Weise, J. B., Laudien, M., Sauerwein, H., and Gorogh, T. (2007) Int J Oncol 30(6), 1381-1387
- Dhanasekaran, S. M., Barrette, T. R., Ghosh, D., Shah, R., Varambally, S., Kurachi, K., Pienta,
 K. J., Rubin, M. A., and Chinnaiyan, A. M. (2001) Nature 412 (6849), 822-826
- Valdman, A., Fang, X., Pang, S. T., Ekman, P., and Egevad, L. (2004) Prostate 60(4), 367-371
- Xu, Y., Zhang, T., Tang, H., Zhang, S., Liu, M., Ren, D., and Niu, Y. (2005) J Surg Oncol 92(4), 326-330
- Lilly, M., Sandholm, J., Cooper, J. J., Koskinen, P. J., and Kraft, A. (1999) Oncogene 18(27), 4022-4031
- Pircher, T. J., Zhao, S., Geiger, J. N., Joneja, B., and Wojchowski, D. M. (2000) Oncogene 19(32), 3684-3692
- Yan, B., Zemskova, M., Holder, S., Chin, V., Kraft, A., Koskinen, P. J., and Lilly, M. (2003) J Biol Chem 278 (46), 45358-45367
- Aho, T. L., Sandholm, J., Peltola, K. J., Mankonen, H. P., Lilly, M., and Koskinen, P. J. (2004) FEBS Lett 571(1-3), 43-49

- Tannock, I. F., de Wit, R., Berry, W. R., Horti, J., Pluzanska, A., Chi, K. N., Oudard, S., Theodore, C., James, N. D., Turesson, I., Rosenthal, M. A., and Eisenberger, M. A. (2004) The New England journal of medicine 351(15), 1502-1512
- Petrylak, D. P., Tangen, C. M., Hussain, M. H., Lara, P. N., Jr., Jones, J. A., Taplin, M. E., Burch,
 P. A., Berry, D., Moinpour, C., Kohli, M., Benson, M. C., Small, E. J., Raghavan, D., and
 Crawford, E. D. (2004) The New England journal of medicine 351(15), 1513-1520
- Kueng, W., Silber, E., and Eppenberger, U. (1989) Anal Biochem 182(1), 16-19
- Leong, P. L., Andrews, G. A., Johnson, D. E., Dyer, K. F., Xi, S., Mai, J. C., Robbins, P. D., Gadiparthi, S., Burke, N. A., Watkins, S. F., and Grandis, J. R. (2003) Proc Natl Acad Sci U S A 100(7), 4138-4143
- Liang, H., Hittelman, W., and Nagarajan, L. (1996) Arch Biochem Biophys 330(2), 259-265
- Paoletti, A., Giocanti, N., Favaudon, V., and Bornens, M. (1997) J Čell Sci 110 (Pt 19), 2403-2415
- Morse, D. L., Gray, H., Payne, C. M., and Gillies, R. J. (2005) Mol Cancer Ther 4(10), 1495-1504
- Kramer, G., Schwarz, S., Hagg, M., Havelka, A. M., and Linder, S. (2006) British journal of cancer 94(11), 1592-1598
- Hernandez-Vargas, H., Palacios, J., and Moreno-Bueno, G. (2007) Oncogene 26(20), 2902-2913
- Flynn, V., Jr., Ramanitharan, A., Moparty, K., Davis, R., Sikka, S., Agrawal, K. C., and Abdel-Mageed, A. B. (2003) Int J Oncol 23(2), 317-323
- Kraus, L. A., Samuel, S. K., Schmid, S. M., Dykes, D. J., Waud, W. R., and Bissery, M. C. (2003) Invest New Drugs 21(3), 259-268
- Qiu, L., Wang, Q., Di, W., Jiang, Q., Schefeller, E., Derby, S., Wanebo, H., Yan, B., and Wan, Y. (2005) Int J Oncol 27(3), 823-830
- Katoh, M., Koninkx, J., and Schumacher, U. (2000) Cancer Lett 161(1), 113-120
- Van Schaeybroeck, S., Kyula, J., Kelly, D. M., Karaiskou-McCaul, A., Stokesberry, S. A., Van Cutsem, E., Longley, D. B., and Johnston, P. G. (2006) Mol Cancer Ther 5(5), 1154-1165
- Sirotnak, F. M., Zakowski, M. F., Miller, V. A., Scher, H. I., and Kris, M. G. (2000) Clin Cancer Res 6(12), 4885-4892
- Ohta, T., Ohmichi, M., Hayasaka, T., Mabuchi, S., Saitoh, M., Kawagoe, J., Takahashi, K., Igarashi, H., Du, B., Doshida, M., Mirei, I. G., Motoyama, T., Tasaka, K., and Kurachi, H. (2006) Endocrinology 147(4), 1761-1769
- Pu, Y. S., Hsieh, M. W., Wang, C. W., Liu, G. Y., Huang, C. Y., Lin, C. C., Guan, J. Y., Lin, S. R., and Hour, T. C. (2006) Biochem Pharmacol 71(6), 751-760
- Herbst, R. S., Oh, Y., Wagle, A., and Lahn, M. (2007) Clin Cancer Res 13(15 Pt 2), s4641-4646
- Hari, M., Loganzo, F., Annable, T., Tan, X., Musto, S., Morilla, D. B., Nettles, J. H., Snyder, J. P., and Greenberger, L. M. (2006) Mol Cancer Ther 5(2), 270-278
- Burns, B. S., Edin, M. L., Lester, G. E., Tuttle, H. G., Wall, M. E., Wani, M. C., and Bos, G. D. (2001) Clin Orthop Relat Res (383), 259-267
- Baker, S. D., Sparreboom, A., and Verweij, J. (2006) Clin Pharmacokinet 45(3), 235-252
- Kyle, A. H., Huxham, L. A., Yeoman, D. M., and Minchinton, A. I. (2007) Clin Cancer Res 13(9), 2804-2810
- Patterson, S. G., Wei, S., Chen, X., Sallman, D. A., Gilvary, D. L., Zhong, B., Pow-Sang, J., Yeatman, T., and Djeu, J. Y. (2006) Oncogene 25(45), 6113-6122
- Nozawa, H., Tadakuma, T., Ono, T., Sato, M., Hiroi, S., Masumoto, K., and Sato, Y. (2006) *Cancer Sci* 97(10), 1115-1124
- Takabatake, D., Fujita, T., Shien, T., Kawasaki, K., Taira, N., Yoshitomi, S., Takahashi, H.,
 Ishibe, Y., Ogasawara, Y., and Doihara, H. (2007) Int J Cancer 120(1), 181-188
- Hammerman, P. S., Fox, C. J., Birnbaum, M. J., and Thompson, C. B. (2005) Blood 105(11), 4477-4483
- Lin, H. L., Liu, T. Y., Chau, G. Y., Lui, W. Y., and Chi, C. W. (2000) Cancer 89(5), 983-994

- Natarajan, V., Scribner, W. M., al-Hassani, M., and Vepa, S. (1998) Environ Health Perspect 106 Suppl 5, 1205-1212
- Kappert, K., Sparwel, J., Sandin, A., Seiler, A., Siebolts, U., Leppanen, O., Rosenkranz, S., and Ostman, A. (2006) Arterioscler Thromb Vasc Biol 26(12), 2644-2651
- Fiaschi, T., Buricchi, F., Cozzi, G., Matthias, S., Parri, M., Raugei, G., Ramponi, G., and Chiarugi, P. (2007) Hepatology 46(1), 130-139
- Frank, G. D., and Eguchi, S. (2003) Antioxid Redox Signal 5(6), 771-780
- Chen, C. H., Cheng, T. H., Lin, H., Shih, N. L., Chen, Y. L., Chen, Y. S., Cheng, C. F., Lian, W. S., Meng, T. C., Chiu, W. T., and Chen, J. J. (2006) Mol Pharmacol 69(4), 1347-1355
- Qiu, L., Di, W., Jiang, Q., Scheffler, E., Derby, S., Yang, J., Kouttab, N., Wanebo, H., Yan, B., and Wan, Y. (2005) Int J Oncol 27(5), 1441-1448
- Simon, A. R., Rai, U., Fanburg, B. L., and Cochran, B. H. (1998) Am J Physiol 275(6 Pt 1), C1640-1652
- Park, S. K., Kim, J., Seomun, Y., Choi, J., Kim, D. H., Han, I. O., Lee, E. H., Chung, S. K., and Joo, C. K. (2001) Biochem Biophys Res Commun 284(4), 966-971
- Liu, T., Castro, S., Brasier, A. R., Jamaluddin, M., Garofalo, R. P., and Casola, A. (2004) J Biol Chem 279 (4), 2461-2469
- Demoulin, J. B., Van Roost, E., Stevens, M., Groner, B., and Renauld, J. C. (1999) J Biol Chem 274(36), 25855-25861
- Matikainen, S., Sareneva, T., Ronni, T., Lehtonen, A., Koskinen, P. J., and Julkunen, I. (1999) Blood 93(6), 1980-1991
- Stout, B. A., Bates, M. E., Liu, L. Y., Farrington, N. N., and Bertics, P. J. (2004) J Immunol 173(10), 6409-6417
- Horinaga, M., Okita, H., Nakashima, J., Kanao, K., Sakamoto, M., and Murai, M. (2005) Urology 66(3), 671-675
- Huang, H. F., Murphy, T. F., Shu, P., Barton, A. B., and Barton, B. E. (2005) Mol Cancer 4(1), 2
- Gao, L., Zhang, L., Hu, J., Li, F., Shao, Y., Zhao, D., Kalvakolanu, D. V., Kopecko, D. J., Zhao, X., and Xu, D. Q. (2005) Clin Cancer Res 11(17), 6333-6341
- Nakahara, C., Nakamura, K., Yamanaka, N., Baba, E., Wada, M., Matsunaga, H., Noshiro, H., Tanaka, M., Morisaki, T., and Katano, M. (2003) Clin Cancer Res 9(14), 5409-5416
- Domingo-Domenech, J., Oliva, C., Rovira, A., Codony-Servat, J., Bosch, M., Filella, X., Montagut, C., Tapia, M., Campas, C., Dang, L., Rolfe, M., Ross, J. S., Gascon, P., Albanell, J., and Mellado, B. (2006) Clin Cancer Res 12(18), 5578-5586
- Li, J., Minnich, D. J., Camp, E. R., Brank, A., Mackay, S. L., and Hochwald, S. N. (2006) J Surg Res 132(1), 112-120
- Hammerman, P. S., Fox, C. J., Cinalli, R. M., Xu, A., Wagner, J. D., Lindsten, T., and Thompson, C. B. (2004) Cancer Res 64(22), 8341-8348
- Yan, B., Wang, H., Kon, T., and Li, C. Y. (2006) Brazilian journal of medical and biological research 39(2), 169-176
- Calabrese, E. J., Bachmann, K. A., Bailer, A. J., Bolger, P. M., Borak, J., Cai, L., Cedergreen, N., Cherian, M. G., Chiueh, C. C., Clarkson, T. W., Cook, R. R., Diamond, D. M., Doolittle, D. J., Dorato, M. A., Duke, S. O., Feinendegen, L., Gardner, D. E., Hart, R. W., Hastings, K. L., Hayes, A. W., Hoffmann, G. R., Ives, J. A., Jaworowski, Z., Johnson, T. E., Jonas, W. B., Kaminski, N. E., Keller, J. G., Klaunig, J. E., Knudsen, T. B., Kozumbo, W. J., Lettieri, T., Liu, S. Z., Maisseu, A., Maynard, K. I., Masoro, E. J., McClellan, R. O., Mehendale, H. M., Mothersill, C., Newlin, D. B., Nigg, H. N., Oehme, F. W., Phalen, R. F., Philbert, M. A., Rattan, S. I., Riviere, J. E., Rodricks, J., Sapolsky, R. M., Scott, B. R., Seymour, C., Sinclair, D. A., Smith-Sonneborn, J., Snow, E. T., Spear, L., Stevenson, D. E., Thomas, Y., Tubiana, M., Williams, G. M., and Mattson, M. P. (2007) Toxicol Appl Pharmacol 222 (1), 122-128
- Liu, G., Gong, P., Bernstein, L. R., Bi, Y., Gong, S., and Cai, L. (2007) Crit Rev Toxicol 37(7), 587-605

- Calabrese, E. J. (2005) Crit Rev Toxicol 35(6), 463-582
- Lechanteur, C., Jacobs, N., Greimers, R., Benoit, V., Deregowski, V., Chariot, A., Merville, M. P., and Bours, V. (2005) Oncogene 24(10), 1788-1793
- Yang, P., He, X. Q., Peng, L., Li, A. P., Wang, X. R., Zhou, J. W., and Liu, Q. Z. (2007) J. Toxicol Environ Health A 70(11), 976-983
- Bullock, A. N., Debreczeni, J. E., Fedorov, O. Y., Nelson, A., Marsden, B. D., and Knapp, S. (2005) J Med Chem 48(24), 7604-7614
- Holder, S., Lilly, M., and Brown, M. L. (2007) Bioorg Med Chem 15(19), 6463-6473
- Pogacic, V., Bullock, A. N., Fedorov, O., Filippakopoulos, P., Gasser, C., Biondi, A., Meyer-Monard, S., Knapp, S., and Schwaller, J. (2007) Cancer Res 67(14), 6916-6924

FOOTNOTES

The work was supported by Award W81XWH-04-1-0087 from the Department of Defense/CDMRP Prostate Cancer Program.

The abbreviations used are: STAT3, signal transducer and activator of transcription 3; NFkB, nuclear factor kappa B; PBS, phosphate buffered solution, TBST, tris-buffered saline Tween-20; SDS, sodium dodecyl sulfate; EDTA, ethylenediaminetetraacetic acid.

FIGURE LEGENDS

- <u>Fig. 1.</u> Time course of PIM1 expression induced by docetaxe<u>l</u> RWPE-1 and RWPE-2 cells were treated with 10nM or 100nM docetaxel for the indicated time. PIM1and β-ACTIN proteins were analyzed by immunoblot analysis. One of three similar blots is shown. Ratio* = ratio PIM1/β-ACTIN from pooled densitometry data from three separate experiments. P value** = probability of no difference in ratios (treated vs untreated cells) by paired T test (n = 3).
- <u>Fig. 2.</u> Up-regulation of PIM1 mRNA transcription in RWPE-1 and RWPE-2 prostate cell lines treated with docetaxel. Real-time PCR was used to measure PIM1 mRNA. Each value represents the mean (± SD) of nine pooled measurements produced by three independent experiments. Bars show the relative fold-increase of PIM1 RNA level (normalized to the RNA level of the housekeeping gene cofilin), and compared to untreated control (0 hours). P values (above error bars) were calculated by T-tests, and represent the probability of no difference between the test and control values.
- <u>Fig. 3.</u> Independence of PIM1 expression and cell cycle arrest. (A). DNA histogram analysis of RWPE-2 cells after docetaxel 10nM or 100nM treatments for 24 hours. "sG1" represents a sub-G1 cell population with less then 2N DNA content. "G1" and "G2" shows the appearance of cells in G0/1 or G2/M phases of cell cycle. (B), Immunoblot analysis of cyclin B1, PIM1 expression after docetaxel 10 nM (B, left panel) or 100 nM (B, right panel) treatment at various time points.
- Fig. 4. PIM1 expression protects RWPE-2 cells from docetaxel induced cell death. RWPE-2 cells transfected with pLNCX (= vector) or pLNCX/PIM1 (= PIM1) constructs were treated with docetaxel for 24, 48, and 72 hours, then cell viability was determined by the MTT assay. Results were normalized to the values for untreated cells. Each value represents the mean (± SD) of nine measurements pooled from three independent experiments. P values were determined by T-tests for comparisons between PIM1- and vector-transfected cells treated similarly. (**) represents a p value of <0.01, indicating that the chance for no difference between PIM1- and vector-transfected cells was less than one percent.

- Fig. 5. Knockdown of PIM1 expression with siRNA sensitizes prostate cells to docetaxel-induced cell death. (A), RWPE-2 cells were transfected with plasmids encoding control siRNA or PIM1 siRNA and treated with 100nM of docetaxel for 6 hours. Expression of PIM1, β-ACTIN proteins was analyzed by Immunobloting. (B), Cell viability measured with MTT assay after docetaxel treatment for up to 72hrs. Each value is the mean (± SD) of nine measurements pooled from three independent experiments. P values were determined by T-tests for comparisons between PIM1 siRNA- and control siRNA-treated cells
- Fig. 6 Expression of a dominant-negative (NT81) PIM1 protein sensitizes prostate cells to docetaxel-induced cell death. (A), RWPE-2 stable pools transfected with vector pLNCX, or pLNCX/PIM1 or pLNCX/NT81 were treated with the indicated concentrations of docetaxel for 24 hours. Cell viability was measured by MTT assay, and showed the proportion of viable cells in treated cultures compared with those in untreated cultures (NC). Each bar shows the mean (± SD) of nine measurements pooled from three independent experiments. P values were calculated by T-tests. (**) = p<0.01 and indicates that the chance of no difference between treated and untreated cultures is less than one percent (B), Identification of PIM1 and NT81 transgene expression in RWPE-1 and RWPE-2 stable pools was determined by Western blot with indicated antibodies. (C), Detection of apoptosis induced by treatment with 100nM docetaxel for 24 hours in RWPE-1 and RWPE-2 cells transfected with vector (pLNCX); pLNCX/PIM1 or pLNCX/NT81. "Percent Apoptotic Cells" represents the percent cells positive for carboxyfluorescein caspase, determined by flow cytometery. The basal percent-positive-cells (typically <5%) from untreated cultures has been subtracted from each bar value. Each bar shows the mean (± SD) of nine measurements pooled from three independent experiments. P values were calculated by T-tests. (**) = p<0.01 and indicates that the chance of no difference between different cell lines is less than one percent.
- Fig. 7. PIM1 kinase protects RWPE-2 prostate cells with proliferative potential from docetaxel cytotoxicity. RWPE-2/PIM1 (wild-type PIM1) and RWPE-2/NT81 cells (dominant-negative PIM1) were treated with docetaxel for 24hrs. Additional cultures of the same cells were treated similarly but without docetaxel. Cells were then trypsinized, diluted, replated in fresh medium, and allowed to grow for 6-7 days. Cultures were then fixed with formalin and stained with crystal violet to measure cell growth. Comparisons of the regrowth of treated cultures were made with similar, untreated cells, but comparisons were always made between wells with OD₅₇₀ values on the linear part of a cell density standard curve. Each point represents the mean (± SD) of 9-18 measurements pooled from two independent experiments. Untreated cell cultures were assigned a relative regrowth value of 1.0.
- Fig. 8. Time course of phosphorylation of STAT3 and induction of PIM1 expression. Immunoblots of RWPE-1 cells (Panel A & B) or RWPE-2 cells (Panel C & D) treated with 10 nM (A and C) or 100 nM (B and D) of docetaxel.
- Fig. 9. STAT3 decoy inhibits PIM1 expression in prostate RWPE-2 cells and prevents PIM1 up regulation in cells treated with docetaxel. (Panel A), RWPE-2 cells were transfected with STAT3 mutant control oligonucleotides or STAT3 decoy oligonucleotides and incubated for 48 hours. Expression of PIM1 and as the known STAT3 target gene BCLX, were analyzed by immunoblotting. (Panel B), RWPE-2 cells were transfected with STAT3 mutant control oligonucleotides or STAT3 decoy oligonucleotides and incubated for 16 hours. Cells were treated with 100nM of docetaxel for 6 hours, then lysed and analyzed for their levels of expression for PIM1, phosphoSTAT3 and total STAT3.
- <u>Fig. 10.</u> Elevated level of PIM1 protein enhances NFκB activity in RWPE-2 prostate cancer cells. A pool of RWPE-2 cells stably expressing a NFκB-luciferase reporter plasmid was infected with retroviruses encoding a PIM1 cDNA. After selection with G418, stable pools were analyzed for expression of PIM1 by immunobloting (data not shown). RWPE-2/NFκB-luciferase/pLNCX cells and

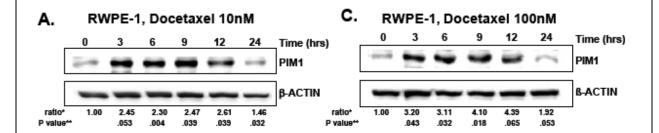
RWPE-2/NFxB-luciferase/PIM1 cells were plated and allowed to grow overnight. On the next day the expression of luciferase was measured and normalized to the protein concentration for each sample. The normalized activity in PIM1 expressing cells was compared to that of vector-transfected cells. The values present the mean (± SD) of the means from five independent experiments. The paired T-test was used to determine statistical significance for the values of luciferase activity measured in the PIM1 expressing cell line as compared to the vector transfected cells.

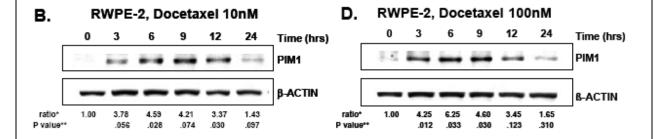
Fig. 11. Expression of a kinase-inactive, dominant-negative PIM1 (NT81) decreases docetaxel-induced activation of NFkB. RWPE-2 cells stably expressing a NFkB -luciferase reporter gene were infected with retroviruses carrying pLNCX vector or pLNCX/NT81 constructs. Pools were selected with G418, and transgene expression was documented by immunoblotting (data not shown). RWPE-2/NFkB-luciferase/pLNCX and RWPE-2/NFkB-luciferase/NT81 cells were treated for 6 hours with indicated concentrations of docetaxel and luciferase activity was determined. Each bar represents the mean (± SD) of triplicate determinations one of three similar experiments. P values were calculated by T-tests. (**) indicates a P value of <0.01, showing that the chance of no difference in luciferase activity between vector and NT81-transduced cells is less than one percent.

Fig. 12. siRNA oligonucleotides inhibit expression of p65/RELA and p50/NFKB1 proteins, and NFκB transcriptional activity. (A), RWPE-2/NFκB-luciferase/PIM1 cells were transfected with control siRNA, siRNAs targeting p50/NFKB1 (= si p50), or p65/RELA (= si p65). After 48 hours the luciferase activity was measured and compared with that of RWPE-2/NFκB-luciferase/pLNCX cells transfected similarly. Each bar represents the relative luciferase activity of the various cells compared with that of vector-transduced cells treated with control siRNA. The values are the mean (± SD) of six measurements pooled from two independent experiments. (B), Immunoblot analysis of NFKB1 (top) and RELA (bottom) protein expression in cells treated with siRNAs. β-ACTIN expression documents equal loading of the lanes.

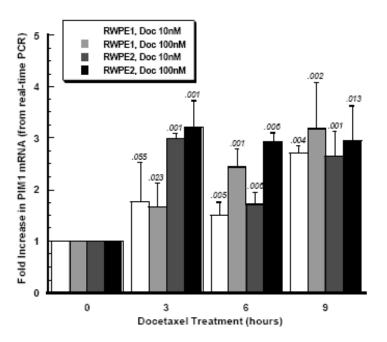
Fig. 13. Inhibition of NFkB activation by siRNA increases docetaxel-induced cell death. (A), RWPE-2/pLNCX and RWPE-2/pIM1 cells were transfected with the indicated siRNAs and allowed to rest for 24 hours. Docetaxel (100nM) was then added for 48 hours. Cell survival was then estimated by MTT assay. Each bar represents the mean (± SD) of six measurements pooled from two independent experiments. P values were calculated by T-test, and represent comparisons between PIM1 expressing cells and vector control cells, as well as among cells treated with different types of siRNAs. (B), MTT survival data from (panel A) for docetaxel-treated cells are re-presented following normalization of the data to the values for control si RNA-treated cells. In this analysis, survival (as OD₄₅₀ from the MTT assay) of cells transfected with NFcB-targeting siRNAs is shown as a percent of the values for the same cells treated with control siRNA. Each bar presents the mean (± SD) of six measurements pooled from two independent experiments. P values were calculated by T-test, and represent the likelihood that there is no difference in the sensitizing effect of the siRNA between vector- and PIM1-transduced cells.

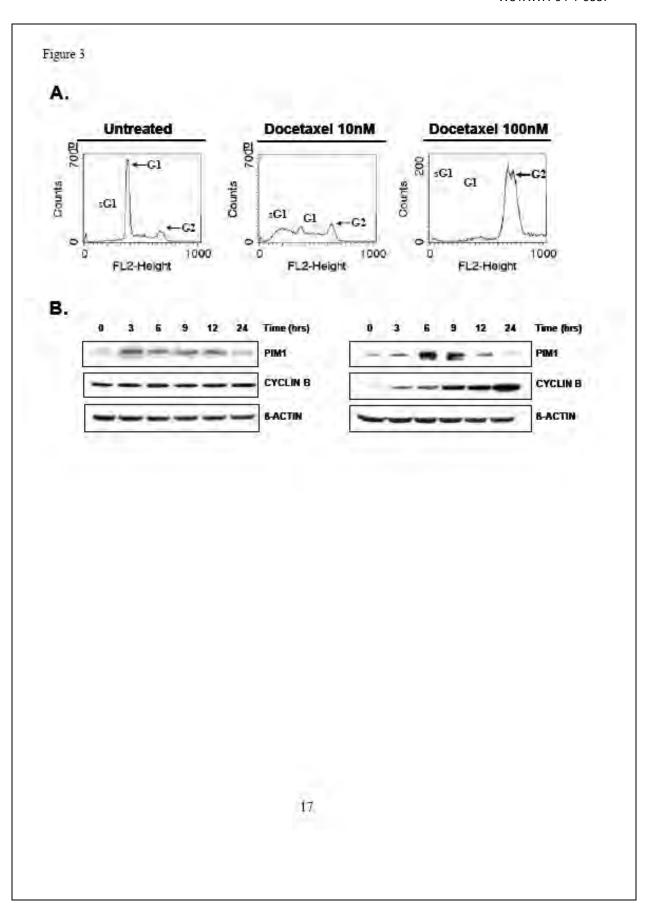
Figure 1

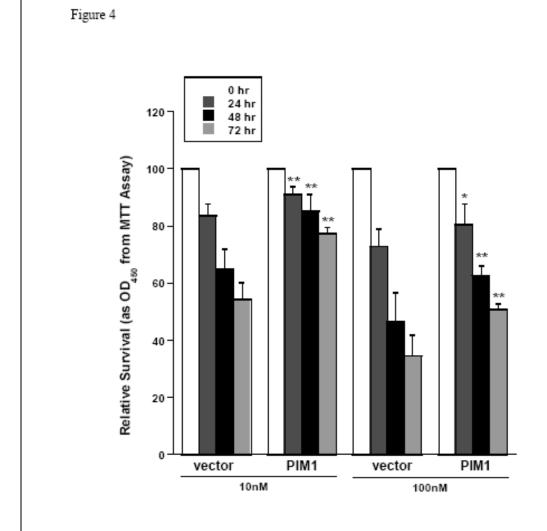


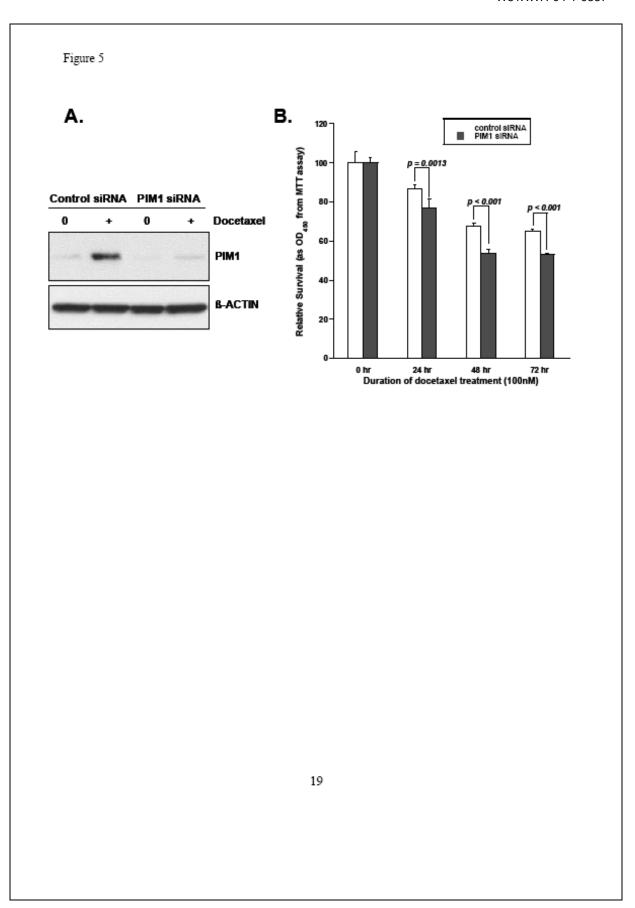


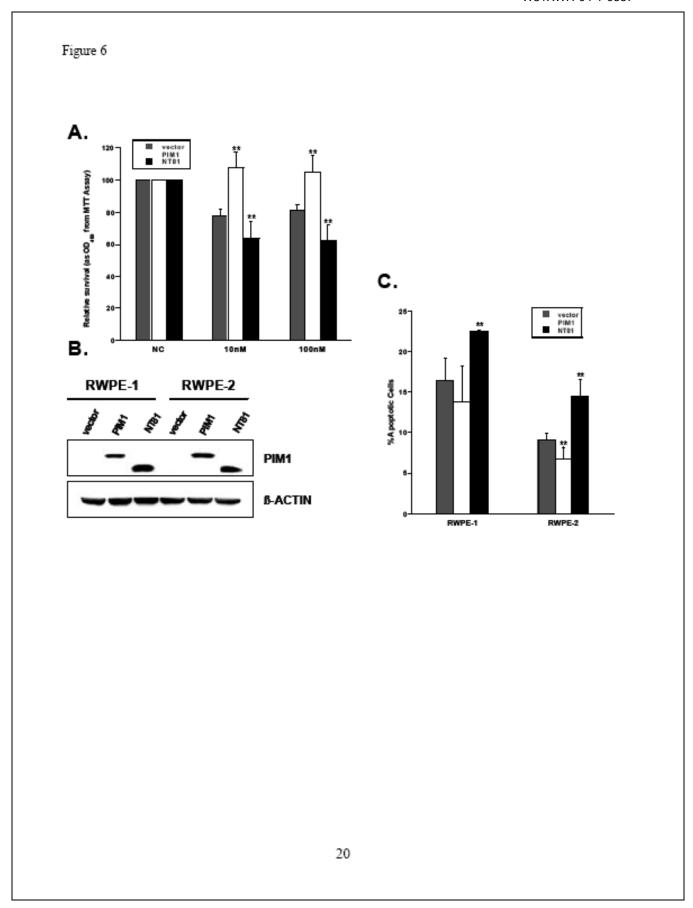


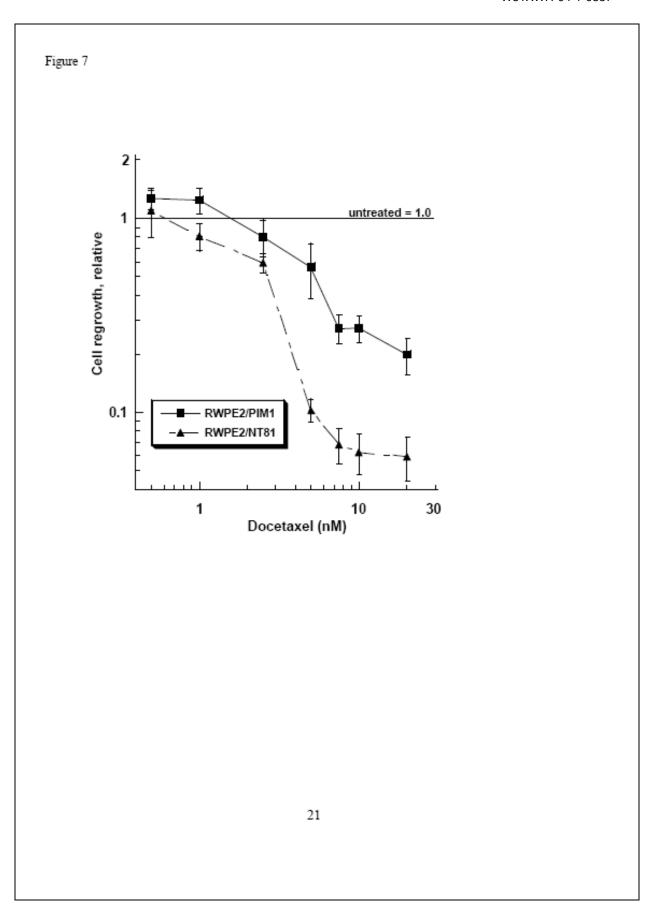


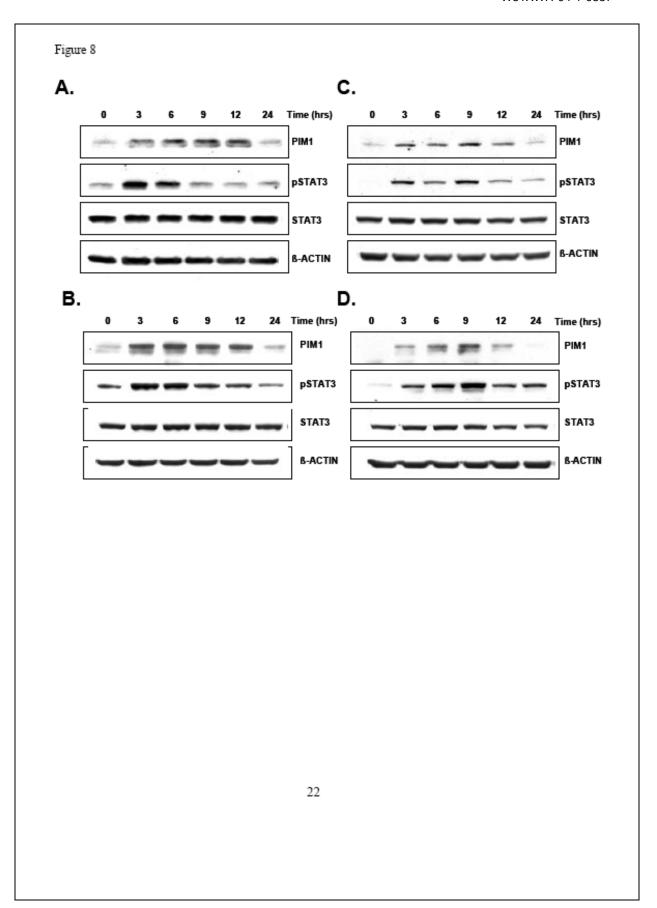


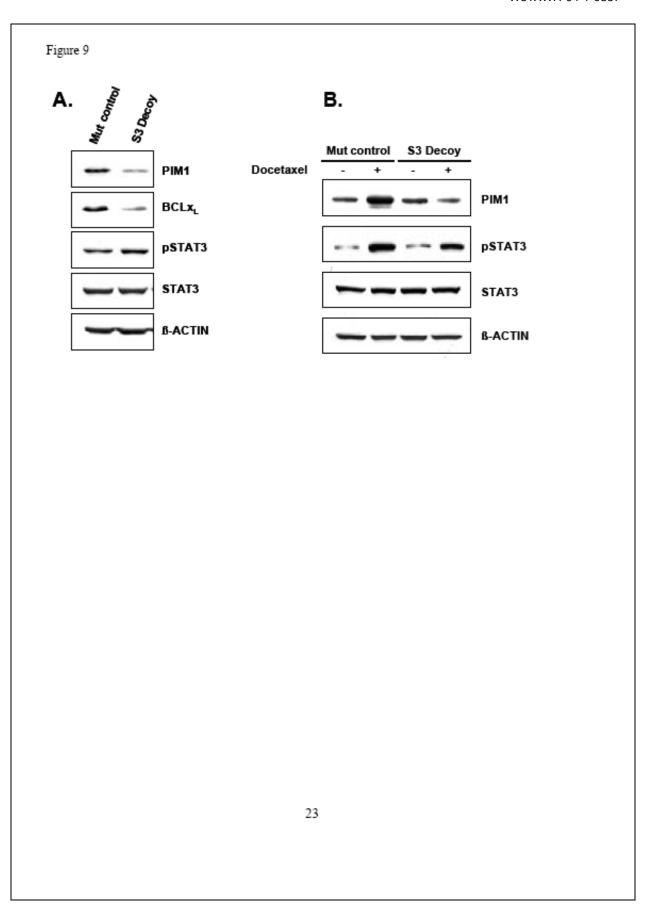


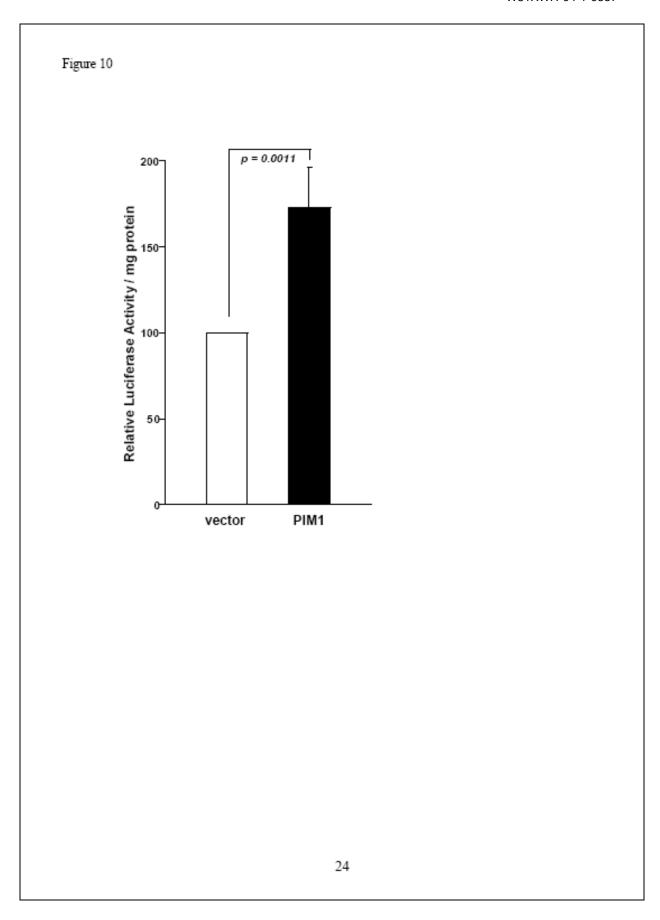


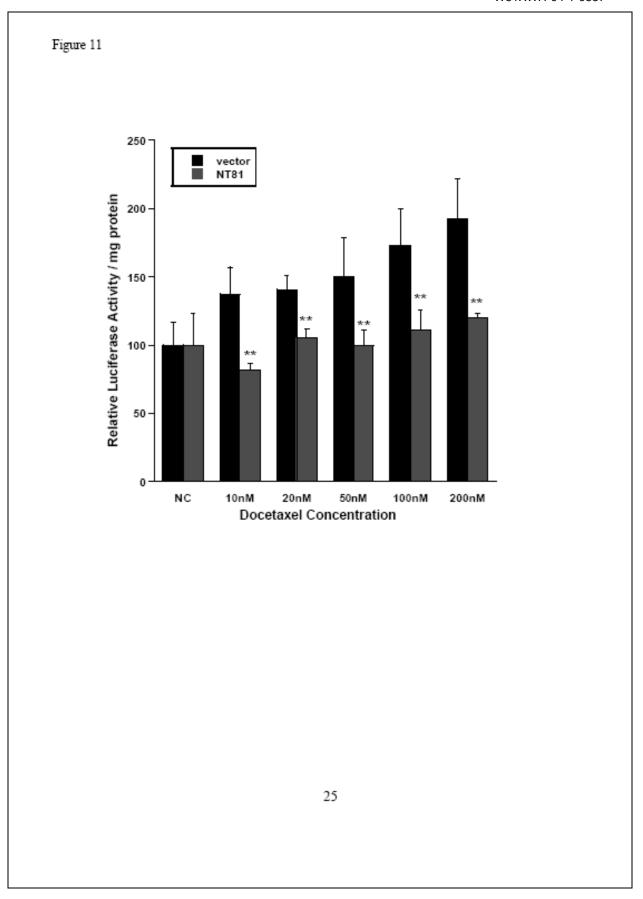


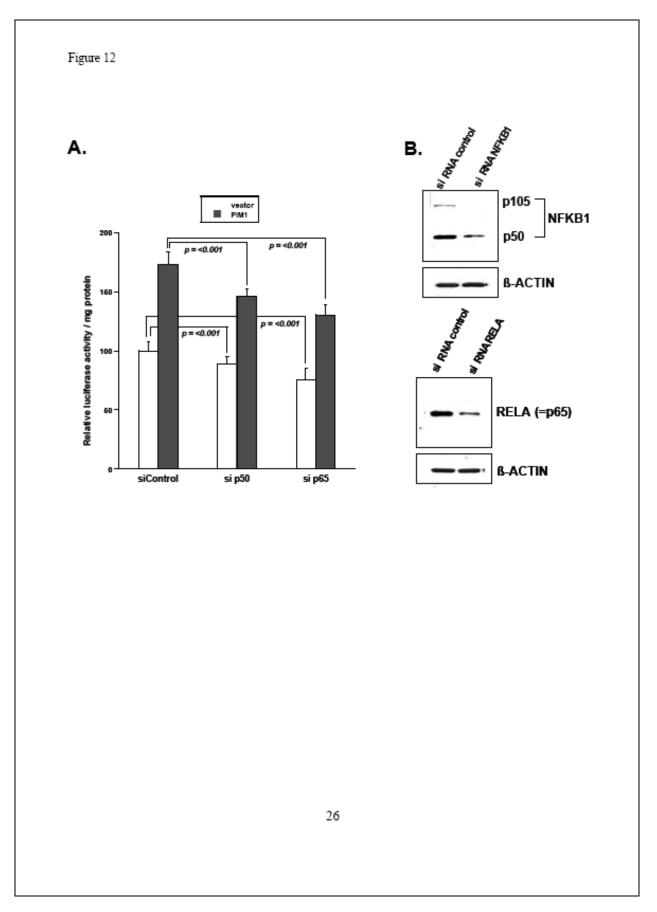






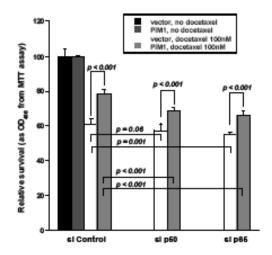




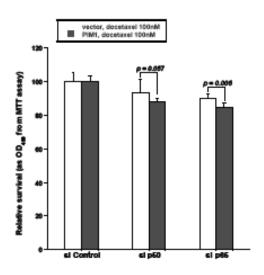




A.



В.



27

CURRICULUM VITAE MICHAEL BRIAN LILLY, MD

Updated 10/2007

Personal Data: Birth: 26 December, 1950, Atlanta, GA

Citizenship: USA

Office: Professor of Clinical Medicine

Vice Chief for Clinical Programs Division of Hematology-Oncology University of California, Irvine

Bldg 56, Rm 248 101 The City Drive Orange, CA 92868

Telephone 714-456-5153

FAX 714-456-2242 e-mail: mlilly@uci.edu

Home: 511 West Olive Avenue

Redlands, CA 92373

(909) 792-5573

Education: Southern Adventist University, Collegedale, TN

1967-1971, B.A. (biology, chemistry)

Loma Linda University, Loma Linda, CA

1971-1975, M.D.

Postgraduate

Training

Internal Medicine residency

University of Alabama at Birmingham

Birmingham, AL 1975-1978

Hematology-Oncology Fellowship University of Alabama at Birmingham

1978-1981

Faculty Positions: 6/81-6/82 Instructor in Medicine

UAB School of Medicine

6/82-10/88 Assistant Professor of Medicine,

UAB School of Medicine

6/82-10/88 Associate Scientist, Lurleen Wallace

Tumor Institute, Birmingham, AL

Faculty Postions (cont'd):

6/89-9/98 Associate Professor of Medicine, University of Washington School of Medicine, Seattle, WA

4/96-10/96 Visiting Scientist, The Walter and Eliza Hall Institute for Medical Research, Melbourne, Victoria, AUSTRALIA

9/98 – 10/06 Professor of Medicine & Microbiology Director, Center for Molecular Biology & Gene Therapy Loma Linda University School of Medicine, Loma Linda, CA

11/06 – present Professor of Clinical Medicine, and Vice Chief for Clinical Programs, Divison of Hematology-Oncology, University of California, Irvine

11/06 – present Co-leader for Translational Oncology Program, Chao Family Comprehensive Cancer Center, University of California, Irvine

Hospital Positions: Alabama

1981-1988 Attending Physician, University of Hospitals and Clinic

1981-1988 Staff Oncologist, Birmingham VA Medical

Center, Birmingham, AL

1989-1998 Staff Oncologist, Seattle VA Medical Center, Seattle, WA

1998-present Attending Physician, Loma Linda University Medical Center, Loma Linda, CA 11/06-present Attending Physician, University of California, Irvine Medical Center, Orange, CA

Honors: 1974 Alpha Omega Alpha

1980 National Research Service Fellow

1981 Fellow, American College of Physicians

Board Certification: 1979 American Board of Internal Medicine

1980 ABIM Subspecialty Exam, Hematology 1981 ABIM Subspecialty Exam, Med. Oncology

Licensure: Alabama Medical License #7730 (3/77-12/91)

Washington State License #27864 (12/91 – 12/00) California Medical License #G84932 (12/98 – present) **Organizations:** Fellow, American College of Physicians

Member, American Society of Hematology Member, American Society for Bone Marrow

Transplantation

Member, American Society for Gene Therapy

National Member, study sections for NIH:
Professional 1987 Diagnostic Radiology

Responsibilities 1988 Experimental Therapeutics

Member, site visit team for program project Dr. George Hahn, PI; Stanford University

1988, 1989

Member, site visit team for program project
Dr. Bayard Clarkson, Pl, Memorial-Sloan

Kettering Inst., 1997

Member, Pathobiology Study Section, DOD/CDMRP

Breast Cancer Program, 2006-2008

Member, Data Safety Monitoring Board for California

Cancer Consortium, 2007 - present

Special Local Responsibilities

Member, Scientific Review Subcommittee SVAMC, 1993, 1994, 1997

Member, Research & Development Committee

SVAMC, 1994, 1995

Member, Hospice Advisory Committee

SVAMC, 1994, 1995

Board Development Committee, Leukemia & Lymphoma Society (Southern California Chapter),

2003

Medical Director, Chao Family Comprehensive Cancer

Center Infusion Center, 2007 – present

Cancer Committee, UCI Medical Center, 2007 -

present

Board of Trustees, Leukemia & Lymphoma Society,

Orange County-Inland Empire Chapter, 2007 - present

Consultant Cetus Corporation (1986)

EncorePharma (2001-present)

Myriad Constint (2002 present)

Myriad Genetics (2002-present)

Exelixis Pharmaceuticals (2005-present)

GRANTS & CONTRACTS (PRINCIPAL INVESTIGATOR) Note: This listing does not include multicenter clinical trials in which Dr. Lilly was the local principal investigator.

National Institutes of Health F32CA27980 *Hyperthermia of animal and human tumors*; 7/80-6/82

National Institutes of Health R01CA18138-11 Prediction of thermal tolerance by in vivo NMR spectroscopy; 7/82-6/83

National Institutes of Health R01CA36790 Assessment of hyperthermia by in vivo ³¹P-NMR spectroscopy; 9/84-9/87

Cetus Corporation Characterization of a human granulocyte CSF; 7/85-6/86

National Institutes of Health R01CA45672 *Cytokine signaling in myeloid leukemia*; 9/87-10/98

VA Merit Review Award Non-protein hematopoietic agents; 10/90-4/97

March of Dimes Birth Defects Foundation Characterization of a 28kd protein related to G-CSF; 7/93-6/96

Lymphoma Research Foundation of America *Mechanism of action of the pim-1 oncogene*; 7/95-7/96

Roche Pharmaceuticals Preclinical study of Roferon and bryostatin 1 in a melanoma model; 1/98-12/99

Department of Defense, National Medical Technology Testbed #76-FY99: *Cell-permeable proteins for cell regulation*. 12/99 – 7/02

Leukemia Society of American Translational Award *Propionic Acid Analogues for CLL*. 9/1/01 – 8/31/05

Celgene Corporation, Phase I-II trial of combined GM-CSF (sargramostim) and thalidomide for hormone-refractory prostate cancer (5/02-5/04).

National Institutes of Health R03CA107820 *Molecular Targets of NSAIDs in Prostate* Cancer; (5/1/04 – 4/30/08)

Department of Defense, CDMRP Prostate Cancer Program PC040635 Pim-1: A Molecular Target to Modulate Cellular Resistance to Therapy in Prostate Cancer (10/04 – 10/09)

Bristol-Myers Squibb, *Phase II Study of Dasatinib in Hormone-refractory Prostate Cancer* (7/07 – present)

GRANTS and CONTRACTS (Co-investigator)

National Institutes of Health R01CA097043 *Molecular pathology of 2-deoxy-5-azacytidine*; L. Sowers, PI; Michael Lilly, co-investigator (10% FTE). 7/1/03 – 6/30/08

National Institutes of Health R43CA119833 *SIMPKIN: a facile mthod for identification of unknown kinase substrates.* Q. Hamid, PI; Michael Lilly, co-investigator (5% FTE) 10/1/06-2/28/07.

PUBLICATIONS IN PEER-REVIEWED JOURNALS

- 1. Brezovich I, **Lilly M**, Durant J, Richards D: A practical system for clinical radiofrequency hyperthermia. *Int J Rad Onc Biol Phys* 7:423-430, 1981
- 2. Ng T, Evanochko W, Hiramoto R, Ghanta V, **Lilly M**, Lawson A Corbett T, Durant J, Glickson J: ³¹P-topical NMR spectroscopy of *in vivo* tumors. *Mag Res* 49:271-286, 1982.
- 3. **Lilly M**, Brezovich I, Chakraborty D, Atkinson W, Durant J, Ingram J, McElvein R: Hyperthermia with implanted electrodes: *in vitro* and *in vivo* correlations. *Int J Rad Onc Biol Phys* 9:373-382, 1983.
- 4. Evanochko W, Ng T, **Lilly M**, Kumar N, Durant J, Glickson J: *In vivo* ³¹P-NMR studies of the effect of cancer therapy on a murine mammary carcinoma. *Proc Natl Acad Sci USA* 80:334-338, 1983.
- 5. **Lilly M**, Ng T, Evanochko W, Kumar N, Elgavish G, Durant J, Hiramoto R, Ghanta V, Glickson J: *in vivo* ³¹P-NMR study of hyperthermia tumor treatment. *Cancer Res* 44:663-638, 1984.
- 6. Hiramoto R, Ghanta V, **Lilly M**: Reduction in tumor burden in murine osteosarcoma by hyperthermia and cyclophosphamide. *Cancer Res* 44:1405-1408, 1984.
- 7. Brezovich I, Atkinson W, **Lilly M**: Local hyperthermia with interstitial techniques. *Cancer Res* 44:46752s-4756s, 1984.
- 8. **Lilly M**, Brezovich I, Atkinson W: Hyperthermia with thermally self-regulating ferromagnetic implants. *Radiology* 154:243-244, 1985.
- 9. **Lilly M**, Katholi C, Ng T: Direct relationship between high-energy phosphate content and blood flow in thermally treated tumors. *JNCl* 75:885-889, 1985.
- 10. **Lilly M**, Omura G: Clinical pharmacology of oral intermediate dose methotrexate with or without probenecid. *Cancer Chemo Pharm* 15:220-222, 1985.

- 11. **Lilly M**, Carroll A, Prchal J: Lack of association between glutathione content and development of thermal tolerance in human fibroblasts. *Radiation Res* 106:41-46, 1986.
- 12. Tucker K, **Lilly M**, Heck L, Rado T: Characterization of a new human diploid myeloid leukemia cell line (PLB985) with granulocytic and monocytic differentiating capacity. *Blood* 70:372-378, 1987.
- 13. Devlin J, Devlin P, Myambo K, **Lilly M**, Rado T, Warren K: Isolation and expression of a cDNA encoding a human granulcyte colony-stimulating factor. *J Leukocyte Biol* 41:302-306, 1987.
- 14. **Lilly M**, Devlin J, Devlin P, Rado T: Production of granulocyte colony-stimulating factor by a human melanoma line. *Exp Hematol* 15:966-971, 1987.
- 15. Barton J, Parmley R, Butler T, Williamson S, **Lilly M**, Gualtieri R, Heck L: Differential staining of neutrophils and monocytes: surface and cytoplasmic iron-binding proteins. *Histochem J* 210:147-155, 1988.
- 16. Csepreghy M, Yielding A, **Lilly M**, Scott C, Prchal J: Characterization of a new G6PD variant: G6PD Central City. *Am J Hematol* 28:61-62, 1988.
- 17. **Lilly M**, Kraft A: Leukemia-differentiating activity expressed by the human melanoma cell line LD1. *Leukemia Res* 12:213-218, 1988
- 18. Prchal J, Hauk M, Csepreghy M, **Lilly M**, Berkow R, Scott C: Two apparent G6PD variants in normal XY man: G6PD Alabama. *Am J Med* 84:517-523, 1988.
- 19. Bailey A, **Lilly M**, Bertoli L, Ball E: An antibody which inhibits in vitro bone marrow proliferation in a patient with system lupus erythematosus and aplastic anemia. *Arthritis and Rheumatism* 32:901-905, 1989.
- 20. Kraft A, Williams F, Pettit R, **Lilly M**: Variable response of human myeloid leukemia lines and fresh cells to differentiating activity of bryostatin 1. *Cancer Res* 49:1287-1293, 1989.
- 21. Everson M, Brown C, **Lilly M**: IL6 and GM-CSF are candidate growth factors for chronic myelomonocytic leukemia cells. *Blood* 74:1472-1476, 1989.
- 22. Nemunaitis J, Andrews F, Mochizuki D, **Lilly M**, Singer J: Human marrow stromal cells: response to IL6 and control of IL6 expression. *Blood* 74:1693-1699, 1989.
- 23. Brezovich I, **Lilly M**, Meredith R, Weppleman B, Brawner W, Henderson R, Salter M: Hyperthermia of pet animal tumors with self-regulating ferromagnetic thermoseeds. *Intl J Hyperthermia* 6:117-130, 1990.

- 24. **Lilly M**, Tompkins C, Brown C, Pettit R, Kraft A: Differentiation and growth modulation of chronic myelogenous leukemia cells by bryostatin 1. *Cancer Res* 50:5520-5525, 1990.
- 25. **Lilly M**, Brown C, Pettit R, Kraft A: Bryostatin 1: a potential cytotoxic agent for chronic myelomonocytic leukemia cells. *Leukemia* 5:282-287, 1991.
- 26. Andrews D, **Lilly M**, Tompkins C, Singer J: Sodium vanadate, a tyrosine phoshpatase inhibitor, affects expression of hematopietic gorwth factors and extracelular matrix RNAs in SV40-transformed human marrow stromal cells. *Exp Hematol* 20:391-400, 1992.
- 27. **Lilly M**, Le T, Holland P, Hendrickson S: Expression of the pim-1 kinase is specifically induced in myeloid cells by growth factors whose receptors are structurally related. *Oncogene* 7:727-732, 1992.
- 28. Takahashi G, Andrews D, Tompkins C, Montgomery R, **Lilly M**, Singer J, Alderson M: Effect of granulocyte macrophage colony-stimulating factor (GM-CSF) and interleukin 3(IL3) on interleukin 8 (IL8) production in neutrophils and monocytes. *Blood* 81:357-364, 1993.
- 29. Polostkya A, Zhao C, **Lilly M**, Kraft A: A critical role for the intracellular domain of the alpha chain of the GM-CSF receptor in cell cycle transition. *Cell Growth & Diff* 4:5250531, 1993
- 30. Polostkya A, Zhao C, **Lilly M**, Kraft A: Mapping the intracytoplasmic regions of the alpha granulocyte-macrophage colony-stimulating factor receptor necessary for cell growth regulation. *J Biol Chem* 269:14607-14613, 1994
- 31. Takahashi G, Montgomery B, Stahl W, Crittenden C, Thorning D, **Lilly M**: Pentoxifylline inhbits tumor necrosis factor-alpha mediated cytotoxicity and activation of phospholipase A2 in L929 murine fibrosarcoma cells. *Intl J Immunopharm* 16:723-736, 1994
- 32. Sensebe L, Li J, **Lilly M,** Crittenden C, Herve P, Charbord P, Singer J: Non-transformed colony-derived stromal cell lines from normal human marrows. I. Growth requirements, characterization ,and myelopoieisis-supportive ability. *Exp Hematol* 23:507-513, 1995
- 33. Asiedu C, Biggs J, **Lilly M**, Kraft A: Inhibition of leukemic cell growth by the protein kinase C activator Bryostatin 1 correlates with the dephosphorylation of cyclin-dependent kinase 2. *Cancer Res* 55:3716-3720, 1995

- 34. **Lilly M**, Vo K, Lee T, Takahashi G: Bryostatin 1 acts synergistically with interleukin 1 to promote the release of G-CSF and other myeloid cytokines from marrow stromal cells. *Exp Hematol* 24:613-621, 1996.
- 35. Matsuguchi T, Zhao Y, **Lilly MB**, Kraft AS: The cytoplasmic domain of the granulocyte-macrophage colony-stimulating factor (GM-CSF) receptor α subunit is essential for both GM-CSF-mediated growth and differentiation. *J Biol Chem* 272:17450-17459, 1997.
- 36. **Lilly M**, Kraft A: Enforced expression of the 33kd pim-1 kinase enhances factor-independent growth and inhibits apoptosis in murine myeloid cells. *Cancer Res* 57:5348-5355, 1997.
- 37. Matsuguchi T, **Lilly MB**, Kraft AS: Cytoplasmic domains of the human granulocyte-macrophage colony-stimulating factor receptor β chain (h β c) responsible for human GM-CSF-induced myeloid cell differentiation. *J Biol Chem* 273:19411-19418, 1998.
- 38. Frankel A, **Lilly M**, Kreitman R, Hogge D, Beran M, Freedman MH, Emanuel PD, McLain C, Hall P, Tagge E, Berger M, Eaves C: Diptheria toxin fused to granulocyte-macrophage colony-stimulating factor is toxic to blasts from patients with juvenile myelomonocytic leukemia and chronic myelomonocytic leukemia. *Blood* 92:4279-4286, 1998.
- 39. **Lilly M,** Kiskonen P, Sandholm J, Cooper JJ, Kraft AS: The Pim-1 kinase prevents apoptosis-associated mitochondrial dysfunction, and supports cytokine-independent survival of myeloid cells in part through regulation of *bcl-2* expression. *Oncogene* 18:4022-4031, 1999.
- 40. **Lilly M**, Zemskova M, Frankel AE, Salo J, Kraft AS: Distinct domains of the human GM-CSF receptor alpha subunit mediate activation of JAK/STAT signaling and differentiation. *Blood* 97:1662-1670, 2001.
- 41. Wu X, Daniels T, Molinaro C, **Lilly MB**, Casiano C: Caspase cleavage of the nuclear autoantigen LEDGF/p75 abrogatres its prosurvival function: implications for autoimmunity in atopic disorders. *Cell Death Differentiation* 9:915-924 (2002).
- 42. Lombano F, Kidder MY, **Lilly M**, Gollin YG, Block BS: Recurrence of microangiopathic hemolytic anemia after apparent recovery from the HELLP syndrome: A case report. *J Reprod Med* 47:875-877 (2002)
- 43. Frankel AE, Powell BL, **Lilly MB**. Diphtheria toxin conjugate therapy of cancer. *Cancer Chemother Biol Response Modif.* 2002;20:301-13. Review
- 44. Ionov Y, Le X, Tunquist BJ, Sweetenham J, Sachs T, Ryder J, Johnson T, **Lilly MB**, Kraft AS: Nuclear localization of the pim-1 protein kinase is necessary for its biologic effects. *Anticancer Res* 23(1A):167-78 (2003).

- 45. Yan B, Zemskova M, Holder S, Chin V, Kraft AS, Koskinen PJ, **Lilly MB**: The PIM-2 kinase phosphorylates BAD on serine-112 and reverses BAD induced cell death. *J Biol Chem* 278:45358-45367 (2003)
- 46. Aho TLT, Sandholm J, Peltola KJ, Mankonen H, **Lilly M**, Koskinen PJ: Pim-1 kinase promotes inactivation of the pro-apoptotic Bad protein by phosphorylating it on the Ser¹¹² gatekeeper site. *FEBS Letters* 571:43-49 (2004).
- 47. Fodor I, Timiryasova T, Denes B, Yoshida J, Ruckle H, **Lilly M**: Vaccinia virus-mediated p53 gene therapy of bladder cancer in an orthotopic murine model. *J Urology* 173, 604-609 (2005).
- 48. Kim K-T, Baird K, Ahn J-Y, Meltzer P, **Lilly M**, Small D: Pim-1 is upregulated in constitutively activating FLT3 mutants and plays a role in FLT3-mediated cell survival. *Blood* 105(4), 1759-1767 (2005).
- 49. Chen WW, Chan DC, Donald C, **Lilly MB**, Kraft AS. Pim family kinases enhance tumor growth of prostate cancer cells. *Mol Cancer Res.* 3:443-51 (2005).
- 50. Zemskova M, Wechter W, Yoshida J, Ruckle H, Reiter RE, **Lilly MB**: Gene expression profiling in R-flurbiprofen-treated prostate cancer: Identification of prostate stem cell antigen as a flurbiprofen-regulated gene. *Biochem Pharmacology* 72:1257-1267 (2006).
- 51. Holder SL, Zemskova M, Bremner R, Neidigh J, **Lilly MB**: Identification of specific, cell-permeable small molecule inhibitor of the PIM1 kinase. *Mol Cancer Therapeutics* Mol Cancer Ther. 6:163-72 (2007).
- 52. Ma J, Arnold HK, **Lilly MB**, Sears R, Kraft AS: Negative regulation of PIM-1 protein kinase levels by the B56b subunit of PP2A. *Oncogene* Feb 12, 2007; [Epub ahead of print]
- 53. Hansen JE, Fischer LK, Chan G, Chang SS, Bladwin SW, Aragon RJ, Carter JJ, **Lilly MB**, Nishimura RN, Weisbart RH, Reeves ME: Antibody-mediated p53 protein therapy prevents liver metastatsis *in vivo*. *Cancer Res* 67:1769-74 (2007).
- 54. Holder SL, **Lilly MB**, Brown ML: Comparative Molecular Field Analysis of Flavonoid Inhibitors of the PIM-1 Kinase. *Bioorg Med Chem* (in press, 2007)
- 55. Zhou J, Pan M, Xie Z, Loh S-L, Bi C, Tai Y-C, **Lilly MB**, Lim Y-P, Han J-H, Glaser KB, Albert DH, Davidsen SK, Chen CS: Synergistic antileukemic effects between ABT-869 and chemotherapy involve downregulation of cell cycle regulated genes and c-Mosmediated MAPK pathway. *Leukemia* (in press, 2007)

BOOKS AND CHAPTERS:

Singer J, Slack J, **Lilly M**, Andrews D: Marrow stromal cells: response to cytokines and control of gene expresssion (in) The Hematopoietic Microenvironment. M. Wicha and M. Long, eds. Johns Hopkins Press, Baltimore, (1993).

RECENT ABSTRACTS:

Hromas R, Collins S, Bavisotto L, Hagen F, Raskind W, **Lilly M**, Kaushansky K: HEM-1, a potential transmembrane protein, is restricted to, yet ubiquitous in, hematopoietic cells. *Blood* 75:98a, 1990

Bianco J, Nemunaitis J, Andrews D, **Lilly M**, Shields A, Singer J: Combined therapy with pentoxifylline, ciprofloxacin, and prednisone reduces regimen related toxicity and accelerates engraftment in patients undergoing bone marrow transplantation. *Blood* 78:237a, 1991.

Lilly M, Sensebe L, Singer J: Characterization of cell-associated granulocyte colonystimulating factor in human marrow stromal cells. *Blood* 78:261a, 1991 (oral presentation)

Takahasi G, **Lilly M**, Bianco J, Crittenden C, Singer J: Pentoxifylline inhibits tumor necrosis factor-alpha cytotoxicity and activation of phospholipase A2 in murine fibrosarcoma cells. *Blood* 78:323a, 1991.

Kirshbaum M, **Lilly M**: Multiple growth factors induce expression of the Bcl-2 protein in 32D murine hematopoietic cells, but differ in their ability to inhibit apotosis. *Blood* 84:423a, 1994.

Lilly M, Pettit G: Identification of the cephalostatins as potent cytotoxic agents for myeloid leukemia cells. *Blood* 86:517a, 1995 (poster presentation)

Lilly M, Kraft A, Rotman E: Enforced expression of the human 33kd Pim-1 kinase enhances autonomous proliferation and tumorgenicity in factor-dependent murine FDCP1 cells. *Blood* 86:588a, 1995 (oral presentation).

Lilly M, Cooper JJ: Enforced expression of the human 33kd Pim-1 kinase prevents apoptosis-associated mitochondrial dysfunction and upregulates *bcl-2* mRNA expression in murine myeloid cells. (oral presentation, ASH 12/97)

Wu X, Molinaro C, **Lilly M**, Casiano C: Caspase-mediated cleavage of the transcription co-activator p75 during apoptosis (abstract #993). *Proc AACR* 41:155 (2000).

- Quiggle DD, **Lilly M**, Murray ED, Gibson K, Leipold D, Gutierrez I, Loughman B, Wechter W: PK guided multi-dose, tolerance, and safety of E-7869 in prostate cancer patients (abstract #3874). *Proc AACR* 41:609 (2000)
- **Lilly M**, Frankel AE, Salo J, Kraft AS: Distinct domains of the human GM-CSF receptor alpha subunit mediate activation of Jak/Stat signaling and differentiation (abstract #2455). *Blood* 96:572a (oral presentation, ASH 12/00)
- Chen CS, **Lilly MB**, Wang FS, Howard FD, Houwen B: Rapid monitoring of peripheral blood stem cells (PBSC) mobilization by using cell membrane phospholipid content correlates well with CD34+ measurements, successful harvest and engraftment (abstract #1642). *Blood* 96:380a (poster presentation, ASH 12/00)
- **Lilly M**, Ruckle H, Quiggle D, Gutierrez I, Murray D, Gibson K, Leipold D, Wechter W, Loughman B: Multi-dose phase I-II trial of E-7869 in prostate cancer patients: safety and time to PSA progression (TPSAP). *Proc AACR* 42:142 (2001)
- Kastaros EP, Casiano C, Colburn KK, **Lilly M**, Weisbart RH, Kim J, Green LM: Lupus associated anti-guanosine antibodies: potential pathogenic effects. *Arthritis* & *Rheumatism* 44:S99 (2001)
- Yan B, Zemskova M, Kraft AS, Koskinen PJ, **Lilly MB**: The pim-2 kinase phosphorylates Bad on serine-112 and reverses Bad induced cell death. (abstract #2919). *Blood* (poster presentation, ASH 12/02).
- **Lilly MB**, Thorn S, Oberg K, Bashirova S, Zemskova M: The pim-1 serine/threonine kinase is primarily expressed in granulocytes and macrophages in inflamed tissues (abstract #981). *Blood* 102:276a (poster presentation, ASH 12/2003)
- Neidigh J, Holder S, **Lilly MB**: Using docking to improve comparative modeling predictions: applications to pim-1 kinase. (poster presentation, *Structure-Based Drug Design 2004*, Boston, MA, April 26-28, 2004)
- Chen CS, Zemskova M, Reiter R, **Lilly MB**: Gene expression profiling in R-flurbiprofentreated prostate cancer: Identification of prostate stem cell antigen as a flurbiprofentegulated gene. (poster presentation, *AACR 3rd Annual Conference on Frontiers in Cancer Prevention*, Seattle, WA; October 2004).
- **Lilly MB,** Holder S, Zemskova M, Neidigh J: Use of a homology model of the PIM-1 kinase to identify variant flavonoids having selective inhibitory activity against PIM-1. *Blood* 104:703a (poster presentation, ASH 12/2004)
- **Lilly MB**, Wechter W, Puuvula L, Henry H: R-Flurbiprofen (RFB) a non-steroidal anti-inflammatory drug (NSAID) with anti-tumor activity, inhibits the expression of CYP24 in murine prostate carcinomas. (poster presentation at *Biennial Vitamin D Conference "Vitamin D and Cancer Chemoprevention"*, NIH, Bethesda, MD, November 2004)

Daniels TR, Ganapathy V, Mediavilla M, Soto U, Zemskova M, **Lilly MB**, Casiano CA The survival protein LEDGF/p75 enhances the resistance of prostate cancer cells to caspase-independent cell death induced by docetaxel *Proc AACR* 46:188 – 189 (2005).

Zemskova M, Sahakian E, **Lilly MB.** The PIM1 kinase is a critical component of a survival pathway that protects prostate cancer cells from docetaxel-induced death *Proc AACR* 47:171 (2006).

Ruckle H, Ebrahimi K, Howard F, Ornstein D, Ahlering T, **Lilly MB**: Post Prostatectomy Adjuvant Multimodality Therapy for Prostate Cancer Patients with High Risk of Relapse. (poster presentation at American Urologic Association annual mtg., 2008)